

On the number of limit cycles
for some families of
planar differential equations

Set Pérez-González

Memòria presentada per aspirar al grau
de doctor en Ciències (Matemàtiques).
Departament de Matemàtiques de la
Universitat Autònoma de Barcelona.

CERTIFICO que aquesta memòria ha
estat realitzada, sota la meva direcció.

Bellaterra, 16 de Juliol de 2012.

Dr. Joan Torregrosa i Arús

”Si las personas no creen que las matemáticas son simples,
es simplemente porque no se dan cuenta de lo complicada
que es la vida.”
John Von Neumann

Agradecimientos

Aunque muchos lo nieguen aquí es donde te lo juegas todo. Donde vas a demostrar si estos años han servido para algo. Si realmente serás una persona de provecho que merece ser laureada con honores académicos. En definitiva, alguien de valía intelectual, con una memoria prodigiosa... para acordarse de todos aquellos que merecen ser agradecidos.

En mi caso será complicado, pues tengo mucho que agradecer y muy mala memoria. Creo que seguiré un orden decreciente, de lo más general a lo más concreto. Por algo estamos aquí, ¿no? Nos gusta darle un orden a las cosas.

En primer lugar me gustaría dar gracias al personal del departamento en general, ya que desde que llegué me sentí uno más y no sólo entre los estudiantes de doctorado. Me gustaría destacar al personal de administración en general, sin favoritismos, porque siempre se han volcado conmigo para resolver cualquier cuestión por pequeña o grande que fuera. Además, y más importante si cabe, siempre tienen una palabra amable y una conversación agradable para quien pasa por la secretaría.

A continuación, querría agradecer a los miembros del Grupo de Sistemas Dinámicos de la UAB por su apoyo y su atención cuando he necesitado de su ayuda. En particular, me gustaría agradecerle a Jaume el trato que me ha dado y confío que estos años haya supuesto algo provechoso para el grupo como el grupo lo ha sido para mí. Sin formar parte del grupo, no se si habría llegado este momento. También quiero nombrar gente de otros grupos de sistemas dinámicos de universidades como la de la UIB, la de Lleida, la de Sevilla, la UPC... Con los que he disfrutado grandes momentos, sobretudo en escuelas y congresos. En particular, me gustaría darle las gracias a los miembros del Grupo de sistemas Dinámicos de la Universidad de Oviedo. Pues aunque salí de su cantera sin conocerles a todos, todos ellos me han apoyado y animado durante estos años.

Querría también dar las gracias a Pedro por acogerme tan amablemente, incluso en su casa, mientras estuve en Granada. A Héctor por ser tan atento en todo para no dejarme sentir sólo durante mi estancia en Tours. Saludos a Jean Claude y Suzie. And I would like to thank Peter and Freddy the opportunity they give me to be in Hasselt working with them. Del mismo modo me gustaría mencionar a Armengol, que siempre ha buscado orientarme y presionarme para sacar adelante este trabajo.

Ha llegado el turno de la juventud. Los estudiantes terminamos siendo gregarios y muchas son las amistades que salen de círculo tan selecto. Querría tener una palabra para todos, y esa es gracias. Gracias por las tertulias, las partidas de ping-pong, las comidas compartidas... Pero sobretudo por ser mejores que cualquier grupo de apoyo de estudiantes de doctorado anónimos para contar las penas. Por eso querría mencionar a

Dong, David, Anna, Elena, Blesa, Ferreiro, Bossa, Ricardo... Tienen un hueco especial Sara y Wolf, y no sólo por el sofá y los platos compartidos. También por la conversaciones, los consejos (no siempre seguidos) y vuestra amistad continuamente demostrada. Además, Leopoldo y Víctor se han ganado un puesto de privilegio, pues han conseguido que no pueda volver a decir que de México no ha salido nada bueno bueno desde el pan Bimbo.

Finalmente, nos acercamos al punto álgido, y he de agradecer a mis padres y mi hermano todo el apoyo recibido y el sacrificio que les ha supuesto el que llegase este día. Por eso les dedico este trabajo, pues es de lo poco que dispongo para devolverles el favor. Y ya no me queda más que dar las gracias a Joan y Eliana, pues sé a ciencia cierta que sin ellos este trabajo sí que no habría llegado a puerto alguno. Joan, creo que nunca llegaré a comprender del todo la suerte que tuve al entrar en tu despacho para pedirte ser mi director. Muchas gracias por tu dirección y mando. Y sólo lamento no haber sido más obediente y mejor estudiante. Eli, sin tu apoyo constante no habría conseguido sobrellevar todo esto. Y no te preocupes que el pedestal que te mereces está ya de camino.

Contents

Introduction	iii
1 Limit cycles on a linear center with extra singular points	1
1.1 Introduction	1
1.2 General results for an arbitrary number of singularities	9
1.2.1 Computations of the Abelian Integrals	9
1.2.2 Upper bounds for the number of zeros	13
1.3 The case of one singularity	15
1.4 The case of two singularities	17
1.4.1 An explicit bound for the maximum configuration	17
1.4.2 Configurations of simultaneous zeros	22
1.4.3 Bifurcation Diagram for perturbations of degree one	33
2 Limit cycles for generalized φ-laplacian Liénard equation	45
2.1 Introduction	45
2.2 Function families	49
2.3 A Polygonal Compactification	50
2.4 State functions	54
2.5 Existence results	54
2.5.1 Local stability of the origin	54
2.5.2 Stability of the infinity	55
2.6 Uniqueness of limit cycle	65
3 On the Bogdanov-Takens bifurcation	69
3.1 Introduction	69
3.2 Changes of variables	73
3.3 Bounds from the origin	75
3.4 Bounds up to infinity	82
3.5 Global bounds for n in \mathbb{R}^+	87
Bibliography	97
Index	102

Introduction

During 17th century, ordinary differential equations were born to explain the movement of the particles in physical systems, such as the translation of the planets around the Sun. Since then they have become a very important tool in many other fields in science and engineering, like biology or electronics. For instance, they are used to model the population growth of species or the evolution of electrical circuits. When the derivation variable just plays an implicit role, the differential equation is said autonomous. The autonomous cases can be considered as dynamical systems. Intuitively, they are rules for the evolution in time of any particle in space. Therefore time is taken as the derivation variable.

Ordinary differential equations of order n take the form

$$F(t, x, x', x'', \dots, x^{(n)}) = 0, \quad (1)$$

where $x^{(n)}$ is the n th derivative of x with respect to t . The autonomous cases take place when F does not depend on t . If x is a vector instead of a real function, equation (1) is called a differential system. In particular, if the space where x is considered is \mathbb{R}^2 or any contained open subset, we refer to it as a planar differential system.

In this thesis the equations considered are, or can be seen as, first-order autonomous planar differential systems,

$$\begin{cases} x' &= f(x, y), \\ y' &= g(x, y), \end{cases} \quad (2)$$

where $x(t)$, $y(t)$, $f(x, y)$ and $g(x, y)$ are real functions.

The aim of the qualitative theory is to understand the behavior of the solutions of any differential system without obtaining their specific expression. The qualitative theory was first introduced by Henri Poincaré in his “Mémoire sur les courbes définies par une équation différentielle”, [Poi81], which was a great breakthrough in the study of differential systems. Poincaré mainly studies the case of planar differential systems and proposes a geometric framework for studying their solutions.

In order to understand this geometric point of view, let us consider the velocity field X , which is the vector field whose components are f and g , the functions in system (2). The solutions of the differential system are the trajectories of the vector field. It means that at any point the tangent vectors to the solution curves and the vector field are parallel. The trajectories are also known as the orbits of the vector field. The advantage of using orbits lies in the fact that if we change the time parametrization, they remain unchanged.

There are some concrete orbits with particular behaviors. Some of them were characterized by Poincaré, among others singular points and cycles. Singular points are the points where the field vanishes. They are also called critical or fixed points. And, cycles are the trajectories of the vector field that repeat themselves along time. Usually, they are also called closed or periodic orbits. Notice that singular points are a particular type of cycles. For a point in a cycle after a time T , its orbit will be again on him. For a fixed point, its orbit is on him for every time t in \mathbb{R} .

The notion of limit cycle was also introduced in the first papers which dealt with qualitative theory. Essentially, a limit cycle, γ , is a periodic orbit such that at least one trajectory of the vector field, different from γ , approaches γ in positive or negative time. See, for example [HS74, Chi06]. Usually, when the vector field is of class \mathcal{C}^1 an alternative definition is given. A closed orbit is named limit cycle if it is isolated from the other periodic orbits. See [Sot79]. This definition is, in general, more restrictive than the previous one, but both are equivalent in the analytic case.

In many senses a cornerstone of the qualitative theory of autonomous systems in dimension two is the Poincaré-Bendixson Theorem. It first appeared in the third volume of [Poi81] for analytic vector fields. In [Ben01], it is extended to the case of differential systems defined by functions of class \mathcal{C}^1 . This result, for a continuous vector field X , establishes that for any orbit contained in positive time in a bounded region, if it approaches a set without singular points, this set is a periodic orbit. Different proofs of this continuous version can be found in [CL55, Har64]. It can be mentioned [Cie02] as a neat summary of the theorem and some related results.

Just for the completeness of the terminology, we should introduce the notions of α and ω limit sets. They were first proposed by George D. Birkhoff in [Bir66]. So the ω -limit of an orbit is the set of points that the orbit approaches in positive time. And the α -limit is the set that the orbit departs from, in negative time.

As a corollary of the Poincaré-Bendixson Theorem we have that the ω -limit set of a positive orbit contained in a bounded region can only be a fixed point, a cycle or a polycycle, a set of fixed points and regular orbits connecting them. The regular orbits connecting fixed points, in particular the ones in polycycles, are said homoclinic or heteroclinic orbits depending in if they connect just one singular point or several ones, respectively. An analogous result is obtained for the α -limit sets. Therefore the behavior of the solutions of a differential equation can be almost reduced to a local study of the singular points, the closed orbits and the connections of regular orbits and fixed points. In this fact lies the importance of the limit sets. We are particularly interested in the limit cycles. And our results are related with the most famous open problem about limit cycles, that is the second part of the Hilbert 16th problem.

In the International Congress of Mathematics in 1900, David Hilbert proposed 23 problems that in his opinion would motivate advances in mathematics during the 20th century. With the 16th problem, Hilbert asked about the topology of algebraic curves and surfaces. He included a second part asking about the maximum number and the

position of the limit cycles of a polynomial planar system,

$$\begin{cases} x' &= P(x, y), \\ y' &= Q(x, y), \end{cases}$$

with P and Q polynomials of degree n . This maximum number depending just on n is usually known as the Hilbert number, $\mathbf{H}(n)$.

There are a lot of published works in relation with this problem. But even the minimum case, $n = 2$, it is yet to be proved. Vladimir I. Arnold in [Arn77, Arn83] establishes a weak version of this problem, that is also still open. Steve Smale, in his list of mathematical problems for the 21st century, includes a modern version of it, see [Sma98]. Moreover, he proposes to found upper bounds of the number of limit cycles of order n^q , where q is a universal constant. In the Smale's list, it occupies the 13th position, so this problem is known as the Smale 13th. For more details in the 16th Hilbert we refer the reader to [Ily02, Li03, CL07].

Smale also says that the computation of the Hilbert number can be notably difficult. So the mathematicians must consider a special class of differential equations 'where the finiteness is simple, but the bounds remain unproved'. In fact, he proposes to seek bounds for a special class of polynomial Liénard systems,

$$\begin{cases} x' &= y - F(x), \\ y' &= -x, \end{cases}$$

where F is a real polynomial of odd degree and satisfying $F(0) = 0$.

In order to achieve the Hilbert number, the lower bounds are as important as the upper bounds. The study of lower bounds for the Hilbert number focus mainly on two standard techniques. One is the computation of the limit cycles that persist after the polynomial perturbation of centers. And the other is the study of necessary conditions for a family of differential systems depending on some parameters such that it succeed the birth of a limit cycle from different kind of singular orbits, such as fixed points or heteroclinic connections. It is known as the bifurcation of a limit cycle. For example, the Hopf bifurcation phenomena implies the birth of a cycle from a singular point satisfying some particular conditions.

This thesis deals with these aspects of limit cycles for some particular families of differential equations. In the first chapter we examine the weak Hilbert 16th problem restricted to the polynomial perturbation of a particular center. The second chapter establishes sufficient conditions for the existence and uniqueness of limit cycles in a generalization of the Liénard equation. Chapter 3 provides a study of the location of a bifurcation curve in the parameter space of the Bogdanov-Takens system. Immediately, we show more details of the problems treated. However, each chapter contains a section devoted to summarize the problems and the main results obtained.

Because of the independence between the different problems proposed, this thesis has been written in a modular form, been each chapter independent to the others. And, therefore, it can be read in any order. To facilitate access to the individual topics, the notation on each chapter is rendered as self-contained as possible.

In Chapter 1 we examine the limit cycles that appear after the perturbation of a linear center with extra singular points. The perturbed system that we consider is

$$\begin{cases} x' &= y K(x, y) + \varepsilon P(x, y), \\ y' &= -x K(x, y) + \varepsilon Q(x, y), \end{cases} \quad (3)$$

where K is a specific family of polynomials, P and Q are any polynomial and ε a small enough real number. This differential system has a center at the origin, equivalent to the generated by the Hamiltonian $H(x, y) = x^2 + y^2$. And the extra singular points that we referred before are the ones that satisfy $K(x, y) = 0$.

In fact we analyze the Abelian integral associated to (3), as it was proposed by Arnold in the statement of the weak Hilbert 16th problem. There are several previous works dealing with the Abelian integral associated to this system where the set of singular points take different forms, like straight lines [LLLZ02] or quadratic curves [BL07]. We consider the case of finite sets of isolated points.

One of the key points of the work included in Chapter 1 is that we are able to consider several period annulus where we can seek limit cycles. Hence, we develop a study of the simultaneity of the limit cycles in the different annuli at the same time. Due to their difficulty, the papers on the simultaneity of limit cycles in several regions are not common at all. But some examples are [CL95, CLP09]. Other key point of the first chapter is the study on the dependence of the number of limit cycles on the location of the parameters included in Section 1.4.3. We have constructed a bifurcation diagram that distinguishes different regions on the parameter space where we have different number of limit cycles.

In this chapter the lack of a partial fraction decomposition for two variable rational functions does not allow us to obtain better upper bounds in the more general cases. But the main difficulty in carrying out better results for this chapter is the amount and the size of the computations that should be done. Some of the results of this chapter appear in [PGT12].

In the second chapter of this thesis we extend some of the classical results about existence and uniqueness of limit cycles for the Liénard equation [YCC⁺86, ZDHD92] to the φ -laplacian case,

$$(\varphi(x'))' + f(x)\psi(x') + g(x) = 0. \quad (4)$$

This equation appears in models that consider definitions of the derivative different from the classic one, such as the relativistic one. In fact, the harmonic relativistic oscillator can be modeled as

$$\left(\frac{x'}{\sqrt{1 - \frac{x'^2}{c^2}}} \right)' + x = 0,$$

see [Gol57, Mic98]. So, our results apply to the relativistic van der Pol equation,

$$\left(\frac{x'}{\sqrt{1 - \frac{x'^2}{c^2}}} \right)' + \mu(x^2 - 1)x' + x = 0,$$

as well as to the ordinary one.

The results included in this chapter involve an ad hoc compactification designed with two objectives. First, to unify the different behaviors of the functions in (4) satisfying our hypothesis. And second, to make possible the comprehension of the global phase portrait. The results of this chapter have also been done in collaboration with Pedro J. Torres. And they appear in [PGTT12].

The aim of the third chapter is to obtain a global knowledge of the homoclinic connection curve in the first quadrant of parameter space, where the limit cycles can appear, in the system associated to this Bogdanov-Takens normal form,

$$\begin{cases} x' &= y, \\ y' &= -n + by + x^2 + xy, \end{cases} \quad (5)$$

where the parameters, n and b , are real numbers. When the parameters vanish, the origin shows a local structure of cusp point, a kind of degenerate singular point. But if we unfold this vector field, they appear several bifurcation curves, a Hopf bifurcation, a saddle-node bifurcation and a homoclinic connection curves. See [GH02] for more details.

It is worth pointing out that the system (5) is a semi-complete family of rotated vector fields with parameter b . So, for any fixed n , the limit cycle grows until it disappears in the homoclinic connection when we range b from its birth in the Hopf bifurcation.

The study of the bifurcation curve of the homoclinic connection is usually restricted to a local region near the origin. It is known, [GH02], that for $n > 0$ there exists a value $b^*(n)$ such that the system has a unique limit cycle if and only if $b^*(n) < b < \sqrt{n}$. Moreover $b^*(n) = \frac{5}{7}\sqrt{n} + \dots$ for n small enough. In [Per92] the quadratic differential system is considered in the whole space and it is proved that $b^*(n)$ is analytic and that the previous inequalities are satisfied for all $n > 0$. A detailed study of the curve $b^*(n)$ for n small enough is presented in [GGT10].

The results obtained in [GGT10] are based on an algebraic method for the location of bifurcation curves. In our work we adapt this procedure to our needs. Finally, we obtain explicit curves such that $b_d(n) < b^*(n) < b_u(n)$ for all $n > 0$. With this result we prove a conjecture proposed by Perko in [Per92], where he predicts that $b^*(n)$ goes to infinity as $\sqrt{n} - 1$. In particular, we prove that $b^*(n)$ goes to infinity as $\sqrt{n} - 1 + O(1/n)$.

This chapter has also been developed in collaboration with Armengol Gasull and Héctor Giacomini.

Chapter 1

Limit cycles on a linear center with extra singular points

1.1 Introduction

One of the main and oldest problems in the qualitative theory of differential systems is the knowledge of the isolated periodic solutions that a concrete system presents. In the plane, the Poincaré-Bendixson theorem ensures that these orbits are α or ω limit sets, so we call them limit cycles. For planar polynomial vector fields, one of the most known unsolved problems is the second part of Hilbert's 16th problem, that can be expressed as follows.

Hilbert 16th Problem. *For the differential system*

$$\begin{cases} \dot{x} = P(x, y), \\ \dot{y} = Q(x, y), \end{cases} \quad (1.1)$$

where P and Q are polynomials of degree n , which is the maximum number of limit cycles, $\mathbf{H}(n)$, for any $n \in \mathbb{N}$? And, which are their relative positions?

A common technique to give lower bounds of this number is based on the perturbation of centers. Hence, the limit cycles bifurcate from the periodic orbits of a center. We say that a limit cycle bifurcates from a periodic orbit $\gamma(r)$ if there exists a continuous family of closed curves $l(\varepsilon)$, where ε is the perturbed parameter, such that $l(\varepsilon)$ is a limit cycle of the perturbed system for $\varepsilon \neq 0$ and $l(0) = \gamma(r)$.

Definition 1.1. *Assume that system (1.1) has a center at the origin. Given a transversal section Σ , parametrized by $r \in [0, r_0)$, the Poincaré map, $\mathbf{P}(r) \in [0, r_0)$, is defined on Σ by the first intersection of the positive semi-orbit of $\Sigma(r)$ with Σ , at $\Sigma(\mathbf{P}(r))$. See Figure 1.1.*

When system (1.1) has a center at the origin, we can extend the Poincaré map, $\mathbf{P}(r, \varepsilon)$, also called the first return map, to the perturbed system

$$\begin{cases} \dot{x} = P(x, y) + \varepsilon f(x, y), \\ \dot{y} = Q(x, y) + \varepsilon g(x, y). \end{cases} \quad (1.2)$$

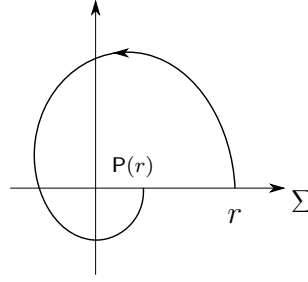


Figure 1.1 Poincaré map, P

Therefore, the periodic orbits of (1.2) coincide with the zeros of the displacement function $d(r, \varepsilon) = P(r, \varepsilon) - r$. From [Poi90] we have that

$$d(r, \varepsilon) = \varepsilon (d_0(r) + \mathcal{O}(\varepsilon)). \quad (1.3)$$

If $d_0(r)$ is not identically zero, then the number of zeros of $d(r, \varepsilon)$ is bounded by the number of zeros of $d_0(r)$ for ε small enough, taking into account its multiplicities. This fact appears for the first time in [Pon34] for Hamiltonian systems and it could be expressed as

Pontrjagin Criterion. *If a limit cycle of (1.2) bifurcates from $\gamma(r)$, a periodic orbit of the unperturbed system, then $d_0(r) = 0$. Conversely, if $d_0(r) = 0$ and $d'_0(r) \neq 0$ then a limit cycle of (1.2) bifurcates from $\gamma(r)$.*

Then it can be considered the weak Hilbert's 16th Problem. V. I. Arnold stated this problem for Hamiltonian systems, see [Arn77] and [Arn83].

Weak Hilbert 16th Problem. *Let $H = H(x, y)$ be a polynomial in x, y of degree $m + 1 \geq 2$, and the level curves $\gamma_h \subseteq \{(x, y) : H(x, y) = h\}$ with $h_1 < h < h_2$. These curves, $\{\gamma_h\}_{h_1 < h < h_2}$, form a continuous family of simple closed curves around the point (x_0, y_0) . Additionally, let us consider the system*

$$\begin{cases} \dot{x} &= \frac{\partial H(x, y)}{\partial y} + \varepsilon f(x, y), \\ \dot{y} &= -\frac{\partial H(x, y)}{\partial x} + \varepsilon g(x, y), \end{cases} \quad (1.4)$$

where $\max(\deg(f), \deg(g)) = n \geq 2$, and (x_0, y_0) is a center of (1.4) when $\varepsilon = 0$. Then, for fixed n and m integer values, the weak Hilbert 16th problem ask for the maximum number of isolated zeros of the Abelian integral, associated to system (1.4),

$$I(h) = \oint_{\gamma_h} (f(x, y)dy - g(x, y)dx). \quad (1.5)$$

For the case considered in the Arnold's statement we have that, see [Poi90, Pon34],

$$I(h) = d_0(h),$$

for $d(h)$ given in (1.3) defined for any Σ , a transversal section of γ_h parametrized by $h \in (h_1, h_2)$.

In general, an Abelian integral, by definition, is the integral of a rational 1-form along an algebraic simple closed curve [CL07, p. 99]. From the above relation between $I(h)$ and $d(h)$ in the weak Hilbert's 16th, $I(h)$ is also known as the Poincaré-Pontrjagin-Melnikov function of system (1.4).

It should be remarked that the study of the Abelian integrals does not give a complete solution of Hilbert's problem, even fixing a value of the degree of the perturbation, n . But, it gives lower bounds for $\mathbf{H}(n)$ when it is applied to specific families of polynomial vector fields. For more details about the Hilbert's 16th problem we refer to [Ily02, Li03].

The problem that we consider in this work and we denote as $\mathcal{P}(n, k)$, is the study of the number of limit cycles, $\mathcal{H}(n, k)$, that bifurcate for ε small enough, from the system

$$\begin{cases} \dot{x} &= y K(x, y) + \varepsilon P(x, y), \\ \dot{y} &= -x K(x, y) + \varepsilon Q(x, y), \end{cases} \quad (1.6)$$

where P and Q are arbitrary real polynomials of degree n and $K(x, y)$ is a concrete polynomial. There are several papers where $K(x, y)$ is considered in different ways. In [LLLZ00, XH04a, XH04b] the set $\{K(x, y) = 0\}$ represents a straight line of simple or multiple singular points. In [BL07, LLLZ02, GL07], the problem when $K(x, y)$ are some concrete quadratic polynomials is considered. When the set $\{K(x, y) = 0\}$ represents a collection of straight lines orthogonal to the axes is studied in [GLT12].

In this chapter we take $K(x, y) = \prod_{j=1}^k ((x - a_j)^2 + (y - b_j)^2)$ where (a_j, b_j) are points of \mathbb{R}^2 . For simplicity, the zeros of $K(x, y)$ are referred as the singularities of system (1.6). As far as we know, the situation when the set $\{K(x, y) = 0\}$ is a set of isolated points and the perturbation is of degree n is only studied in [GPT08]. This last work can be considered as our starting point.

Most of the papers referenced previously study problems with a unique period annulus, the ones that contains the origin. In our problem, there are other period annuli and they are all nested. Our aim is to obtain the maximum number of limit cycles that bifurcate from the periodic orbits of all period annuli simultaneously, for a fixed collection of singularities. This can be considered as a continuation of the work [GPT08], where only the first period annulus is studied. In [GL07], among other general conics, the case of one singularity is also done for both period annuli, but only under cubic perturbations. Moreover, for some particular cases, we also study how this maximum number changes when we move the singularities.

There are not so many papers focused on the study of the simultaneous bifurcation of limit cycles for perturbed systems. Some of them are [GGJ08, CLP09] that deal with the simultaneity between two different regions, or [DL03] where three separated period annuli appear. A study of the simultaneity of limit cycles to obtain a lower bound

of $\mathbf{H}(n)$ is done in [CL95] and, more recently, in [Li03]. In our general case, when k singularities are considered, the problem presents $k + 1$ nested period annuli.

We should distinguish the general problem $\mathcal{P}(n, k)$, that studies the limit cycles in terms of the values n and k , from the one that, for a particular k , the location of the zeros of $K(x, y)$ are fixed, $\mathcal{P}_a(n)$.

When $K(x, y)$ does not vanish, after a time rescaling, system (1.6) is equivalent to

$$\begin{cases} \dot{x} &= y + \varepsilon \frac{P(x, y)}{K(x, y)}, \\ \dot{y} &= -x + \varepsilon \frac{Q(x, y)}{K(x, y)}. \end{cases} \quad (1.7)$$

The previous system corresponds to a rational perturbation of the linear center, and the level curves of the unperturbed system are given by the circles

$$\gamma_r = \{(x, y) \in \mathbb{R}^2 : x^2 + y^2 = r^2\}.$$

As we have showed before, the number of perturbed limit cycles that equation (1.7) can have up to a first order analysis, $\mathcal{H}(n, k)$, can be lower bounded by the number of simple zeros of the Abelian integral

$$I(r) = \oint_{\gamma_r} \frac{P(x, y)dy - Q(x, y)dx}{K(x, y)}. \quad (1.8)$$

In fact, this is the problem that we consider along this chapter: the study of the number of simultaneous zeros of $I(r)$ for

$$K(x, y) = \prod_{j=1}^k ((x - a_j)^2 + (y - b_j)^2) \quad (1.9)$$

where (a_j, b_j) are points of \mathbb{R}^2 . In most cases, we consider only the generic situation where these points are everyone different, isolated, nonaligned with the origin and $\tilde{r}_j = \sqrt{a_j^2 + b_j^2}$ does not vanish for $j = 1, \dots, k$. Since the different regions that we should consider are the annuli between consecutive zeros of $K(x, y)$, we suppose that these points are located at different distances from the origin. We do not consider the case $\tilde{r}_j = 0$ for any j because, as it can be easily checked, the number of zeros of the corresponding Abelian integral would have less zeros. As the associated Abelian integral is not well defined for any r , we restrict our results to the level curves, γ_r , completely contained in

$$\mathcal{R}_j = \{(x, y) \in \mathbb{R}^2 : \tilde{r}_j^2 = a_j^2 + b_j^2 < x^2 + y^2 < a_{j+1}^2 + b_{j+1}^2 = \tilde{r}_{j+1}^2\},$$

for $j = 0, \dots, k - 1$, $(a_0, b_0) = (0, 0)$ and $\mathcal{R}_k = \{(x, y) \in \mathbb{R}^2 : a_k^2 + b_k^2 < x^2 + y^2\}$. See Figure 1.2 for a particular configuration with three singularities. The above regions $\mathcal{R}_0, \dots, \mathcal{R}_3$ are also showed.

For the general case, we prove the following result.

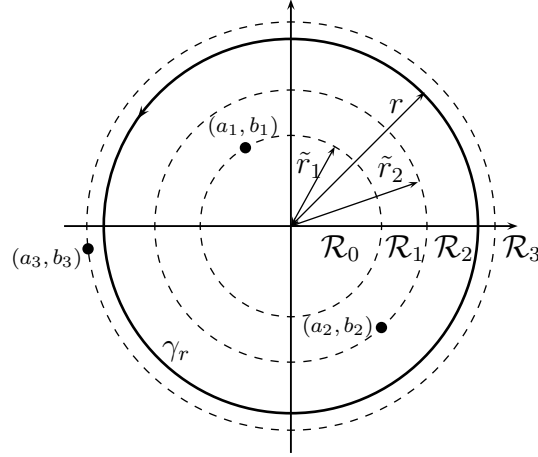


Figure 1.2 Example of location of the singularities (a_j, b_j) and the regions \mathcal{R}_j

Theorem 1.2. Let k and n be any pair of natural numbers. Given system

$$\begin{cases} \dot{x} = y K(x, y) + \varepsilon P(x, y), \\ \dot{y} = -x K(x, y) + \varepsilon Q(x, y), \end{cases} \quad (1.10)$$

where $K(x, y) = \prod_{j=1}^k ((x - a_j)^2 + (y - b_j)^2)$ and P and Q are polynomials of degree n .

Then the Abelian integral associated to system (1.10), $I(r)$ as it is defined in (1.8), is a piecewise rational function in r^2 . Moreover, the expression of $I(r)$ depends on the position of γ_r with respect to the period annuli \mathcal{R}_j , so we can identify I with the vector (I_0, \dots, I_k) where $I_j(r) = I(r)$ if $\gamma_r \subset \mathcal{R}_j$ for $j = 0, \dots, k$.

From this vectorial behavior of the Abelian integral, we can extend it to all the aspects of our problem. Hence, we consider the following definitions.

Definition 1.3. Fixed any natural number k and a collection of points (a_i, b_i) for $i = 1, \dots, k$, a vector $\mathcal{Z} = (z_0, \dots, z_k) \in \mathbb{N}^{k+1}$ is called a configuration of simultaneous zeros of $\mathcal{P}_a(n)$ if the Abelian integral $I(r)$ satisfies that $I_j(r)$ has exactly z_j zeros contained in J_j , for any $j = 0, \dots, k$.

Definition 1.4. Fixed any natural number k , a vector $\mathcal{Z} = (z_0, \dots, z_k) \in \mathbb{N}^{k+1}$ is called a configuration of simultaneous zeros of $\mathcal{P}(n, k)$ if there exists a collection of points (a_i, b_i) for $i = 1, \dots, k$ such that the Abelian integral $I(r)$ satisfies that $I_j(r)$ has exactly z_j zeros contained in J_j for any $j = 0, \dots, k$.

Since the set of configurations of $\mathcal{P}(n, k)$ is contained in the Cartesian product, \mathbb{N}^{k+1} , we can induce some structure on it. Consequently, we can define a partial order relation (known as the product order) and a norm (the norm of the sum) on the set of configurations.

Definition 1.5. Given \mathcal{Z}^1 and \mathcal{Z}^2 two configurations of simultaneous zeros of $\mathcal{P}(n, k)$, we say that $\mathcal{Z}^1 \leq \mathcal{Z}^2$ if $z_j^1 \leq z_j^2$ for any $j = 0, \dots, k$.

Definition 1.6. Given \mathcal{Z} a configuration of simultaneous zeros of $\mathcal{P}(n, k)$ or $\mathcal{P}_a(n)$, we define the norm of \mathcal{Z} as $|\mathcal{Z}| = z_0 + \dots + z_k$.

Remark 1.7. For each value of n , there is only one configuration of $\mathcal{P}_a(n)$, but for each n and k there is more than one configuration of $\mathcal{P}(n, k)$.

Since we have defined a partial order on the set of configurations of $\mathcal{P}(n, k)$, Theorem 1.2 provides the existence of an upper bound of this set. This can be done because the Abelian integral is obtained as a vector of rational functions. And it allows us to prove next result.

Corollary 1.8. There exists the maximum of the configurations of simultaneous zeros of $\mathcal{P}(n, k)$. We call it $\mathcal{Z}^M(n, k)$.

Additionally, as the set of configurations of $\mathcal{P}(n, k)$ is bounded, it should be finite. This fact proves the existence of maximal configurations of $\mathcal{P}(n, k)$.

Definition 1.9. A configuration \mathcal{Z} of $\mathcal{P}(n, k)$ is a maximal configuration if there not exist any other configuration of simultaneous zeros of $\mathcal{P}(n, k)$ greater than \mathcal{Z} .

Remark 1.10. The maximum configuration of $\mathcal{P}(n, k)$, $\mathcal{Z}^M(n, k)$, is unique, but the maximal configurations of $\mathcal{P}(n, k)$, in general, are not.

Although the expressions of the corresponding I_j are unique, the bounds that can be achieve on its degrees depend on the Partial Fraction Decomposition of $1/K(x, y)$, that is not unique. As we can see in this chapter it is not easy to achieve the exact value of $\mathcal{Z}^M(n, k)$ for all n and k and neither to give explicit upper bounds, i.e. $k + 1$ -tuples (z_0, z_1, \dots, z_k) so that $\mathcal{Z}_j \leq z_j$ for $j = 0, \dots, k$.

Proposition 1.11. Under the hypotheses of Theorem 1.2, we have

$$\mathcal{Z}^M(n, k) \leq (N, \dots, N, N - \min\{n + 1, (2k - 1)(k - 1)\}),$$

where $N = \left\lceil \frac{\max\{n + 1, (2k - 1)(k - 1)\}}{2} \right\rceil + n + 1 + (2k - 1)(k - 1)$. So,

$$|\mathcal{Z}^M(n, k)| \leq kn + (k + 3) \left\lceil \frac{\max\{n + 1, (2k - 1)(k - 1)\}}{2} \right\rceil + k(2k^2 - 3k + 2).$$

Where $\lceil \cdot \rceil$ is the integer part function.

For fixed values of k the above result can be improved. In this work we present better explicit values of upper bounds for $k = 1$ and $k = 2$.

Theorem 1.12. *Let $k = 1$. Under the conditions stated in Theorem 1.2 and denoting by $[\cdot]$ the integer part function, we get*

$$(i) \ n + [(n + 1)/2] \leq \mathcal{H}(n, 1), \text{ and,}$$

(ii) *given any $(i, j) \leq (n, [(n + 1)/2])$, there exist polynomials P, Q of degree n such that system (1.10) has at least i, j bifurcated limit cycles in $\mathcal{R}_0, \mathcal{R}_1$, respectively.*

Theorem 1.13. *Let $k = 2$. Under the assumptions of Theorem 1.2 and denoting by $[\cdot]$ the integer part function,, we have that*

$$\mathcal{Z}^M(n, 2) \leq \left(n + 4, n + 5, \left\lfloor \frac{n + 1}{2} \right\rfloor + 4 \right)$$

and $|\mathcal{Z}(n, 2)| \leq 2n + [(n + 1)/2] + 13$.

In particular, if $a_1/b_1 = a_2/b_2$ we have that

$$\mathcal{Z}^M(n, 2) \leq \left(n + 1, n + 2, \left\lfloor \frac{n + 1}{2} \right\rfloor + 1 \right)$$

and $|\mathcal{Z}(n, 2)| \leq 2n + [(n + 1)/2] + 4$.

Moreover, Theorem 1.12 generalizes the result of [GL07] for the case of two complex straight lines intersecting in a real point. We consider any value of n instead of a perturbation inside the cubic class.

Theorem 1.13 provides upper bounds of $\mathcal{Z}^M(n, 2)$. However for fixed values of n , the exact value can be computed. For example the maximum configuration of $\mathcal{P}(0, 2)$ and $\mathcal{P}(1, 2)$ are $\mathcal{Z}^M(0, 2) = (1, 1, 1)$ and $\mathcal{Z}^M(1, 2) = (3, 2, 3)$, respectively. But these maximums are not configurations of simultaneous zeros. In fact, we prove that there are no configurations with three zeros for $\mathcal{P}(0, 2)$ nor configurations with seven or eight zeros for $\mathcal{P}(1, 2)$. The following results summarize these facts.

Theorem 1.14. *For $\mathcal{P}(0, 2)$, the Abelian integral $I(r^2)$ can have at most two simple zeros. Moreover, its configurations are: $(0, 0, 0)$, $(1, 1, 0)$ and $(0, 1, 1)$ for every pair of points (a_i, b_i) , $i = 1, 2$.*

Theorem 1.15. *The maximum number of simple zeros of $\mathcal{P}(1, 2)$ is six. The maximal configurations are $(3, 1, 2)$, $(2, 2, 2)$ and $(2, 1, 3)$. Additionally, an element in \mathbb{N}^3 is a configuration if, and only if, it is lower or equal to any of the maximal ones.*

One question still unanswered is whether the maximal configurations of $\mathcal{P}(1, 2)$ are configurations, or not, for every pair of points (a_i, b_i) , $i = 1, 2$. In order to answer this question a bifurcation diagram should be constructed, distinguishing the regions where the maximum number of zeros of $I(r)$ changes. As the configurations with four zeros can be found for every particular choice of points, see Proposition 1.29, there should be just represented by the regions with four, five or six maximum zeros.

Before showing the results on the bifurcation diagram, let us assume the following hypothesis. The zeros of $K(x, y)$ are ordered because they are located at different

distances from the origin. Moreover, as the number of zeros of the Abelian integral does not depend on any rescaling or rotation with respect to the origin in the variables (x, y) in \mathbb{R}^2 . Then, without loss of generality, we can suppose, that $(a_1, b_1) = (1, 0)$. Hence, the bifurcation diagram can be represented in \mathbb{R}^2 , because the coordinates of the second singularity, (a_2, b_2) , are the free variables of this problem.

Hence the bifurcation diagram can be computed from any maximal configuration. Consider now the maximal configuration $(3, 1, 2)$ and fix any perturbation such that system (1.10) presents three zeros in the inner annulus and one in the middle one. Therefore, the bifurcation regions $\tilde{\mathcal{S}}_0$, $\tilde{\mathcal{S}}_1$ and $\tilde{\mathcal{S}}_2$, in (a_2, b_2) plane, are defined by the number of zeros of I in the outer annulus, that is 0, 1 and 2. Hence, the total number of zeros of I is 4, 5 and 6 for the maximal configuration $(3, 1, 2)$, or $(2, 1, 3)$, by symmetry. This regions are plotted in Figure 1.3.

The complete bifurcation diagram could be done doing a similar procedure for the case $(2, 2, 2)$. This global result exceeds the scope of this work due to the difficulties to obtain the diagram of Figure 1.3, as it can be seen in Section 1.4.2.

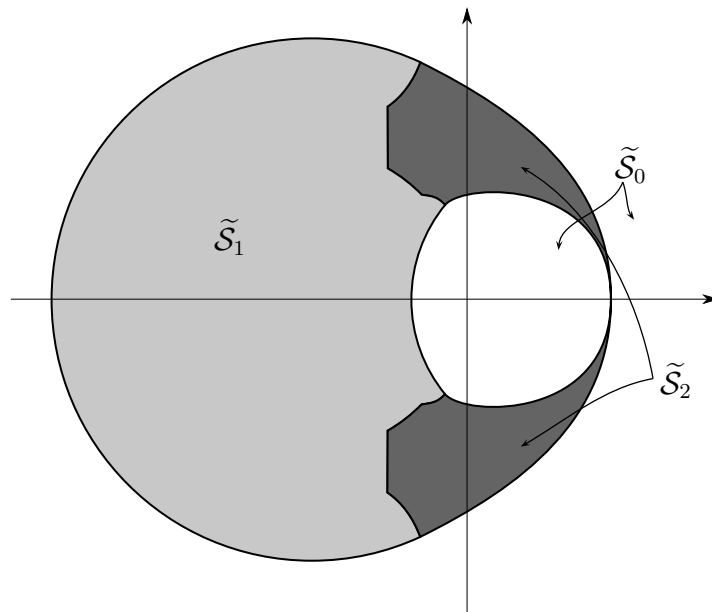


Figure 1.3 *Bifurcation diagram for the maximal $(3, 1, 2)$ configuration*

This chapter is organized as follows. In Section 1.2, we unfold the computations needed to found an expression of the Abelian integral, (1.8). We include also the proofs of Theorem 1.2 and Proposition 1.11. Section 1.3 is devoted to the study of the case of a unique singularity and the proof of Theorem 1.12. The case with two singularities is studied in Section 1.4. First, we provides the upper bound given in Theorem 1.13 and we improve this result for the first values of n , $n \leq 6$. Secondly, Theorems 1.14 and 1.15 are proved. Finally, the bifurcation diagram showed in Figure 1.3 is constructed.

1.2 General results for an arbitrary number of singularities

This section is devoted to prove the rationality of $I(r)$ and the general bounds of its number of zeros. Next technical lemma ensures that locating a singular point at $(1, 0)$, for example the closer to the origin, is not restrictive.

Lemma 1.16. *System (1.6) is invariant under dilations and rotations with the center at the origin*

Proof. Rotations and dilations are linear transformation of the space. So, they do not change the form of system (1.6) nor the degree of the polynomials. Moreover, the transformed system has also the inner structure of being a polynomial perturbation of a linear center multiplied by a function like $K(x, y)$ with the zeros located in other place, but with the same properties of the original one. \square

1.2.1 Computations of the Abelian Integrals

Although there is not a unique way to express $1/K(x, y)$, for K given in (1.9), as a sum of partial fractions, the following lemma gives us a possible decomposition for any value of k . In this section we show other rational decompositions of lower degrees, but only for small values of k .

Lemma 1.17. *For all k ,*

$$\frac{1}{\prod_{j=1}^k F_j(r, \cos t, \sin t)} = \sum_{j=1}^k \frac{A_j(r^2, r \cos t, r \sin t)}{D(r^2)F_j(r, \cos t, \sin t)},$$

where $F_j(r, \cos t, \sin t) = r^2 - 2a_j r \cos t - 2b_j r \sin t + a_j^2 + b_j^2$, A_j and D , for $j = 1, \dots, k$, are polynomials with degree $(2k - 1)(k - 1)$ and $2k(k - 1)$, respectively.

Proof. We consider the conjugate of each term in the denominator of the expression of the statement, i.e. the polynomial $G_j(r, \cos t, \sin t) = r^2 - 2a_j r \cos t + 2b_j r \sin t + a_j^2 + b_j^2$ for $j = 1, \dots, k$. Thus

$$\begin{aligned} F_j G_j &= 4(a_j^2 + b_j^2)r^2 \cos^2 t - 4a_j(a_j^2 + b_j^2 + r^2)r \cos t \\ &\quad + (r^2 + a_j^2 - 2rb_j + b_j^2)(r^2 + a_j^2 + 2rb_j + b_j^2). \end{aligned}$$

This polynomial, seen as a one variable polynomial respect to $r \cos t$, has a negative discriminant, $-16(a_j^2 + b_j^2 - r^2)^2 b_j^2 < 0$. Therefore, by the one variable Partial Fraction Decomposition Theorem, there exist polynomials, B_j , with degree one such that for any k ,

$$\left(\prod_{j=1}^k F_j G_j \right)^{-1} = \sum_{j=1}^k \frac{B_j(r \cos t)}{F_j G_j}.$$

In fact $B_j(r \cos t) = \rho_j(r^2)r \cos t + \xi_j(r^2)$, with ρ_j and ξ_j been rational functions. The expressions of ρ_j and ξ_j can be found solving a linear system with $2k$ equations and $2k$ variables. This system can be constructed from equation

$$1 = \sum_{i=1}^k \left(\prod_{\substack{j=1 \\ j \neq i}}^k F_j G_j \right) (\rho_i(r^2)r \cos t + \xi_i(r^2)).$$

We just study the degrees of the polynomials involved in the matrix of the system. Let us denote by Δ_l any non-fixed polynomial of degree l with respect to r^2 . Consequently the system can be written as

$$\begin{pmatrix} 0 & \cdots & 0 & \Delta_{2k-2} & \cdots & \Delta_{2k-2} \\ \Delta_{2k-2} & \cdots & \Delta_{2k-2} & \Delta_{2k-3} & \cdots & \Delta_{2k-3} \\ \vdots & \ddots & \vdots & \vdots & \ddots & \vdots \\ \Delta_1 & \cdots & \Delta_1 & \Delta_0 & \cdots & \Delta_0 \\ \Delta_0 & \cdots & \Delta_0 & 0 & \cdots & 0 \end{pmatrix} \begin{pmatrix} \rho_1 \\ \vdots \\ \rho_k \\ \theta_1 \\ \vdots \\ \theta_k \end{pmatrix} = \begin{pmatrix} 1 \\ 0 \\ \vdots \\ 0 \end{pmatrix}. \quad (1.11)$$

Therefore, by Cramer's Rule, the solutions ρ_j and θ_j , as products of one term for each different row and column of the previous matrix, have the following rational form

$$\rho_j = \frac{\Delta_{-k + \sum_1^{2(k-1)} l}}{\Delta_{k-1 + \sum_1^{2(k-1)} l}} = \frac{\Delta_{2(k-1)^2 - 1}}{\Delta_{2k(k-1)}}, \quad \text{and} \quad \theta_j = \frac{\Delta_{-(k-1) + \sum_1^{2(k-1)} l}}{\Delta_{k-1 + \sum_1^{2(k-1)} l}} = \frac{\Delta_{2(k-1)^2}}{\Delta_{2k(k-1)}},$$

both denominators are the same, the determinant of system (1.11).

Now we can consider

$$\frac{1}{\prod_{j=1}^k F_j} = \frac{\prod_{l=1}^k G_l}{\prod_{j=1}^k F_j G_j} = \sum_{j=1}^k \frac{B_j(\cos t) \prod_{l=1}^k G_l}{F_j G_j} = \sum_{j=1}^k \frac{B_j(\cos t) \prod_{\substack{l=1 \\ l \neq j}}^k G_l}{F_j}.$$

Hence we just need to take $A_j(r^2, r \cos t, r \sin t)$ as the numerator of $B_j(\cos t) \prod_{\substack{l=1 \\ l \neq j}}^k G_l$ and

$D(r^2)$ as the determinant of M , so D is a polynomial of degree $2k(k-1)$.

Additionally, by the definition of G_l ,

$$\prod_{\substack{l=1 \\ l \neq j}}^k G_l = \Delta_0(r^2) \Delta_{k-1}(r \cos t, r \sin t) + \cdots + \Delta_{k-2}(r^2) \Delta_1(r \cos t, r \sin t) + \Delta_{k-1}(r^2),$$

and it follows that

$$A_j = (\Delta_{2(k-1)^2-1}(r^2)r \cos t + \Delta_{2(k-1)^2}(r^2)) \prod_{\substack{l=1 \\ l \neq j}}^k G_l = \Delta_{(2k-1)(k-1)}(r^2, r \cos t, r \sin t).$$

This completes the proof. \square

Next lemma gives us another rational decomposition. It has lower degree than the one given in Lemma 1.17, for some particular values of k . In fact it seems to be true for any value of k (taking fixed values for the points (a_i, b_i)). But to obtain a proof for any k requires a deeper knowledge of the structure of the decomposition. In Section 1.4 we include the explicit expressions for case $k = 2$.

Lemma 1.18. *For all $k = 2, 3, 4$,*

$$\frac{1}{\prod_{j=1}^k F_j(r, \cos t, \sin t)} = \frac{A(r^2)}{D(r^2)} + \sum_{j=1}^k \frac{B_j(r^2)(r \cos t + 1) + C_j(r^2)r \sin t}{E_j(r^2)F_j(r, \cos t, \sin t)},$$

where $F_j(r, \cos t, \sin t) = r^2 - 2a_j r \cos t - 2b_j r \sin t + a_j^2 + b_j^2$ and A, B_j, C_j, D and E_j for $j = 1, \dots, k$ are polynomials of degrees $k(k-1), k-1, k-1, k^2$ and $2k-1$, respectively.

Proof. Straightforward computations with an algebraic manipulator¹ give as the sought expression. \square

In addition to the previous lemmas we need the following one. It is a generalization of [GPT08, Lemma 2.2]. Our proof is considered as a corollary of that one, instead of an adapted one. Our statement is given in terms of Chebyshev's polynomials, see more information about them in [Con65].

Lemma 1.19. *For all $l \in \mathbb{N}$, we have that*

$$\begin{aligned} I_l^c(r) &= \int_0^{2\pi} \frac{\cos(lt)}{r^2 + a^2 + b^2 - 2ar \cos t - 2br \sin t} dt \\ &= \begin{cases} \frac{2\pi}{(a^2 + b^2)^{l/2}} T_l \left(\frac{a}{\sqrt{a^2 + b^2}} \right) \frac{r^l}{a^2 + b^2 - r^2} & 0 \leq r < \sqrt{a^2 + b^2}, \\ 2\pi (a^2 + b^2)^{l/2} T_l \left(\frac{a}{\sqrt{a^2 + b^2}} \right) \frac{r^{-l}}{r^2 - (a^2 + b^2)} & r > \sqrt{a^2 + b^2}, \end{cases} \\ I_l^s(r) &= \int_0^{2\pi} \frac{\sin(lt)}{r^2 + a^2 + b^2 - 2ar \cos t - 2br \sin t} dt \\ &= \begin{cases} \frac{2\pi b}{(a^2 + b^2)^{(l+1)/2}} U_{l-1} \left(\frac{a}{\sqrt{a^2 + b^2}} \right) \frac{r^l}{a^2 + b^2 - r^2} & 0 \leq r < \sqrt{a^2 + b^2}, \\ 2\pi b (a^2 + b^2)^{(l-1)/2} U_{l-1} \left(\frac{a}{\sqrt{a^2 + b^2}} \right) \frac{r^{-l}}{r^2 - (a^2 + b^2)} & r > \sqrt{a^2 + b^2}, \end{cases} \end{aligned}$$

¹All the computations have been made using MAPLE.

where T_l and U_l are the Chebyshev's polynomials of first and second kind of degree l , respectively.

Proof. We consider the change $t = \tau + \theta$ taking the unique value of $\theta \in (0, 2\pi)$ such that $\sin \theta = b/\sqrt{a^2 + b^2}$ and $\cos \theta = a/\sqrt{a^2 + b^2}$, so

$$\begin{aligned} I_l^c(r) &= \int_0^{2\pi} \frac{\cos(l(\tau + \theta))}{r^2 + a^2 + b^2 - 2ar \cos(\tau + \theta) - 2br \sin(\tau + \theta)} d\tau \\ &= \int_0^{2\pi} \frac{\cos(l\tau) \cos(l\theta) - \sin(l\tau) \sin(l\theta)}{r^2 + a^2 + b^2 - 2r(a \cos \theta + b \sin \theta) \cos \tau - 2r(b \cos \theta - a \sin \theta) \sin \tau} d\tau \quad (1.12) \\ &= \int_0^{2\pi} \frac{\cos(l\theta) \cos(l\tau) - \sin(l\theta) \sin(l\tau)}{r^2 + a^2 + b^2 - 2r\sqrt{a^2 + b^2} \cos \tau} d\tau. \end{aligned}$$

The change of variable $r = \rho\sqrt{a^2 + b^2}$ transforms equation (1.12) to the form given on the hypothesis of [GPT08, Lemma 2.2]. Therefore,

$$\begin{aligned} I_l^c(r) &= \frac{\cos(l\theta)}{a^2 + b^2} \int_0^{2\pi} \frac{\cos(l\tau)}{\rho^2 + 1 - 2\rho \cos \tau} d\tau + \frac{\sin(l\theta)}{a^2 + b^2} \int_0^{2\pi} \frac{\sin(l\tau)}{\rho^2 + 1 - 2\rho \cos \tau} d\tau = \\ &= \begin{cases} 2\pi \frac{\cos(l\theta)}{a^2 + b^2} \frac{\rho^l}{1 - \rho^2} & 0 \leq \rho < 1, \\ 2\pi \frac{\cos(l\theta)}{a^2 + b^2} \frac{1}{(\rho^2 - 1)\rho^l} & \rho > 1, \end{cases} \end{aligned}$$

now, if we undo the change in r , we have that

$$I_l^c(r) = \begin{cases} 2\pi \frac{\cos(l\theta)}{a^2 + b^2 - r^2} \frac{r^l}{\sqrt{a^2 + b^2}^l} & 0 \leq r < \sqrt{a^2 + b^2}, \\ 2\pi \frac{\cos(l\theta)}{r^2 - (a^2 + b^2)} \frac{\sqrt{a^2 + b^2}^l}{r^l} & r > \sqrt{a^2 + b^2}. \end{cases}$$

By the definition of θ and the properties of the Chebyshev's polynomials T_l , see [Phi03], we obtain

$$\cos(l\theta) = T_l(\cos \theta) = T_l\left(\frac{a}{\sqrt{a^2 + b^2}}\right).$$

This gives us the expression of the statement of the lemma.

The proof finishes doing analogous computations for

$$I_l^s(r) = \begin{cases} 2\pi \frac{\sin(l\theta)}{a^2 + b^2 - r^2} \frac{r^l}{\sqrt{a^2 + b^2}^l} & 0 \leq r < \sqrt{a^2 + b^2}, \\ 2\pi \frac{\sin(l\theta)}{r^2 - (a^2 + b^2)} \frac{\sqrt{a^2 + b^2}^l}{r^l} & r > \sqrt{a^2 + b^2} \end{cases}$$

and

$$\sin(l\theta) = \sin \theta U_{l-1}(\cos \theta) = \frac{b}{\sqrt{a^2 + b^2}} U_{l-1}\left(\frac{a}{\sqrt{a^2 + b^2}}\right).$$

□

Now we have the tools to see the rationality of (1.8).

Proof of Theorem 1.2. After changing to polar coordinates and using usual trigonometric identities, the expression of $I(r)$ at (1.8) writes as

$$\begin{aligned} I(r) &= \int_0^{2\pi} \frac{Q(r \cos t, r \sin t) r \sin t + P(r \cos t, r \sin t) r \cos t}{\prod_{j=1}^k (r^2 - 2ra_j \cos t - 2rb_j \sin t + a_j^2 + b_j^2)} dt = \\ &= \sum_{m=1}^{n+1} r^m \int_0^{2\pi} \frac{\sum_{l=0}^m (\alpha_{lm} \cos(lt) + \beta_{lm} \sin(lt))}{\prod_{j=1}^k (r^2 - 2ra_j \cos t - 2rb_j \sin t + a_j^2 + b_j^2)} dt, \end{aligned} \quad (1.13)$$

where α_{lm} and β_{lm} are independent real coefficients such that if l and m are not of the same parity then $\alpha_{lm} = \beta_{lm} = 0$. Finally, ordering and gathering coefficients,

$$\begin{aligned} I(r) &= \sum_{l=0}^{n+1} r^l R_l(r^2) \int_0^{2\pi} \frac{\cos(lt)}{\prod_{j=1}^k (r^2 - 2ra_j \cos t - 2rb_j \sin t + a_j^2 + b_j^2)} dt \\ &+ \sum_{l=1}^{n+1} r^l S_l(r^2) \int_0^{2\pi} \frac{\sin(lt)}{\prod_{j=1}^k (r^2 - 2ra_j \cos t - 2rb_j \sin t + a_j^2 + b_j^2)} dt, \end{aligned} \quad (1.14)$$

where $R_l(r^2)$ and $S_l(r^2)$ are polynomials of degree at most $[(n+1-l)/2]$ with arbitrary coefficients for all $l = 0, \dots, n+1$.

Lemma 1.17 allows us to break up the rational functions in the integrand of (1.14) as a sum of more simple functions and Lemma 1.19 gives us an expression for the integral of each term. As everyone of those expressions is a rational piecewise function of r^2 , we can assure that the sum of them is also a rational piecewise function of r^2 . \square

1.2.2 Upper bounds for the number of zeros

$I(r)$ is a piecewise rational function. See Theorem 1.2. Then the number of its zeros is bounded. This section is devoted to prove Proposition 1.11 that provides an explicit bound studying the degree of the numerator.

Proof of Proposition 1.11. From the proof of Theorem 1.2, the numerator of $I(r)$ can be studied from the numerator of the integrand of (1.14), that is

$$R_0(r^2) + \sum_{l=1}^{n+1} r^l (R_l(r^2) \cos(lt) + S_l(r^2) \sin(lt)).$$

The numerators, that appear applying Lemma 1.17, are

$$A_j(r^2, r \cos t, r \sin t) = \sum_{i=0}^{\kappa} \sum_{m=i}^{\kappa} \alpha_{i,m}(r^2) r^m \cos^i t \sin^{m-i} t$$

for any $j = 1, \dots, k$, where $\kappa = (2k-1)(k-1)$ and $\alpha_{i,m}$ are polynomials of degree $\kappa - m$.

We can write $\cos(lt) \cos^i t \sin^{m-i} t$ as a real combination of the functions

$$\begin{aligned} & \cos((l+m)t), \cos((l+m-2)t), \cos((l+m-4)t), \dots \text{ if } m-i \text{ is even,} \\ & \sin((l+m)t), \sin((l+m-2)t), \sin((l+m-4)t), \dots \text{ if } m-i \text{ is odd,} \end{aligned}$$

and function $\sin(lt) \cos^i t \sin^{m-i} t$ as a real combination of

$$\begin{aligned} & \sin((l+m)t), \sin((l+m-2)t), \sin((l+m-4)t), \dots \text{ if } m-i \text{ is even,} \\ & \cos((l+m)t), \cos((l+m-2)t), \cos((l+m-4)t), \dots \text{ if } m-i \text{ is odd.} \end{aligned}$$

Therefore, the numerator of the integrand for any term in the Abelian integral can be written as

$$\tilde{R}_0(r^2) + \sum_{\lambda=1}^{n+1+\kappa} r^\lambda (\tilde{R}_\lambda(r^2) \cos(\lambda t) + \tilde{S}_\lambda(r^2) \sin(\lambda t)), \quad (1.15)$$

where $\tilde{R}_\lambda(r^2)$ and $\tilde{S}_\lambda(r^2)$ are polynomials of degree

$$\max \left\{ \left[\frac{n+1-l}{2} \right] + \kappa - m : \begin{array}{l} l = \max\{0, \lambda - \kappa\}, \dots, n+1 \\ m = \max\{0, \lambda - (n+1)\}, \dots, \kappa \end{array} \right\},$$

for any $\lambda = 0, \dots, n+1+\kappa$ and $[\cdot]$ denotes the integer part function. That is

$$\deg \tilde{R}_\lambda = \deg \tilde{S}_\lambda = \begin{cases} [(n+1)/2] + \kappa & \text{if } \lambda \leq \min\{n+1, \kappa\}, \\ [(n+1)/2] + \kappa - \lambda + n + 1 & \text{if } n+1 < \lambda \leq \kappa, \\ [(n+1+\kappa-\lambda)/2] + \kappa & \text{if } \kappa < \lambda \leq n+1, \\ [(n+1+\kappa-\lambda)/2] + \kappa - \lambda + n + 1 & \text{if } \max\{n+1, \kappa\} \leq \lambda. \end{cases}$$

Then, using (1.15), the degree of the numerator of the Abelian integral, $\hat{I}(r)$, depends on the region where r is considered. That is

$$\deg \hat{I}(r) = \begin{cases} \deg \hat{I}_j(r) = \max_{\lambda=0, \dots, n+1+\kappa} \{\deg \tilde{R}_\lambda + \lambda\}, & \text{if } r^2 < a_{j+1}^2 + b_{j+1}^2, j = 0, \dots, k-1, \\ \deg I_k(r) = \max_{\lambda=0, \dots, n+1+\kappa} \{\deg \tilde{R}_\lambda\}, & \text{if } r^2 > a_k^2 + b_k^2 \end{cases}$$

where $\hat{I}_j(r)$ denotes the numerator of $I_j(r)$ for $j = 0, \dots, k$. Hence,

$$\begin{aligned} \deg \hat{I}_j(r) = & 2 \max \left\{ \left[\frac{n+1}{2} \right] + \kappa + \min\{n+1, \kappa\}, \left[\frac{n+1}{2} \right] + \kappa, \left[\frac{\kappa}{2} \right] + \kappa + n + 1, \right. \\ & \left. \left[\frac{\max\{n+1, \kappa\}}{2} \right] + \kappa + n + 1 \right\} = 2 \left(\left[\frac{\max\{n+1, \kappa\}}{2} \right] + \kappa + n + 1 \right) \end{aligned}$$

for $j = 0, \dots, k - 1$ and

$$\begin{aligned} \deg \widehat{I}_k(r) &= 2 \max \left\{ \left[\frac{n+1}{2} \right] + \kappa, \left[\frac{\max\{n+1, \kappa\}}{2} \right] + \max\{n+1, \kappa\} \right\} \\ &= 2 \left(\left[\frac{\max\{n+1, \kappa\}}{2} \right] + \max\{n+1, \kappa\} \right). \end{aligned}$$

Finally, the total number of zeros, except the origin, is bounded by the sum of all the degrees. So, the bound is given by

$$\begin{aligned} |\mathcal{Z}(n, k)| &\leq k(n+1+\kappa) + (k+1) [\max\{n+1, \kappa\}/2] + \max\{n+1, \kappa\} - 1 \\ &\leq kn + (k+3) [\max\{n+1, \kappa\}/2] + k(2k^2 - 3k + 2). \end{aligned}$$

□

1.3 The case of one singularity

The aim of this section is to prove the bound, given in Theorem 1.12, for the number of zeros of the Abelian integral when we have only one singularity.

Proposition 1.20. *When $k = 1$, the singularity of system (1.10) is located at $(1, 0)$ and the function $I(r)$, defined in (1.8), is the piecewise rational function*

$$I(r) = \begin{cases} 2\pi \frac{r^2}{1-r^2} \Phi(r^2) & \text{if } 0 < r < 1, \\ 2\pi \frac{1}{1-r^2} \Psi(r^2) & \text{if } 1 < r, \end{cases} \quad (1.16)$$

where Φ and Ψ are polynomials of degree less or equal to n and $[(n+1)/2]$, respectively. So, $|\mathcal{Z}^M(n, 1)| \leq n + [(n+1)/2]$. $[\cdot]$ denotes the integer part function.

Proof. Lemma 1.16 allows us to prove that the singularity is located at $(1, 0)$.

Fixed P and Q in (1.6) we have

$$I(r) = \int_0^{2\pi} \frac{Q(r \cos t, r \sin t) r \sin t + P(r \cos t, r \sin t) r \cos t}{r^2 - 2r \cos t + 1} dt.$$

Following the procedure in the proof of Theorem 1.2, $I(r)$ can be written as

$$I(r) = \sum_{l=0}^{n+1} r^l R_l(r^2) \int_0^{2\pi} \frac{\cos(lt)}{r^2 - 2r \cos t + 1} dt + \sum_{l=1}^{n+1} r^l S_l(r^2) \int_0^{2\pi} \frac{\sin(lt)}{r^2 - 2r \cos t + 1} dt.$$

By Lemma 1.19, the terms corresponding to the second addition vanish. Then, we only need to consider the first one taking into account the relative position of the point $(1, 0)$ and the curve γ_r . When $0 < r < 1$ we have

$$I(r) = I_0(r) = 2\pi \frac{1}{1-r^2} \sum_{l=0}^{n+1} r^{2l} R_l(r^2) = 2\pi \frac{r^2}{1-r^2} \Phi(r^2)$$

where

$$\Phi(s) = \sum_{l=0}^{n+1} s^{l-1} R_l(s) = \sum_{i=0}^n \phi_i s^i. \quad (1.17)$$

and, when $1 < r$,

$$I(r) = I_1(r) = 2\pi \frac{1}{r^2 - 1} \sum_{l=0}^{n+1} R_l(r^2) = 2\pi \frac{1}{1 - r^2} \Psi(r^2)$$

where

$$\Psi(s) = - \sum_{l=0}^{n+1} R_l(s) = \sum_{j=0}^{[(n+1)/2]} \psi_j s^j. \quad (1.18)$$

Moreover, the coefficients $\{\phi_i\}$ and $\{\psi_i\}$ are linear combinations of the coefficients $\{\alpha_{l,m}\}$ given by (1.13) in the proof of Theorem 1.2. \square

Proposition 1.21. *Fixed n in \mathbb{N} . If $k = 1$, given i and j such that $i \leq n$ and $j \leq [(n+1)/2]$ and given $x_1, \dots, x_i \in J_0 = (0, 1)$, $x_{i+1}, \dots, x_n \notin J_0$, $y_1, \dots, y_j \in J_1 = (1, \infty)$ and $y_{j+1}, \dots, y_{[(n+1)/2]} \notin J_1$ then there exist P and Q of degree n such that $I(r)$, defined in (1.8), has exactly i zeros in J_0 located on $\{x_k\}$ and j zeros in J_1 located on $\{y_l\}$.*

Proof. When $n = 0$, Φ and Ψ are constants. Hence there are no isolated zeros and the statement is proved.

For the other cases, $n \geq 1$, we can choose P and Q , from the proof of Theorem 1.2, such that the values of $\{\alpha_{l,m}\}$ are arbitrary. Then the proof follows showing that the polynomials $\Phi(s)$ and $\Psi(s)$, from (1.17) and (1.18), have exactly the configuration of zeros given in the statement. The main problem is that, from expressions (1.17) and (1.18), it can be checked that

$$\Phi(1) + \Psi(1) = 0 \quad (1.19)$$

and, consequently, the values of $\{\phi_i\}$ and $\{\psi_i\}$ are not independent. We apply this relation in the coefficient of the leading term of Ψ , so

$$\psi_{[(n+1)/2]} = - \sum_{i=0}^n \phi_i - \sum_{j=0}^{[(n+1)/2]-1} \psi_j.$$

First we show, when n is even, that the coefficients $\{\alpha_{l,m}\}$ can be given in terms of $\{\phi_i\}$ and $\{\psi_j\}$. When n is odd follows similarly. The system given by the expressions of $\{\phi_i\}$ and $\{\psi_j\}$ with respect to $\{\alpha_{l,m}\}$, (1.13), is solvable if we take out one equation. In fact, if we eliminate the equation relative to the expression of $\psi_{[(n+1)/2]}$, the solution

$\{\alpha_{l,m}\}$ can be written as

$$\alpha_{l,m} = \begin{cases} \sum_{i=0}^{m/2-1} (\phi_i + \phi_{n-i}) + \sum_{j=0}^{m/2-1} \psi_j & \text{if } l = 0, m = 2, 4, \dots, n, \\ -\phi_n - \psi_0 & \text{if } l = 1, m = 1, \\ -\sum_{i=0}^{(m+1)/2-2} \phi_i - \sum_{i=0}^{(m+1)/2-1} \phi_{n-i} - \sum_{j=0}^{(m+1)/2-1} \psi_j & \text{if } l = 1, m = 3, 5, \dots, n-1, \\ \phi_{n/2+(l-1)/2} & \text{if } l = 1, 3, \dots, n+1, m = n+1 \\ 0 & \text{in other cases.} \end{cases} \quad (1.20)$$

Second, we compute the values $\{\phi_i\}$ and $\{\psi_j\}$ for a fixed choice of the corresponding zeros, taking into account the relation (1.19). Given $x_i \neq 1$, $i = 1, \dots, n$ and $y_j \neq 1$, $j = 1, \dots, [(n+1)/2]$, there exists a unique collection of numbers, $\tilde{\phi}_i$ for $i = 0, \dots, n-1$ and $\tilde{\psi}_j$ for $j = 0, \dots, [(n+1)/2] - 1$, such that $s^n + \sum_{i=0}^{n-1} \tilde{\phi}_i s^i = \prod_{i=0}^{n-1} (s - x_i) := \tilde{\Phi}(s)$ and $s^{[(n+1)/2]} + \sum_{j=0}^{[(n+1)/2]-1} \tilde{\psi}_j s^j = \prod_{j=0}^{[(n+1)/2]-1} (s - y_j) := \tilde{\Psi}(s)$ with $\tilde{\Phi}(1) \neq 0$ and $\tilde{\Psi}(1) \neq 0$.

Then fixing $\phi_n = 1$ and $\psi_{[(n+1)/2]} = -\tilde{\Phi}(1)/\tilde{\Psi}(1)$ we can define $\Phi(s) = \phi_n \tilde{\Phi}(s)$ and $\Psi(s) = \psi_n \tilde{\Psi}(s)$. These two functions satisfy the condition (1.19) and the solution (1.20) provides the existence of a perturbation where the functions $\Phi(s)$ and $\Psi(s)$ defined in (1.16) are done. Due to the arbitrariness of choosing the zeros, x_i and y_j , the proof is finished. \square

Finally, we conclude this section with the proof of Theorem 1.12.

Proof of Theorem 1.12. Propositions 1.20 and 1.21 allow us to choose the perturbation in (1.6) that has an associated Abelian integral with a fixed configuration of simple zeros. So, see [Pon34], there exist perturbations with at least any configuration of limit cycles less or equal than $(n, [(n+1)/2])$. \square

1.4 The case of two singularities

The rationality of $I(r)$ guarantees a solution for the problem $\mathcal{P}(n, k)$. But the solution can not be optimal because an example with such quantity of zeros can not be obtained. We present, in this section, some optimal bounds for $k = 2$ and small values of n . The cases $n \leq 6$ are studied with more detail. The computations that are needed, for larger values of n , exceed the capacity of our computers.

1.4.1 An explicit bound for the maximum configuration

Theorem 1.2 provides, using that function $I(r)$ is piecewise rational, the existence of a maximum configuration. Although the proof is constructive, it does not give the lowest

value for the degree of functions I_j . So just if we fix concrete values of k , explicit lower upper bounds of these degrees can be obtained. This section deals with the case $k = 2$, where Theorem 1.13 gets a better upper bound of $\mathcal{Z}^M(n, 2)$. Before to prove Theorem 1.13, we introduce some technical results. Lemma 1.23 gives a better rational decomposition than Lemma 1.17. And Proposition 1.24 provides an explicit expression for $I(r)$. Therefore, we can study the degrees of the numerator of $I(r)$ in each interval J_l for $l = 0, 1, 2$, defined in the introduction.

As Lemma 1.16, next result transforms (1.6) into another one which simplifies the computations.

Lemma 1.22. *Given system (1.6),*

$$\begin{cases} \dot{x} &= y K(x, y) + \varepsilon P(x, y), \\ \dot{y} &= -x K(x, y) + \varepsilon Q(x, y), \end{cases} \quad (1.21)$$

where $K(x, y) = \prod_{j=1}^2 ((x - a_j)^2 + (y - b_j)^2)$ and P and Q are polynomials of degree n . And such that (a_1, b_1) , (a_2, b_2) and the origin are not collinear, equivalently $a_1/b_1 \neq a_2/b_2$. Then, there exists a change of variables, in fact a rotation centered at the origin, that restricts the study of (1.21) to the case $a_1 = a_2 = a > 0$. Moreover, the value $a_j^2 + b_j^2$ remains unchanged.

Proof. Let us consider that the change of variable (\tilde{x}, \tilde{y}) is a rotation, in the plane (x, y) , with respect to the origin of angle $\theta = \arctan((a_1 - a_2)/(b_1 - b_2))$. As it is a linear transformation it does not modify the structure of the system, nor the degree of the perturbation (P, Q) . More concretely, the singularities are located at $(\tilde{a}_1, \tilde{b}_1)$ and $(\tilde{a}_2, \tilde{b}_2)$ with

$$\tilde{a}_1 = \tilde{a}_2 = \tilde{a} = \text{sign}(b_1 - b_2) \frac{-b_1 a_2 + a_1 b_2}{\sqrt{(a_1 - a_2)^2 + (b_1 - b_2)^2}}.$$

If \tilde{a} is negative then we make a rotation of angle $\theta + \pi$ instead of θ . □

The following lemma gives us a decomposition with addends of degree one, for $k = 2$. It is proved just for the case $a_1 = a_2 > 0$, but with this structure can be found a decomposition's result less restrictive.

Lemma 1.23. *Under the hypothesis of Theorem 1.2 for $k = 2$ assuming that $a_1 = a_2 = a > 0$ and $b_1 \neq b_2$ we have that:*

$$\frac{1}{\prod_{j=1}^2 F_j(r, \cos t, r \sin t)} = A(r^2) + \sum_{j=1}^2 \frac{B_j(r^2)(r \cos t + 1) + C_j(r^2)r \sin t}{F_j(r, \cos t, r \sin t)}, \quad (1.22)$$

where

$$\begin{aligned}
A(r^2) &= \frac{r^4 + 2(a^2 - b_1 b_2)r^2 + (a^2 + b_1^2)(a^2 + b_2^2) - 4a^2}{D_1(r^2)D_2(r^2)E(r^2)}, \\
B_1(r^2) &= \frac{4ar^2 + 2a(a^2 + b_1^2)(b_1 - b_2)}{(b_1 - b_2)D_1(r^2)E(r^2)}, \\
B_2(r^2) &= \frac{-4ar^2 + 2(a^2 + b_2^2)(b_1 - b_2)}{(b_1 - b_2)D_2(r^2)E(r^2)}, \\
C_1(r^2) &= \frac{-2(a^2 - b_1^2)r^2 + 2(a^2 + b_1^2)(a^2 + 2a + b_1 b_2)}{(b_1 - b_2)D_1(r^2)E(r^2)}, \\
C_2(r^2) &= \frac{2(a^2 - b_2^2)r^2 + 2(a^2 + b_2^2)(a^2 + 2a + b_1 b_2)}{(b_1 - b_2)D_2(r^2)E(r^2)}, \\
D_j(r^2) &= r^2 + a^2 + 2a + b_j^2, \\
E(r^2) &= r^4 - 2(a^2 + b_1 b_2)r^2 + (a^2 + b_1^2)(a^2 + b_2^2), \\
F_j(r, \cos t, r \sin t) &= r^2 - 2ar \cos t - 2b_j r \sin t + a^2 + b_j^2,
\end{aligned}$$

for $j = 1, 2$.

Proof. The numerator of equation (1.22) can be written as

$$\eta_0 + \eta_1 r \cos t + \eta_2 r \sin t + \eta_3 r^2 \cos(2t) + \eta_4 r^2 \sin(2t) = 1,$$

and the system of equations $\{\eta_0 = 1, \eta_1 = \eta_2 = \eta_3 = \eta_4 = 0\}$ takes the form

$$M \begin{pmatrix} A \\ B_1 \\ B_2 \\ C_1 \\ C_2 \end{pmatrix} = \begin{pmatrix} 1 \\ 0 \\ 0 \\ 0 \\ 0 \end{pmatrix}, \quad (1.23)$$

where M is the matrix of the corresponding linear system. The determinant of M ,

$$\det(M) = - (4a^2 + (b_1 + b_2)^2) D_1(r^2) D_2(r^2) E(r^2),$$

does not vanish because, for $r \in \mathbb{R}$, none of the bi-quadratic factors do. This is due to the fact that the discriminant of $\det(M)$, considered as a polynomial in r^2 , is $-4a^2(b_2 - b_1)^2$, which is negative for any value of the parameters under the hypothesis of the statement. The factors in r^2 vanish only when $r^2 = -(a^2 + b_j^2 + 2a) < 0$, which is impossible for $r \in \mathbb{R}$.

The values of A , B_j , C_j , D_j and E , for $j = 1, 2$, come from solving equation (1.23). \square

Proposition 1.24. *Let A, D_j, E be the functions defined in Lemma 1.23. Under the same hypotheses of this lemma, the Abelian integral $I(r)$ writes as*

$$I(r) = 2\pi A(r^2)R_0(r^2) + 2\pi \sum_{j=1}^2 \sum_{l=0}^{n+2} \frac{\phi_{j,l}(r^2)r^{l(1+(-1)^{\delta_j})}}{(-1)^{\delta_j}(a^2 + b_j^2 - r^2)}, \quad (1.24)$$

where $\delta_j = \begin{cases} 0 & \text{if } r^2 < a^2 + b_j^2 \\ 1 & \text{if } r^2 > a^2 + b_j^2 \end{cases}$, $l = 0, \dots, n+2$ for $j = 1, 2$. Moreover, if $s = r^2$, $R_0(s)$ is a polynomial of degree $[(n+1)/2]$ and $\phi_{j,l}(s)$ are rational functions that depend on a, b_1, b_2 and n . The numerator of any $\phi_{j,l}$ has lower or equal degree to $2 + [(n-l)/2]$ and the denominator is the polynomial $D_j(s)E(s)$, which has degree 3, for $j = 1, 2$ and $l = 0, \dots, n+2$.

Proof. The expression of the Abelian integral, from the proof of Theorem 1.2, is given by (1.14). Hence, using Lemma 1.23, we have

$$\begin{aligned} I(r) &= \sum_{l=0}^{n+1} r^l A(r) \left(R_l(r^2) \int_0^{2\pi} \cos(lt) dt + S_l(r^2) \int_0^{2\pi} \sin(lt) dt \right) \\ &+ \sum_{j=1}^2 \sum_{l=0}^{n+2} r^l \left[B_j(r^2) \left(R_l(r^2) + \frac{r^2}{2} R_{l+1}(r^2) + \frac{1}{2} R_{l-1}(r^2) \right) \right. \\ &\quad \left. + C_j(r^2) \left(\frac{r^2}{2} S_{l+1}(r^2) - \frac{1}{2} S_{l-1}(r^2) \right) \right] \int_0^{2\pi} \frac{\cos(lt)}{F_j(r, \cos t, \sin t)} dt \\ &+ \sum_{j=1}^2 \sum_{l=0}^{n+2} r^l \left[B_j(r^2) \left(S_l(r^2) + \frac{r^2}{2} S_{l+1}(r^2) + \frac{1}{2} S_{l-1}(r^2) \right) \right. \\ &\quad \left. + C_j(r^2) \left(-\frac{r^2}{2} R_{l+1}(r^2) + \frac{1}{2} R_{l-1}(r^2) \right) \right] \int_0^{2\pi} \frac{\sin(lt)}{F_j(r, \cos t, \sin t)} dt, \end{aligned}$$

where $F_j(r, \cos t, \sin t) = r^2 - 2ar \cos t - 2b_j r \sin t + a^2 + b_j^2$ and $R_l(r^2)$ and $S_l(r^2)$ are polynomials of degree at most $[(n+1-l)/2]$ with arbitrary coefficients for all $l = 0, \dots, n+1$, see (1.14). For simplicity we have denoted $R_{-1} = S_{-1} = S_0 = R_{n+2} = S_{n+2} = R_{n+3} = S_{n+3} = 0$.

Finally, the expression given in the statement follows, using also that $\int_0^{2\pi} \cos(lt) dt = 0$ for $l > 0$ and $\int_0^{2\pi} \sin(lt) dt = 0$ for $l \geq 0$, replacing the integrals in the previous formula for I with the corresponding expressions of $I_l^c(r)$ and $I_l^s(r)$ given in Lemma 1.19. Additionally, straightforward computations show that the numerators of $\phi_{j,l}$ are polynomials in r^2 of degree lower or equal to

$$1 + \max \left(\left\lceil \frac{n+1-l}{2} \right\rceil, 1 + \left\lceil \frac{n+1-(l+1)}{2} \right\rceil, \left\lceil \frac{n+1-(l-1)}{2} \right\rceil \right) = 2 + \left\lceil \frac{n-l}{2} \right\rceil.$$

□

Proof of Theorem 1.13. For $k = 2$ there are three regions to study, J_j for $j = 0, 1, 2$. See the introduction for the definition of J_j . Moreover, we distinguish two cases: when the singularities (a_j, b_j) are collinear with the origin and when they are not.

First we study the non collinear case. From Lemma 1.22, as in the previous proofs, we assume $a_1 = a_2 = a$ and we apply Proposition 1.24, which provides explicit expressions for I in each region.

In the first region $r \in J_0$, that is $r^2 < a^2 + b_1^2 < a^2 + b_2^2$, we apply Proposition 1.24 with $\delta_j = 0$ for $j = 1, 2$. Then the Abelian integral (1.24) writes as

$$I(r) = I_0(r) = 2\pi A(r)R_0(r) + 2\pi \sum_{j=1}^2 \sum_{l=0}^{n+2} \frac{\phi_{j,l}(r^2)r^{2l}}{a^2 + b_j^2 - r^2},$$

where the degree of the numerator of $I_0(r)$ is lower or equal to

$$2 \left(\max_{l=0, \dots, n+2} \left(2 + \left\lfloor \frac{n+1}{2} \right\rfloor + 2, l + 2 + \left\lfloor \frac{n-l}{2} \right\rfloor + 2 \right) \right) = 2(n+5).$$

Furthermore, $I(r)$ is a function of r^2 and from the expression of $I(r)$ in polar coordinates, (1.13), it can be checked that $I_0(0) = 0$. So, in fact, $\mathcal{Z}_0(n, 2) \leq n + 4$.

Doing the same procedure for the second region $r \in J_1$, $a^2 + b_1^2 < r^2 < a^2 + b_2^2$, (1.24) writes as

$$I(r) = I_1(r) = 2\pi A(r^2)R_0(r^2) + 2\pi \sum_{l=0}^{n+2} \frac{\phi_{1,l}(r^2)}{r^2 - (a^2 + b_1^2)} + 2\pi \sum_{l=0}^{n+2} \frac{\phi_{2,l}(r^2)r^{2l}}{a^2 + b_2^2 - r^2},$$

and the degree of the numerator of $I_1(r)$ is lower or equal to

$$2 \left(\max_{l=0, \dots, n+2} \left(2 + \left\lfloor \frac{n+1}{2} \right\rfloor + 2, l + 2 + \left\lfloor \frac{n-l}{2} \right\rfloor + 2 \right) \right) = 2(n+5).$$

Hence $\mathcal{Z}_1(n, 2) \leq n + 5$.

As in the above cases, for the last region $r \in J_2$, $a^2 + b_1^2 < a^2 + b_2^2 < r^2$, we have that

$$I(r) = I_2(r) = 2\pi A(r^2)R_0(r^2) + 2\pi \sum_{j=1}^2 \sum_{l=0}^{n+2} \frac{\phi_{j,l}(r^2)}{r^2 - (a^2 + b_j^2)}.$$

The proof for this case finishes showing that the degree of the numerator of $I_2(r)$ is lower or equal to

$$2 \left(\max_{l=0, \dots, n+2} \left(2 + \left\lfloor \frac{n+1}{2} \right\rfloor + 2, 2 + \left\lfloor \frac{n-l}{2} \right\rfloor + 2 \right) \right) = 2 \left(\left\lfloor \frac{n+1}{2} \right\rfloor + 4 \right).$$

Therefore we have that $\mathcal{Z}_2(n, 2) \leq [(n+1)/2] + 4$.

The collinear case, $a_1/b_1 = a_2/b_2$, follows similarly but using the decomposition introduced in [GPT08]. Straightforward computations show that I_j are functions of r^2 and the degrees of the corresponding numerators are bounded by $2(n+1)$, $2(n+2)$ and $2[(n+1)/2] + 1$, for $j = 0, 1, 2$. \square

Improvements of upper bounds when $n \leq 6$ and $k = 2$

It is clear that the expression of $I(r)$ is unique, although the differences given by the decompositions in Lemmas 1.17 and 1.23 can mislead us of this fact. For concrete values of n and k , straightforward computations² show that the bounds provided by Theorem 1.13 are larger than the explicit ones obtained by direct calculations. These differences are due to some simplifications that appear during the procedure to obtain $I(r)$. Therefore, this phenomenon is still an open question.

Proposition 1.25. *Table 1.1 summarizes the values of the maximum configuration for $k = 2$ and $n \leq 6$.*

n	$\mathcal{Z}^M=(\mathcal{Z}_0, \mathcal{Z}_1, \mathcal{Z}_2)$	$ \mathcal{Z}^M $	$\tilde{\mathcal{Z}}$
0	(1,1,1)	3	13
1	(3,2,3)	8	16
2	(4,3,3)	10	18
3	(5,4,4)	13	21
4	(6,5,4)	15	23
5	(7,6,5)	18	26
6	(8,7,5)	20	28

Table 1.1: Degree of the numerators of I in each region. $\tilde{\mathcal{Z}}$ shows the value given by Theorem 1.13

The computations involved in obtaining the values of Table 1.1 are not difficult but the memory requirements are too high. In fact our computers needed some hours to obtain the explicit expressions for $n = 5$ and over a week for $n = 6$. Hence other techniques should be developed to obtain them for higher values of n . Extrapolating the exact values of Table 1.1 for $n \geq 1$ we have

$$\mathcal{Z}^M(n, 2) \leq \left(n + 2, n + 1, \left\lfloor \frac{n + 1}{2} \right\rfloor + 2 \right)$$

and so

$$|\mathcal{Z}^M(n, 2)| \leq 2n + \left\lfloor \frac{n + 1}{2} \right\rfloor + 5.$$

This values match with the ones given in Table 1.1 for $n \leq 6$. Next section presents also the explicit expressions for I for the values $n = 0$ and $n = 1$.

1.4.2 Configurations of simultaneous zeros

In this section we see that, in general, there is no perturbation nor singular points such that the configuration of zeros is the maximum one. Therefore the maximality of the

²All the computations of this section have been done with MAPLE.

total number of zeros of $I(r^2)$ is a simultaneity problem of zeros and the three different period annulus should be studied all together. The main difficulty is studying the different functions in the same parameter space defined in fixed but different domains.

As we have already mention in the introduction, and for simplicity, we restrict our analysis to the case

$$(a_1, b_1) = (1, 0) \quad \text{and} \quad (a_2, b_2) = (a, b), \quad \text{with} \quad a^2 + b^2 \geq 1.$$

Let n be the degree of the perturbation (P, Q) in (1.6). The explicit expression of the Abelian integral I given by (1.9) can be explicitly obtained in terms of the coefficients of P and Q . From the results and the notation of this chapter, I is defined by the three functions $I_0(r^2)$, $I_1(r^2)$ and $I_2(r^2)$. Hence the problem reads as: *For any n , given a point in the plane (a, b) , which is the maximum number of simultaneous zeros of I_j in J_j for $j = 0, 1, 2$?* This section provides a detailed presentation of our results for $n = 0$ and $n = 1$.

Configurations for degree zero perturbations

In the previous section we conclude that $\mathcal{Z}^M(0, 2) = (1, 1, 1)$. Hence we can prove the result which gives the configurations of zeros for the Abelian integral for $n = 0$.

Proof of Theorem 1.14. Let $P(x, y) = p_0$ and $Q(x, y) = q_0$ be the perturbation functions given in (1.6) for $n = 0$. In this case following the procedure and notation described in Section 1.2 we obtain I , from (1.8),

$$\begin{aligned} I_0(r^2) &= 2\pi \frac{r^2 ((a\alpha + b\beta + \alpha)r^2 - b\beta - a\alpha - b^2\alpha - a^2\alpha)}{(a^2 + b^2 - r^2) ((r^2 - a)^2 + b^2) (r^2 - 1)}, \\ I_1(r^2) &= 2\pi \frac{(a\alpha + b\beta - \alpha)r^2 - b\beta - a\alpha + b^2\alpha + a^2\alpha}{(a^2 + b^2 - r^2) ((a - 1)^2 + b^2) (r^2 - 1)}, \\ I_2(r^2) &= -I_0(r^2). \end{aligned} \tag{1.25}$$

Each I_j , $0, 1, 2$ is defined in the intervals $(0, 1)$, $(1, \sqrt{a^2 + b^2})$ and $(\sqrt{a^2 + b^2}, \infty)$, respectively. α and β are independent combinations of p_0 and q_0 , so they can be considered as the parameters of this problem. In fact, in this case $\alpha = p_0$ and $\beta = q_0$. Hence, the simple zeros different from the origin are given from the respective numerators. That is, from three polynomials of degree one in r^2 , denoted by \widehat{I}_j for each $j = 0, 1, 2$, which depend on a, b, α, β .

Finally, we show which are the possible configurations less or equal to the maximum, $(1, 1, 1)$.

From (1.25), I_0 and I_2 have exactly the same zeros. Hence the configuration $(1, 1, 1)$ can not be done, because \widehat{I}_0 and \widehat{I}_2 can not have simultaneously one zero in $(0, 1)$ and another one in $(\sqrt{a^2 + b^2}, \infty)$. So, $I(r^2)$ have, at most, two simple zeros.

Let us denote by x_0 the zero of \widehat{I}_0 . Then we have the condition

$$(a\alpha + b\beta + \alpha)x_0 - b\beta - a\alpha - b^2\alpha - a^2\alpha = 0.$$

Solving the previous expression in terms of α/β we have that

$$\frac{\alpha}{\beta} = \frac{b(-1 + x_0)}{-a - b^2 - a^2 + x_0 + ax_0}.$$

Then, the following properties hold

$$\begin{aligned}\widehat{I}_0(0) &= -x_0\omega, \\ \widehat{I}_0(1) &= (1 - x_0)\omega, \\ \widehat{I}_1(1) &= (1 - x_0)\omega, \\ \widehat{I}_1(\sqrt{a^2 + b^2}) &= (x_0 - (a^2 + b^2))\omega, \\ \widehat{I}_2(\sqrt{a^2 + b^2}) &= (x_0 - (a^2 + b^2))\omega, \\ \widehat{I}_2(\infty) &= \text{sign}(-\omega)\omega,\end{aligned}$$

where $\omega = b\beta(a^2 + b^2 - 1)/(a + b^2 + a^2 - x_0 - ax_0)$. The proof ends studying the sign of the above expressions in terms of x_0 . When x_0 is in $(0, 1)$ or in $(\sqrt{a^2 + b^2}, \infty)$, \widehat{I}_1 has a zero in $(1, \sqrt{a^2 + b^2})$. But when x_0 is in $[1, \sqrt{a^2 + b^2}]$ then \widehat{I}_1 has no zeros in $(1, \sqrt{a^2 + b^2})$. These last assertions prove that the only possible configurations are $(1, 1, 0)$, $(0, 1, 1)$ and $(0, 0, 0)$. \square

Configurations for degree one perturbations

The configurations in Theorem 1.15 are obtained looking for fixed values of (a, b) and specific perturbations for each of them. This section deals with all possible configurations less than the maximum $(3, 2, 3)$, given in Section 1.4, for degree one perturbations. A different problem is, for a fixed configuration, which are all the points (a, b) such that this configuration is obtained studying all the possible perturbations of fixed degree. Section 1.4.3 studies this last problem for the configurations $(3, 1, 2)$. However it is necessary to obtain beforehand some results for some lower configurations. The following definition is also useful to study this case.

Definition 1.26. *We say that $\mathcal{Z}(n, k) = (\mathcal{Z}_0, \dots, \mathcal{Z}_k)$ is a minimal configuration of $\mathcal{P}(n, k)$ in (a, b) if for some choice of values of the parameters, we have at least a configuration of zeros $\mathcal{Z}(n, k)$ for I defined by (1.8).*

For the case $k = 2$ and $n = 1$, following the procedure and notation described in Section 1.2 we obtain I , from (1.8),

$$\begin{aligned}I_0(r^2) &= 2\pi \frac{r^2 \widehat{I}_0}{(a^2 + b^2 - r^2)(a^2 + b^2)((r^2 - a)^2 + b^2)(r^2 - 1)}, \\ I_1(r^2) &= 2\pi \frac{\widehat{I}_1}{(a^2 + b^2 - r^2)(a^2 + b^2)((a - 1)^2 + b^2)(r^2 - 1)}, \\ I_2(r^2) &= 2\pi \frac{\widehat{I}_2}{(a^2 + b^2 - r^2)((r^2 - a)^2 + b^2)(r^2 - 1)},\end{aligned}$$

where

$$\begin{aligned}
\widehat{I}_0 &= -(a\alpha_2 + b\beta_2)r^6 + \left((a^2 + b^2)\alpha_0 + ((a+1)^2 + b^2)(a\alpha_2 + b\beta_2) \right) r^4 \\
&\quad + \left((1+a)(a^2 + b^2)\alpha_1 + b(a^2 + b^2)\beta_1 - ((a^2 + b^2)^2 + a(a^2 + b^2) + a^2 - b^2)\alpha_2 \right. \\
&\quad \left. - b((a+1)^2 + b^2 - 1)\beta_2 \right) r^2 - (a^2 + b^2)^2\alpha_0 - ((a+1)^2 + b^2 - 1)(a^2 + b^2)\alpha_1 \\
&\quad - b(a^2 + b^2)\beta_1, \\
\widehat{I}_1 &= ((a^2 - b^2 - a)\alpha_2 + b(2a - 1)\beta_2)r^4 + \left((a^2 + b^2 - 1)(a^2 + b^2)\alpha_0 + (a - 1)(a^2 + b^2)\alpha_1 \right. \\
&\quad \left. + b(a^2 + b^2)\beta_1 + a((a - 1)^2 + b^2)\alpha_2 + b((a - 1)^2 + b^2)\beta_2 \right) r^2 \\
&\quad + (a^2 + b^2 - a)(a^2 + b^2)\alpha_1 - b(a^2 + b^2)\beta_1 + (a^2 + b^2 - a)(a^2 + b^2)\alpha_2 - b(a^2 + b^2)\beta_2, \\
\widehat{I}_2 &= -\alpha_0 r^6 + \left(-(a+1)\alpha_1 - b\beta_1 + (-a^2 + b^2 - a - 1)\alpha_2 - b(1 + 2a)\beta_2 \right) r^4 \\
&\quad + \left((a^2 + b^2)\alpha_0 + (a^2 + b^2 + a)\alpha_1 + b\beta_1 + a((a+1)^2 + b^2)\alpha_2 + b((a+1)^2 + b^2)\beta_2 \right) r^2 \\
&\quad - a(a^2 + b^2)\alpha_2 - b(a^2 + b^2)\beta_2.
\end{aligned} \tag{1.26}$$

The second subindex of α_i 's and β_i 's that appeared in (1.13) has been deleted to simplify the previous expressions. Thus, we have that all the coefficients α_i and β_i are arbitrary real constants. And together with a and b , they compose the set of seven essential parameters of problem $\mathcal{P}(1, 2)$. Moreover, expressions (1.26) show also that the maximum configuration for this problem is $(3, 2, 3)$.

As it has been explained in the introduction, the limit cycles correspond with the simple zeros of $I(r^2)$. Then we can study only the configuration of the simultaneous zeros of the polynomials \widehat{I}_0 , \widehat{I}_1 and \widehat{I}_2 in their corresponding intervals. This can be done rewriting these polynomials in the proper way and doing an exhaustive and meticulous application of the Descartes's rule of signs.

Next result shows that, for this case, there exists a symmetry that reduces the number of cases we need to study.

Proposition 1.27. *For any (a, b) , if (z_0, z_1, z_2) is a configuration of problem $\mathcal{P}(1, 2)$ then (z_2, z_1, z_0) is also a configuration.*

Proof. From expressions (1.26), according to Definition 1.4 and equation (1.13) we prove that if there are $\alpha_0, \alpha_1, \alpha_2, \beta_1$ and β_2 so that (z_0, z_1, z_2) is a configuration, then there are $\alpha_0^*, \alpha_1^*, \alpha_2^*, \beta_1^*$ and β_2^* for which the configuration of zeros is (z_2, z_1, z_0) .

With the change of variables

$$(x, y) = \left(\frac{aw + bz}{w^2 + z^2}, \frac{bw - az}{w^2 + z^2} \right) \text{ and its inverse } (w, z) = \left(\frac{ax + by}{y^2 + x^2}, \frac{bx - ay}{y^2 + x^2} \right),$$

we have that

$$(a, b) \mapsto (1, 0), \quad (1, 0) \mapsto (a, b), \quad \text{and} \quad w^2 + z^2 = \frac{a^2 + b^2}{y^2 + x^2}. \tag{1.27}$$

The relation between the new Abelian integral (I_0^*, I_1^*, I_2^*) and the old one is given by

$$(I_0^*, I_1^*, I_2^*) = (I_2, I_1, (a^2 + b^2)I_0),$$

where the new parameters are

$$\begin{aligned}\alpha_0^* &= \frac{(a^2 + b^2)\alpha_0 + (a^2 + a + b^2)\alpha_1 + \beta_1 b}{a^2 + b^2}, \\ \alpha_1^* &= \frac{-\alpha_1 a - \beta_1 b}{a^2 + b^2}, \\ \alpha_2^* &= \frac{(a - a^2 - b^2)\alpha_1 + \beta_1 b + (a - b)(a + b)\alpha_2 + 2\beta_2 g c}{a^2 + b^2}, \\ \beta_1^* &= \frac{-(a^2 + a + b^2)(a^2 - a + b^2)\alpha_1 + c\beta_1 b}{b(a^2 + b^2)}, \\ \beta_2^* &= \frac{a(a^2 - a + b^2)\alpha_1 - c\beta_1 b + 2\alpha_2 b^2 a - b(a - b)(a + b)\beta_2}{b(a^2 + b^2)}.\end{aligned}$$

Finally we have, from the change of variables (1.27), the following correspondence between intervals

$$\begin{aligned}r \in (0, 1) &\mapsto r^* \in (a^2 + b^2, \infty), \\ r \in (1, a^2 + b^2) &\mapsto r^* \in (1, a^2 + b^2), \\ r \in (a^2 + b^2, \infty) &\mapsto r^* \in (0, 1),\end{aligned}$$

that provides the symmetric configuration. \square

Due to the symmetry given by the last proposition, let us consider, from now on, only configurations (z_0, z_1, z_2) with $z_0 \geq z_2$.

First we prove some technical results to know which vectors of integers are configurations and which are not. More concretely, Lemma 1.28 shows how some of zeros of $\widehat{I}_j(r^2)$ for $j = 0, 1, 2$ can be fixed a priori. This allow us to found the minimal configurations of $\mathcal{P}(1, 2)$. See Proposition 1.29. From these facts, we prove that $I(r)$ has not eight positive zeros. Because there are no configurations with three zeros in the inner annulus and two in the middle one. See Proposition 1.30. Moreover the properties that satisfy the polynomials \widehat{I}_0 , \widehat{I}_1 and \widehat{I}_2 are studied in order to apply, in most cases, the Descartes' rule of signs.

Lemma 1.28. *Fixed (a, b) with $b \neq 0$. Given x_0, x_1, x_2 non-zero and different real numbers such that $(a + 1)^2 + b^2 \neq x_0 + x_1 + x_2$ and y_0 a real number such that $y_0 \neq 1$ and $y_0 \neq a^2 + b^2$, then there exist $\alpha_0, \alpha_1, \beta_1, \alpha_2, \beta_2$ satisfying:*

$$\begin{aligned}\widehat{I}_0(r^2) &= -\alpha_0(r^2 - x_0)(r^2 - x_1)(r^2 - x_2), \\ \widehat{I}_1(r^2) &= \alpha_0(r^2 - y_0)((\mu - y_0)(1 - x_0)(1 - x_1)(1 - x_2)(r^2 - \mu) \\ &\quad + (1 - y_0)(\mu - x_0)(\mu - x_1)(\mu - x_2)(r^2 - 1)), \\ \widehat{I}_2(r^2) &= \alpha_0(\phi_3(r^2 - \mu)^3 + \phi_2(r^2 - \mu)^2 + \phi_1(r^2 - \mu) + \phi_0) := \alpha_0\phi(r^2 - \mu),\end{aligned}\tag{1.28}$$

where $\mu = a^2 + b^2$ and

$$\begin{aligned}\phi_3 &= \mu + 1 + 2a - (x_0 + x_1 + x_2), \\ \phi_2 &= 3\mu^2 + (4a + 1 - 3(x_0 + x_1 + x_2))\mu + x_0x_1 + x_1x_2 + x_0x_2 - 2a, \\ \phi_1 &= 3\mu^3 + (2a - 3(x_0 + x_1 + x_2))\mu^2 + (1 - 2a + 2(x_0x_1 + x_1x_2 + x_0x_2))\mu - x_0x_1x_2, \\ \phi_0 &= \mu(\mu - x_0)(\mu - x_1)(\mu - x_2).\end{aligned}$$

Proof. From equation (1.26), the proof follows checking that the system of equations

$$\left\{ \widehat{I}_0(x_0) = 0, \widehat{I}_0(x_1) = 0, \widehat{I}_0(x_2) = 0, \widehat{I}_1(y_0) = 0 \right\},$$

has only one solution with respect to the variables $\alpha_1, \beta_1, \alpha_2, \beta_2$. Because the determinant of its associated matrix M ,

$$\begin{aligned}\det(M) &= b^2x_0x_1x_2(x_2 - x_0)(x_1 - x_0)(x_2 - x_1)(y_0 - 1)(a^2 + b^2 - 1) \\ &\quad (a^2 + b^2)^3(a^2 + b^2 - y_0)((a + 1)^2 + b^2 - x_0 - x_1 - x_2),\end{aligned}$$

does not vanish. \square

Previous lemma shows that $(3, 1, 0)$ is a minimal configuration. Similar results give other minimal configurations for this case.

Proposition 1.29. *The configurations which are minimal of $\mathcal{P}(1, 2)$ in any (a, b) are $(3, 1, 0)$, $(3, 0, 1)$, $(2, 2, 0)$, $(2, 1, 1)$, $(2, 0, 2)$, $(1, 2, 1)$, $(1, 1, 2)$, $(1, 0, 3)$, $(0, 2, 2)$ and $(0, 1, 3)$.*

Next result shows that there are configurations that can not be done. An immediate consequence of next result is that the maximum configuration is not maximal. Hence, there are no perturbations providing eight simultaneous zeros.

Proposition 1.30. *Given $w \in \{0, 1, 2, 3\}$, $(3, 2, w)$ is not a configuration of $\mathcal{P}(1, 2)$.*

Proof. With the change $r^2 = (\mu - 1)s + 1$, the expression of \widehat{I}_1 in Lemma 1.28 writes as

$$\widehat{I}_1(s) = \alpha_0(\mu - 1)^2(s - y_0)\varphi(s) \tag{1.29}$$

where $\varphi(s) = -y_0(\mu - x_0)(\mu - x_1)(\mu - x_2)s + (1 - y_0)(1 - x_0)(1 - x_1)(1 - x_2)(s - 1)$, and the interval of definition is moved to $(0, 1)$. Consequently, if $x_0, x_1, x_2, y_0, s \in (0, 1)$ we have that y_0 is the unique zero of $\widehat{I}_1(s)$ in $(0, 1)$, because the polynomial of degree one, $\varphi(s)$, is always negative in this interval,

$$\begin{aligned}\varphi(0) &= -(1 - y_0)(1 - x_0)(1 - x_1)(1 - x_2) < 0, \\ \varphi(1) &= -y_0(\mu - x_0)(\mu - x_1)(\mu - x_2) < 0.\end{aligned}$$

Therefore it is not possible that $\widehat{I}_1(s)$ has two zeros in the interval $(1, a^2 + b^2)$ and the statement is done. \square

The list of impossible configurations follows studying the number of zeros of \widehat{I}_2 or $\phi(s)$, see (1.28), given in Lemma 1.28. The Descartes' rule of signs, [Kos82], allows us to describe them. But first we need some technical results and notations to describe the signs of the coefficients ϕ_i , when we move the parameters on the plane (μ, a) . More concretely, Lemmas 1.32, 1.33 and 1.34 provide the shapes and locations of the equations $\phi_i = 0$. On the plane (μ, a) , with $\mu = a^2 + b^2$, in all these relations a can be written as a function of μ . We denote them by $a = a_i(\mu)$. Lemma 1.35 gives some relations between the coefficients that are very useful in the proof of Proposition 1.36. This last result exposes that there are not configurations with six positive and simultaneous zeros of I , three in the inner annulus and three more in the outer one. This result together with Proposition 1.30 shows that there are not configurations with seven zeros.

Definition 1.31. Given a polynomial $\phi(s) = \sum_{j=0}^n \phi_j s^j$, we say that ϕ has the configuration of signs $[s_n, \dots, s_1, s_0]$ with $s_i \in \{+, -, ?\}$ if and only if $\text{sign}(\phi_j) = s_j$ for $j = 0, \dots, n$ and the symbol $?$ denotes the case when $\text{sign}(\phi_j)$ is unknown.

For example, for a polynomial of degree three, we say that $\phi(s) = \phi_3 s^3 + \phi_2 s^2 + \phi_1 s + \phi_0$, has the configuration $[-, +, -, +]$ if $\phi_3 < 0$, $\phi_2 > 0$, $\phi_1 < 0$ and $\phi_0 > 0$, and we say that it has a configuration $[?, +, +, +]$ if we don't know the sign of ϕ_3 but $\phi_2, \phi_1, \phi_0 > 0$.

Lemma 1.32. Given $x_0, x_1, x_2 \in (0, 1)$, let us consider $a_1 = a_1(\mu)$ such as $\phi_1(\mu, a_1(\mu)) = 0$. Then

$$a_1 = \frac{3\mu^3 - 3(x_0 + x_1 + x_2)\mu^2 + (2x_0x_2 + 2x_0x_1 + 1 + 2x_1x_2)\mu - x_0x_1x_2}{2\mu(1 - \mu)}. \quad (1.30)$$

Furthermore, for $\mu > 1$, the graph of the function $a_1(\mu)$ has a vertical asymptote on $\mu = 1$ and an oblique one on $a = -3(\mu + 1 - (x_0 + x_1 + x_2))/2$. Moreover, $\lim_{\mu \rightarrow 1^+} a_1 = -\infty$. See the graph of function $a_1(\mu)$ and the sign of coefficient ϕ_1 in Figure 1.4.

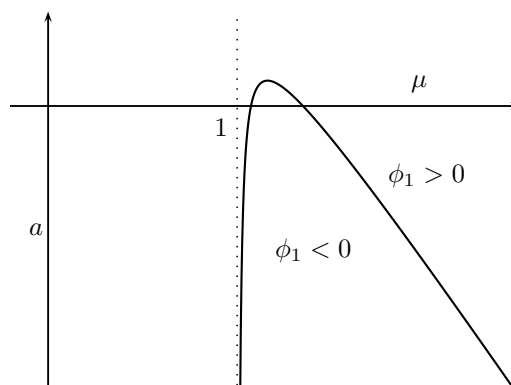


Figure 1.4 Graph of the curve $\phi_1(\mu, a) = 0$ defined in Lemma 1.32

Proof. The graph of a_1 has $\mu = 0$ and $\mu = 1$ as vertical asymptotes. The limit of a_1 when μ nears 1 on the right side is

$$\lim_{\mu \rightarrow 1^+} a_1 = \text{sign}(-4 + 3(x_0 + x_2 + x_1) - 2(x_0x_2 + x_0x_1 + x_1x_2) + x_0x_1x_2) \infty,$$

that for the values of x_0 , x_1 and x_2 consider, is always negative. The proof finishes studying the graph close to the asymptote. \square

Lemma 1.33. *Given $x_0, x_1, x_2 \in (0, 1)$, let us consider $a_2 = a_2(\mu)$ with $\phi_2(\mu, a_2(\mu)) = 0$, then*

$$a_2 = \frac{3\mu^2 + (1 - 3x_0 - 3x_1 - 3x_2)\mu + x_0x_2 + x_0x_1 + x_1x_2}{2(1 - 2\mu)}. \quad (1.31)$$

Moreover, the graph of a_2 presents a vertical asymptote on $\mu = 1/2$ and an oblique one with equation $a = (6(x_0 + x_1 + x_2) - 6\mu - 5)/8$. Figure 1.5 shows the graph of the function $a_2(\mu)$ for $\mu > 1/2$ in terms of the sign of the limit

$$\lim_{\mu \rightarrow \frac{1}{2}^+} a_2 = \text{sign}(-5 + 6(x_0 + x_1 + x_2) + 4(x_0x_2 - x_0x_1 + x_1x_2)) \infty$$

and the sign of the coefficient ϕ_2 .

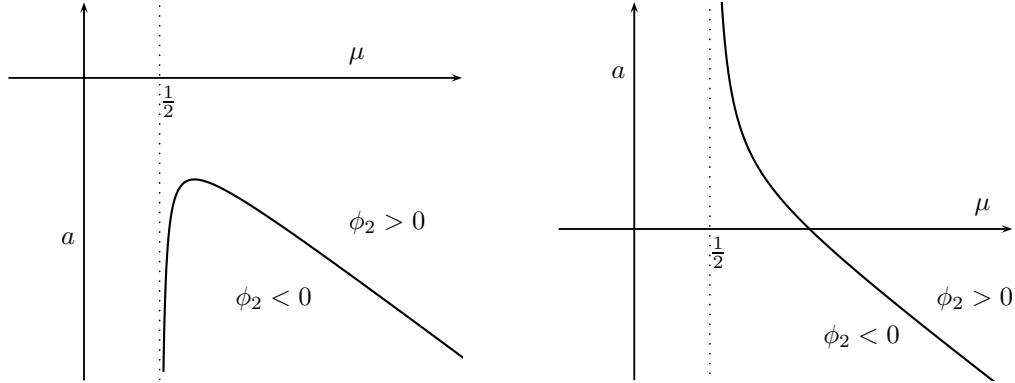


Figure 1.5 Graphs for the curves $\phi_2(\mu, a) = 0$ defined in Lemma 1.33

Lemma 1.34. *Given $x_0, x_1, x_2 \in (0, 1)$, let us consider $a_3 = a_3(\mu)$ with $\phi_3(\mu, a_3(\mu)) = 0$,*

$$a_3 = -\frac{1}{2}(\mu + 1 - (x_0 + x_1 + x_2)). \quad (1.32)$$

Moreover, the graph of the function $a_3(\mu)$ is a straight line with negative slope. Figure 1.6 shows also the sign of the coefficient ϕ_3 .

Lemma 1.35. *Given $x_0, x_1, x_2 \in (0, 1)$, let $a_i = a_i(\mu)$ for $i = 1, 2, 3$ be the functions defined in (1.30), (1.31) and (1.32). If $\mu > 1$ then $a_2(\mu) > a_1(\mu)$. See the relative positions of the respective graphs and the sign configurations in Figure 1.7.*

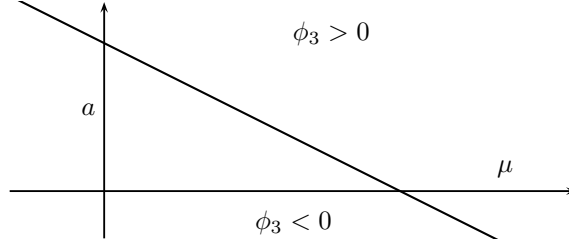


Figure 1.6 Graph of the curve $\phi_3(\mu, a) = 0$ defined in Lemma 1.34

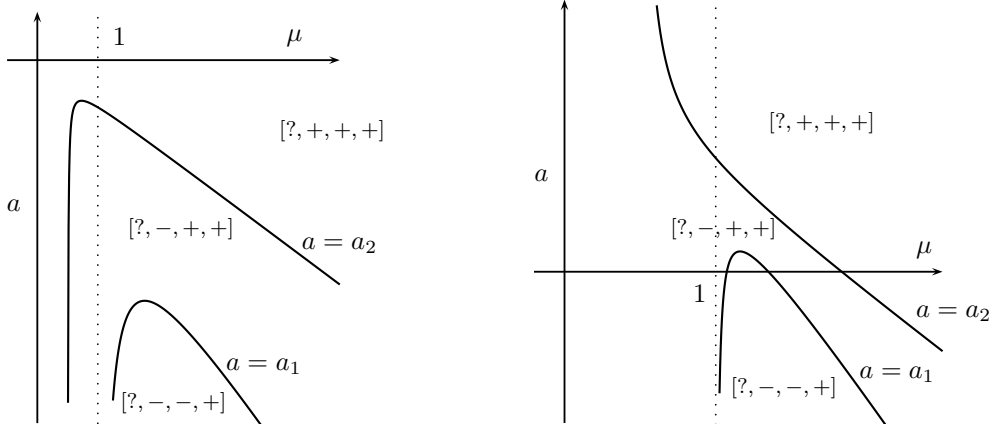


Figure 1.7 The two situations for the curves $\phi_1(\mu, a) = 0$ and $\phi_2(\mu, a) = 0$, defined on Lemma 1.35. The sign configurations of the function $\phi(s)$ are also indicated

Proof. The proof follows showing that there are no tangential contact points between a_1 and a_2 for any choice of values of x_0 , x_1 and x_2 . Then, for fixed values of x_0 , x_1 and x_2 , it is checked that the relative position is the given in the statement.

First we compute the resultant, $R_{1,2}$, between the numerator of the difference of a_1 and a_2 and the difference of its derivatives, with respect to the parameter x_2 . That is

$$\begin{aligned} R_{1,2} = & (9\mu^6 - 18(x_1 + x_0)\mu^5 + 3(3(x_1^2 + x_0^2 - 1) + 4(x_0 + x_1) + 9x_0x_1)\mu^4 \\ & - 2(x_1 - 3 + 6x_0^2x_1 + 11x_0x_1 + 3x_1^2 + 6x_1^2x_0 + x_0 + 3x_0^2)\mu^3 \\ & + 3x_0x_1(3x_1 + 2x_0x_1 + 3 + 3x_0)\mu^2 - 6x_0x_1(x_0x_1 + 1)\mu \\ & + x_0x_1(x_0x_1 + 1))(2\mu - 1)\mu(\mu - 1). \end{aligned}$$

The last three terms of $R_{1,2}$ do not vanish when $\mu > 1$ and the first one, which is the unique term that could be null, with the change $\tilde{\mu} = \mu - 1$ writes as

$$\begin{aligned} \tilde{R}_{1,2}(\tilde{\mu}) = & 9\tilde{\mu}^6 + 18(3 - x_1 - x_0)\tilde{\mu}^5 + 3(42 - 26(x_0 + x_1) + 9x_0x_1 + 3(x_1^2 + x_0^2))\tilde{\mu}^4 \\ & + 2(-6(x_1^2x_0 + x_0^2x_1) + 15(x_0^2 + x_1^2) - 67(x_0 + x_1) + 75 + 43x_0x_1)\tilde{\mu}^3 \\ & + 3(35x_0x_1 + 12(x_0^2 + x_1^2) - 9(x_0^2x_1 + x_1^2x_0) - 38(x_0 + x_1) + 33 + 2x_0^2x_1^2)\tilde{\mu}^2 \\ & + 6(6 - 3(x_0^2x_1 + x_1^2x_0) + 3(x_0^2 + x_1^2) + x_0^2x_1^2 - 8(x_0 + x_1) + 9x_0x_1)\tilde{\mu} \\ & + 6 + 9x_0x_1 - 8x_0 - 8x_1 + x_0^2x_1^2 - 3x_0^2x_1 + 3x_1^2 + 3x_0^2 - 3x_1^2x_0. \end{aligned}$$

Hence, $\tilde{R}_{1,2}$ is always positive because for all x_0 and x_1 in $(0, 1)$, all the coefficients of this polynomial are positive. So there is not tangential contact.

Straightforward computations finish the proof showing that $a_2 > a_1$ for fixed $x_0 = 1/8$, $x_1 = 1/4$ and $x_2 = 1/2$. That is

$$a_2 - a_1 = \frac{192\tilde{\mu}^4 + 536\tilde{\mu}^3 + 690\tilde{\mu}^2 + 460\tilde{\mu} + 115}{128(2\tilde{\mu} + 1)(\tilde{\mu} + 1)\tilde{\mu}} > 0.$$

□

Proposition 1.36. *Given $w \in \{0, 1, 2\}$, $(3, w, 3)$ is not a configuration for the problem $\mathcal{P}(1, 2)$.*

Proof. In the expression of $\widehat{I}_2(r^2)$ given in Lemma 1.28, or equivalently in function $\phi(s)$, y_0 does not appear. So if $\widehat{I}_0(r^2)$ has three zeros in $(0, 1)$, the zeros of $\widehat{I}_2(r^2)$ do not depend on the zeros of $\widehat{I}_1(r^2)$.

From equation (1.28), ϕ can be considered in the variables (μ, a) with $\mu = a^2 + b^2$. Moreover, ϕ is a function in b^2 , then we can restrict our study to $b > 0$. The number of zeros of ϕ can be done studying the number of positive zeros, considering $\phi(s)$ with $r^2 = s + a^2 + b^2$ and applying the Descartes' rule, [Kos82].

When \widehat{I}_0 has three zeros in the first region, $x_0, x_1, x_2 \in (0, 1)$, as $\mu > 1$ ϕ_0 is always positive. This forces that \widehat{I}_2 has also three zeros if and only if, for $s > 0$ we have $\phi_3 < 0$, $\phi_2 > 0$, $\phi_1 < 0$. The proof follows showing that this relative position of the curves, see Figure 1.8, is in fact impossible.

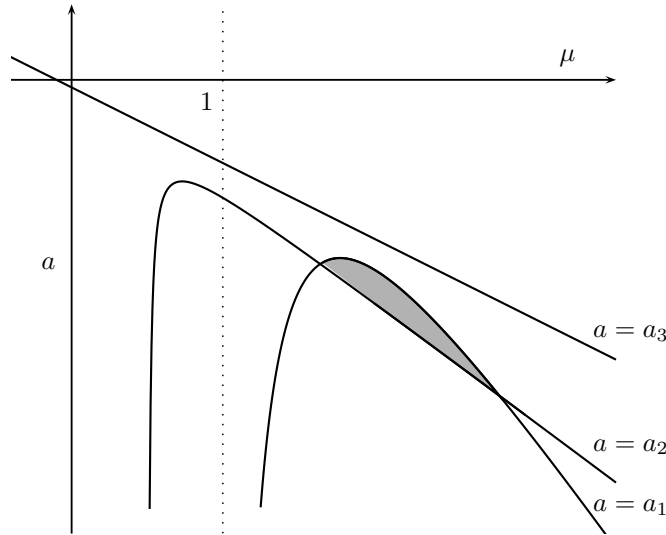


Figure 1.8 *Impossible configuration of the graphs of the functions $a = a_i(\mu)$, $i = 1, 2, 3$. The shadowed region corresponds to the situation $\phi_0, \phi_2 > 0$, $\phi_1, \phi_3 < 0$ with a sign configuration $[-, +, -, +]$*

When $\mu > 1$, it can be checked that for each $i = 1, 2, 3$, $\phi_i > 0$ if and only if $a > a_i(\mu)$. Lemma 1.35 guaranties that $a_2 > a_1$. Therefore there is not a value of a such as $a < a_1$ and $a > a_2$. So the conditions $\phi_1 < 0$ and $\phi_2 > 0$ are incompatible. \square

Proposition 1.37. *For any (a, b) and given $w \in \{0, 1, 2\}$, $(3, 0, w)$ is a configuration if, and only if $(3, 1, w)$ is a configuration also.*

Proof. From the functions (1.28), if we fix x_0, x_1, x_2 and y_0 , the expression \widehat{I}_2 is independent to the choice of y_0 . Then when \widehat{I}_0 has three zeros, independently of the number of zeros of \widehat{I}_2 , \widehat{I}_1 has one zero for y_0 in $(0, 1)$ and no zeros when $y_0 > 1$. Because equation (1.29) guaranties that the other zero of \widehat{I}_1 is negative. Moreover, the point (a, b) remains unchanged, but the perturbation changes with y_0 . \square

Maximum number of zeros for degree one perturbations

Now we prove Theorem 1.15, the main result of Section 1.4, that asserts that the maximum number of zeros of $\mathcal{P}(1, 2)$ is six. And the maximal configurations are $(3, 1, 2)$, $(2, 2, 2)$ and $(2, 1, 3)$. In fact it is also proved that a vector of integers is a configuration if, and only if, is less or equal to one of the maximal ones.

Proof of Theorem 1.15. Proposition 1.25 provides that all the configurations are lower than $(3, 2, 3)$. Propositions 1.27, 1.30 and 1.36 guarantee that $(3, 2, 3)$, $(3, 2, 2)$, $(3, 1, 3)$ and $(2, 2, 3)$ are not configurations. Therefore the maximum number of simultaneous zeros cannot be seven nor eight. Same results imply that neither $(3, 2, 1)$, $(3, 0, 3)$, $(1, 2, 3)$ are configurations. Hence the only configurations with six zeros are the ones from the statement.

The proof finishes proving that all the vectors (z_0, z_1, z_2) less or equal to $(3, 1, 2)$, $(2, 2, 2)$ or $(2, 1, 3)$ are configurations. This is done providing concrete values of (a, b) and perturbation parameters such that the exact number of zeros of \widehat{I}_j is z_j for $j = 0, 1, 2$. We only show that $(2, 2, 2)$ is a configuration because the other cases follows similarly and next section deals with the configurations of type $(3, 1, w)$.

Fixed $(a, b) = (1/2, 1)$, we have $J_0 = (0, 1)$, $J_1 = (1, \sqrt{5}/2)$ and $J_2 = (\sqrt{5}/2, \infty)$. From Proposition 1.29 we know that $(2, 2, 0)$ is a minimal configuration. In a similar way that Lemma 1.28, we can found the functions \widehat{I}_0 and \widehat{I}_1 , see (1.26), such that $x_0 = 7/10$, $x_1 = 9/10$ and $y_0 = 11/10$, $y_1 = 12/10$, are their corresponding pair of zeros. Then

$$\left\{ \alpha_0 = 1, \alpha_1 = -\frac{508}{6745}, \beta_1 = \frac{20609}{26980}, \alpha_2 = -\frac{1155}{1349}, \beta_2 = -\frac{6995}{2698} \right\}.$$

and the functions (1.26) write as

$$\begin{aligned} \widehat{I}_0 &= -\frac{1}{10792} (326r^2 - 403) (10r^2 - 9) (10r^2 - 7), \\ \widehat{I}_1 &= -\frac{231}{10792} (10r^2 - 11) (5r^2 - 6), \\ \widehat{I}_2 &= r^6 - \frac{34916}{6745}r^4 + \frac{214097}{26980}r^2 - \frac{20375}{5396}. \end{aligned}$$

Moreover, \widehat{I}_0 has two zeros in J_0 , the third one $\sqrt{403/326}$ is not in J_0 . \widehat{I}_1 has the two zeros in J_1 . \widehat{I}_2 has only two zeros in J_2 , two in the intervals $(9/8, 5/4)$ and $(3/2, 2)$ and the third one in $(1, 17/6)$ which is not in J_2 . Hence, $(2, 2, 2)$ is a configuration. \square

Remark 1.38. *To find the values of (a, b) and the suitable perturbation to prove that a given configuration is done can be, in general, very difficult. Because the region of the parameters can be really small. The configuration $(2, 1, 2)$, for example, is achieved for the values $(a, b) = (999/1000, 9/200)$, $x_0 = \sqrt{19999/20000} \approx 0.999975$, $x_1 = \sqrt{19997/20000} \approx 0.999925$, $x_2 = y_0 = \sqrt{100001/100000} \approx 1.000005$. Next section shows these difficulties.*

1.4.3 Bifurcation Diagram for perturbations of degree one

For $k = 2$ and perturbations of degree one, problem $\mathcal{P}(1, 2)$, the maximal configurations are given in Theorem 1.15. In this section we look for the region on the parameter space, (a, b) , where the maximal configuration $(3, 1, 2)$ can be achieved. This is done studying all the perturbations that provide configurations of type $(3, 1, w)$, for $w = 0, 1, 2$. Given the symmetry of Proposition 1.27, this problem is equivalent to study the maximal configuration $(2, 1, 3)$, because both regions are the same. For the configuration $(2, 2, 2)$ a similar study can be obtained.

From Lemma 1.28, given $x_0, x_1, x_2 \in (0, 1)$, the zeros of \widehat{I}_0 , the bifurcation diagram follows studying the number of zeros of the function \widehat{I}_2 in $J_2 = (a^2 + b^2, \infty)$. Or equivalently, looking for the zeros of

$$\phi(s) = \phi_3 s^3 + \phi_2 s^2 + \phi_1 s + \phi_0 \quad (1.33)$$

in $(0, \infty)$, where

$$\begin{aligned} \phi_3 &= \mu + 1 + 2a - \rho, \\ \phi_2 &= 3\mu^2 + (4a + 1 - 3\rho)\mu + \sigma - 2a, \\ \phi_1 &= 3\mu^3 + (2a - 3\rho)\mu^2 + (1 - 2a + 2\sigma)\mu - \tau, \\ \phi_0 &= \mu(\mu - x_0)(\mu - x_1)(\mu - x_2), \end{aligned}$$

and $\mu = a^2 + b^2$, $\rho = x_0 + x_1 + x_2$, $\sigma = x_0x_1 + x_1x_2 + x_0x_2$, $\tau = x_0x_1x_2$. Moreover, as \widehat{I}_2 does not depend on y_0 , the zero of \widehat{I}_1 , all the results are also valid for the configurations of type $(3, 0, w)$, for $w = 0, 1, 2$.

The main tool to describe the bifurcation diagram is the Descartes' rule of signs. See [Kos82]. But a complete comparative study between the curves $\phi_i(\mu, a) = 0$, $i = 0, 1, 2, 3$ is not necessary. See Lemmas 1.35 and 1.40. First, we provide the bifurcation curves, on the plane (a, b) for a fixed values of x_i , $i = 0, 1, 2$. Second, we construct the general bifurcation curves studying how they change when we move the parameters x_0, x_1 and x_2 in $(0, 1)$.

Bifurcation diagram for fixed zeros in the inner region

The first step to obtain the bifurcation diagram on plane (a, b) from the sign distribution of the coefficients of function ϕ , see (1.33), is doing it when the values of x_0 , x_1 and x_2 are fixed.

Lemma 1.39. *For fixed $x_0, x_1, x_2 \in (0, 1)$ and $(a, b) \in \mathbb{R}^2$ with $\mu = a^2 + b^2 > 1$, the changes of signs in the coefficients of ϕ , see (1.33), are*

(i) zero in $\mathcal{S}_0^* := \{(a, b) \in \mathbb{R}^2 : \phi_2 > 0, \phi_3 > 0\}$,

(ii) one in $\mathcal{S}_1^* := \{(a, b) \in \mathbb{R}^2 : \phi_3 < 0\}$, and

(iii) zero or two in $\mathcal{S}_2^* := \{(a, b) \in \mathbb{R}^2 : \phi_2 < 0, \phi_3 > 0\}$.

Furthermore, the vertexes of these regions are

$$\begin{aligned} R &= \left(\frac{3\rho - \sigma}{2} - 2, \frac{\sqrt{-9\rho^2 + 6\rho\sigma - \sigma^2 + 24\rho - 8\sigma - 12}}{2} \right), \\ S &= \left(\frac{\rho - 2}{2}, \frac{\sqrt{\rho(4 - \rho)}}{2} \right), \\ T &= \left(\frac{\rho - 2 - \zeta}{4}, \frac{\sqrt{(\rho + 2)\zeta + 4\rho - \rho^2 + 2\sigma}}{2\sqrt{2}} \right). \end{aligned} \quad (1.34)$$

Where $\zeta = \sqrt{\rho^2 + 4\rho - 4 - 4\sigma}$, $\rho = x_0 + x_1 + x_2$, $\sigma = x_0x_1 + x_0x_2 + x_1x_2$ and $\tau = x_0x_1x_2$. See Figure 1.9.

Proof. By definition of a_1 , a_2 and a_3 in Lemmas 1.32, 1.33 and 1.34, respectively, we already know the sign configurations according to the value of a with respect to $a_1(\mu)$, $a_2(\mu)$ and $a_3(\mu)$. Following these lemmas, we have that

- if $a > \max(a_2(\mu), a_3(\mu))$ the sign configuration is $[+, +, +, +]$,
- if $a_2(\mu) < a < a_3(\mu)$ the sign configuration is $[-, +, +, +]$,
- if $a < \min(a_2(\mu), a_3(\mu))$ the sign configuration is $[-, -, +, +]$ or $[-, -, -, +]$, and
- if $a_3(\mu) < a < a_2(\mu)$ the sign configuration is $[+, -, +, +]$ or $[+, -, -, +]$.

Since $\mu = a^2 + b^2$ we obtain the regions and the intersection points defined in the statement. \square

As the region \mathcal{S}_2^* can be empty, the following two lemmas give us the necessary conditions on x_0, x_1, x_2 to avoid this possibility.

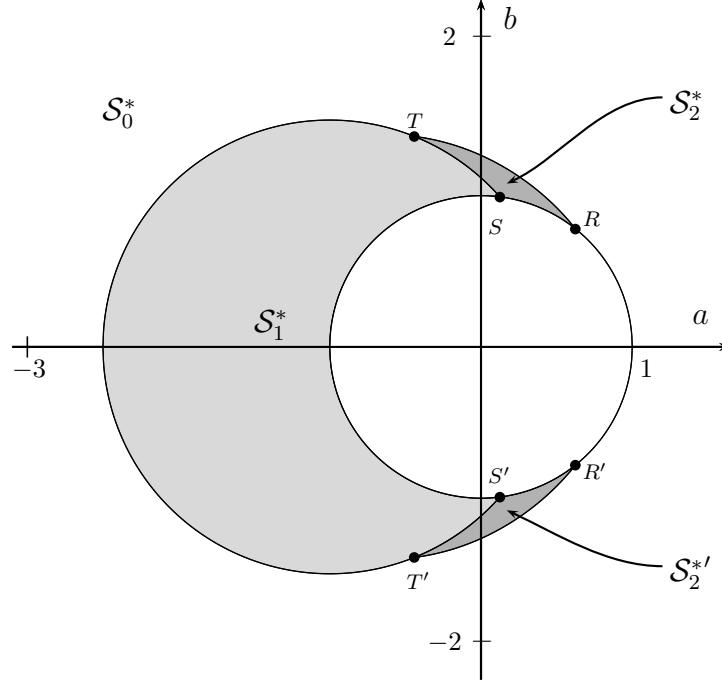


Figure 1.9 The regions and points defined in Lemma 1.39. The respective symmetric ones, with respect to the line $b = 0$, are denoted by R' , S' , T' and $S_2'^*$

Lemma 1.40. For $\mu > 1$, the curves $\phi_2 = 0$ and $\phi_3 = 0$, given in Lemmas 1.33 and 1.34, do not have intersection points (Type I) or just one (Type II). See Figure 1.10. Moreover, given x_0, x_1, x_2 , the region S_2^* is non empty when the curves $\phi_2 = 0$ and $\phi_3 = 0$ are of Type II and the abscise of the intersection point is greater than 1.

Proof. First we prove when the region S_2^* is non empty. As it follows in the proof of Lemma 1.39, this occurs when we have the configuration $[+, -, ?, +]$. This situation is only possible, see Figure 1.10, on Type II and under the conditions of the statement. Second, we show how are the graphs of curves $\phi_2 = 0$ and $\phi_3 = 0$.

When the graph of $\{(\mu, a) : a = a_2(\mu)\}$ is monotonous, there is only one intersection point of the curve with $a = a_3(\mu)$ for $\mu > 1/2$. Because the slope of the oblique asymptote, $-3/2$, is less than the slope of $a = a_3(\mu)$, $-1/2$. So we are in a Type II.

If the graph $\{(\mu, a) : a = a_2(\mu)\}$ is not monotonous, we prove that for $\mu > 1$ there are no intersection points with the graph of $\{(\mu, a) : a = a_3(\mu)\}$. We show it by contradiction, that is, they can exist only for $\mu \leq 1$. In fact we prove that $\mu < 1$.

Assume that the intersection points are $(\mu_0, a_2(\mu_0)) = (\mu_0, a_3(\mu_0))$ and $(\mu_1, a_2(\mu_1)) = (\mu_1, a_3(\mu_1))$. Then, from (1.31) and (1.32), we have that the numerator of $a_3(\mu) - a_2(\mu)$, $N(a_3 - a_2)$, is a quadratic polynomial that vanishes at μ_0 and μ_1 , that is

$$\begin{aligned} N(a_3 - a_2) &= (\mu - \mu_0)(\mu - \mu_1) \\ &= \mu^2 - (x_0 + x_2 + x_1)\mu + x_0x_1 + x_0x_2 + x_1x_2 - (x_0 + x_1 + x_2) + 1, \end{aligned} \quad (1.35)$$

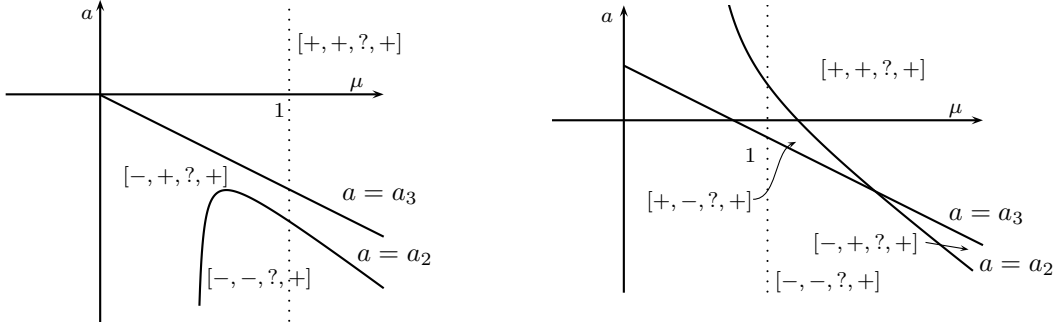


Figure 1.10 Graphs of Types I (left) and II (right) for the curves $\phi_2 = 0$ and $\phi_3 = 0$

with

$$\begin{aligned}\xi_1(x_0, x_1, x_2) &:= \mu_0 + \mu_1 = x_0 + x_1 + x_2, \\ \xi_2(x_0, x_1, x_2) &:= \mu_0 \mu_1 = x_0 x_1 + x_0 x_2 + x_1 x_2 - (x_0 + x_1 + x_2) + 1.\end{aligned}\tag{1.36}$$

The possible values of x_0, x_1, x_2 satisfy the next conditions: the discriminant of $N(a_3 - a_2)$, see (1.35), is non negative, the function $a_2(\mu)$, see (1.31), is not monotonous and $x_0, x_1, x_2 \in (0, 1)$. All these conditions can be expressed as the next set of inequalities:

$$\begin{aligned}C_1 &= x_0^2 + x_1^2 + x_2^2 - 2(x_0 x_1 + x_0 x_2 + x_1 x_2) + 4(x_0 + x_1 + x_2) - 4 \geq 0, \\ C_2 &= 5 - 6(x_0 + x_1 + x_2) + 4(x_0 x_1 + x_0 x_2 + x_1 x_2) \geq 0, \\ C_3 &= x_0(1 - x_0) \geq 0, \\ C_4 &= x_1(1 - x_1) \geq 0, \\ C_5 &= x_2(1 - x_2) \geq 0.\end{aligned}\tag{1.37}$$

The Karush-Kuhn-Tucker (KKT) Theorem, see [AEGP85], provides the maximum and minimum values of the functions (1.36) in the set (1.37). The functions

$$\begin{aligned}\Xi_1^\pm(x_0, x_1, x_2) &:= \pm \xi_1 + \lambda_1 C_1 + \lambda_2 C_2 + \lambda_3 C_3 + \lambda_4 C_4 + \lambda_5 C_5, \text{ and} \\ \Xi_2^\pm(x_0, x_1, x_2) &:= \pm \xi_2 + \lambda_1 C_1 + \lambda_2 C_2 + \lambda_3 C_3 + \lambda_4 C_4 + \lambda_5 C_5,\end{aligned}$$

are defined to look for the maximum(+) or the minimum(-) with $\lambda_j \in \mathbb{R}^+$ for all $j \in \{1, 2, 3, 4, 5\}$.

The candidates to obtain the maximum value of ξ_1 are the solutions of the system $\{\nabla \Xi_1^+ = 0, \lambda_j C_j, j = 1, \dots, 5\}$, where ∇ denotes the gradient operator. This system has eight equations and eight variables, $(x_0, x_1, x_2, \lambda_1, \lambda_2, \lambda_3, \lambda_4, \lambda_5)$, and it has only two solutions satisfying $x_i \in [0, 1]$ and $\lambda_j \geq 0$ for $i = 0, 1, 2$ and $j = 1, \dots, 5$. That is $(1, 1, 1, 0, 0, 1, 1, 1)$ and $(x_M, x_M, x_M, 0, 8\sqrt{3/7}, 0, 0, 0)$ where $x_M = (9 - \sqrt{21})/12$. However, the first point is not in the set (1.37) because $C_2(1, 1, 1) = -1$. Hence, the maximum is obtained at the point (x_M, x_M, x_M) and $\xi_1 \leq (9 - \sqrt{21})/4$.

It can be shown, similarly, that the minimum of ξ_1 is done at the point (x_m, x_m, x_m) with $x_m = 2 - 2\sqrt{2/3}$ and the maximum and the minimum of ξ_2 are done at the points

(x_m, x_m, x_m) and (x_M, x_M, x_M) , respectively. Therefore, we can concluded that

$$\begin{aligned} 1.10102051 &\approx 6 - 2\sqrt{6} \leq \xi_1 \leq \frac{9 - \sqrt{21}}{4} \approx 1.10435608, \\ 0.30217804 &\approx \frac{7 - \sqrt{21}}{8} \leq \xi_2 \leq 15 - 6\sqrt{6} \approx 0.30306154. \end{aligned}$$

Finally, from (1.36) we have

$$\begin{aligned} \mu_0 &= \frac{1}{2} \left(\xi_1 - \sqrt{\xi_1^2 - 4\xi_2} \right), \\ \mu_1 &= \frac{1}{2} \left(\xi_1 + \sqrt{\xi_1^2 - 4\xi_2} \right), \end{aligned}$$

and therefore

$$\max(\mu_0, \mu_1) \leq \frac{1}{2} \left(\max \xi_1 + \sqrt{(\max \xi_1)^2 - 4 \min \xi_2} \right) = \frac{7 - \sqrt{21}}{4} \approx 0.60435608.$$

This contradicts the condition $\mu > 1$. \square

Region \mathcal{S}_2^* contains the configurations $(3, 1, 2)$ and $(3, 1, 0)$, the boundary between these two regions is given when $\phi(s)$ has a positive zero of multiplicity 2. This can be seen in the next result.

Proposition 1.41. *For fixed $x_0, x_1, x_2 \in (0, 1)$ and $(a, b) \in \mathbb{R}^2$ with $\mu = a^2 + b^2 > 1$, the number of zeros of \hat{I}_2 in the outer region is*

- (i) zero if (a, b) is in $\tilde{\mathcal{S}}_0^* := \mathcal{S}_0^* \cup \{(a, b) \in \mathcal{S}_2^* : \mathcal{D}^* > 0\}$,
- (ii) one simple if (a, b) is in $\tilde{\mathcal{S}}_1^* := \mathcal{S}_1^*$,
- (iii) one double if (a, b) is in $\tilde{\mathcal{D}}^* := \{(a, b) \in \mathcal{S}_2^* : \mathcal{D}^* = 0\}$, and
- (iv) two simple if (a, b) is in $\tilde{\mathcal{S}}_2^* := \{(a, b) \in \mathcal{S}_2^* : \mathcal{D}^* < 0\}$.

Therefore the respective configurations are $(3, 1, 0)$ in the case (i), $(3, 1, 1)$ in the cases (ii) and (iii) and $(3, 1, 2)$ in the case (iv). With

$$\begin{aligned} \mathcal{D}^* &= 4\mu^7 + (3 - 4a^2 - 4\rho - 12a)\mu^6 + (-30\rho + 30 + 12\rho a + 4\sigma a + 22\sigma - 12\tau + 8a \\ &\quad + 16a^3)\mu^5 + (3 + 8a - 44a^2 - 16a^4 - 30\rho + 24a^2\rho - 32\sigma a^2 + 8\tau a^2 - 12\rho a + 4\sigma a \\ &\quad - 20\tau a + 8\tau + 27\rho^2 - 18\rho\sigma + 12\rho\tau - \sigma^2 - 4\sigma)\mu^4 + (4 - 12a + 32a^4 - 4\rho - 36\rho a\sigma \\ &\quad + 12\rho\tau a - 8\tau a\sigma - 32\rho a^3 + 24a^2\rho + 24\sigma a^2 - 16\tau a^2 + 16a^3\sigma - 26\tau\sigma + 20\sigma^2 a + 16\tau a^3 \\ &\quad + 12\tau^2 + 12\rho a + 4\sigma a + 48\tau a + 8\tau - 18\rho\sigma - 12\rho\tau + 22\sigma^2 + 22\sigma)\mu^3 \\ &\quad + (-4\sigma^2 a^2 + 18\rho\tau\sigma - 16\tau a^2\sigma - 4a^2\tau^2 - 68\tau a\sigma - \sigma^2 + 2\tau\sigma^2 + 12\rho\tau a - 16a^4 \\ &\quad - 12\tau + 20\tau^2 - 4\sigma^3 - 32\sigma a^2 - 16\tau a^2 - 20\tau a + 12\rho\tau + 48\tau a^2\rho + 16a^3 + 40\tau^2 a \\ &\quad + 16a^3\sigma - 26\tau\sigma + 20\sigma^2 a - 64\tau a^3 - 12\rho\tau^2 - 4a^2 + 4\sigma a)\mu^2 + 2\tau(-2\tau^2 + 6\tau + 20\tau a \\ &\quad + 2\tau\sigma + 20\tau a^2 - 12\rho\tau a + 2\tau a\sigma - 6\rho\tau + \sigma^2 + 8a^3 - 8\sigma a^2 - 4\sigma a + 4a^2 + 2\sigma^2 a)\mu \\ &\quad - \tau^2(4\tau - 4\rho\tau + 8\tau a + 4a^2 + \sigma^2 - 4\sigma a) \end{aligned}$$

where ρ , σ and τ are defined in Lemma 1.39. Additionally the point T , (1.34), is in the curve $\mathcal{D}^* = 0$. In fact it is a tangential contact point between $\mathcal{D}^* = 0$ and $\phi_3 = 0$.

Proof. Lemma 1.39 gives us the possible sign configurations and therefore the number of zeros module two. For that reason, we just consider the curve, $\mathcal{D}^* = 0$, of zeros of multiplicity two inside \mathcal{S}_2^* . This curve is a factor of the resultant, with respect to the variable r , of $\widehat{I}_2(r)$ and its derivative also respect to r . This resultant has the extra factor $\mu + 2a + 1 - \rho$ that we do not consider, because it corresponds to the expression of $\phi_3 = 0$, the boundary of \mathcal{S}_2^* .

Straightforward computations show that T belongs to $\mathcal{D}^* = 0$ and that the tangential property is also satisfied. \square

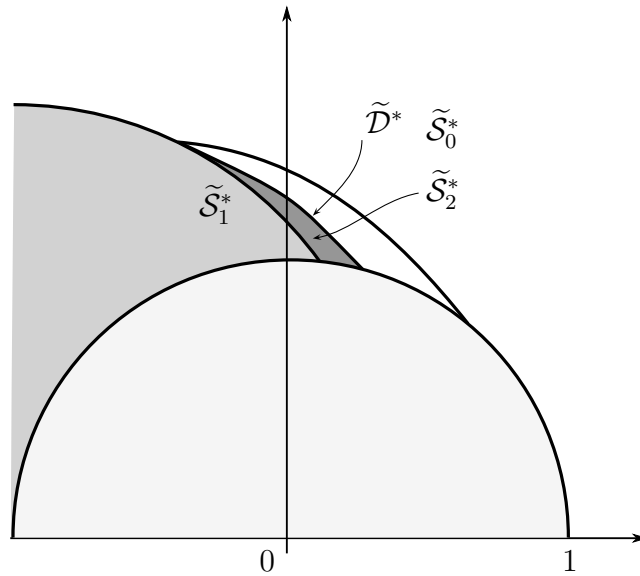


Figure 1.11 Regions where \widehat{I}_2 has 0, 1 or 2 zeros for fixed x_0, x_1, x_2

Remark 1.42. Drawing the implicit expression given in Proposition 1.41 for the curve $\widetilde{\mathcal{D}}^* = 0$, we observe that it is the graph of a function $b^*(a)$. Moreover, it goes from the point T to a point in the circumference $\{a^2 + b^2 = 1\}$ which is situated between the points R and S defined in Lemma 1.39. See Figure 1.11.

Bifurcation diagram varying the zeros of the inner region

The diagram of the maximum number of changes of sign follows studying how the curves of Figures 1.9 and 1.11 are modified under the different values of (x_0, x_1, x_2) in $(0, 1)^3$ or (ρ, σ, τ) in $(0, 3)^2 \times (0, 1)$. See Lemma 1.39. We use these two coordinates indistinctly.

First we write the functions $a_1(\mu)$, $a_2(\mu)$ and $a_3(\mu)$ given in Lemmas 1.32, 1.33 and 1.34 with these new coordinates.

$$\begin{aligned} a_1(\mu) &= \frac{3\mu^3 - 3\rho\mu^2 + (1 + 2\sigma)\mu - \tau}{2\mu(1 - \mu)}, \\ a_2(\mu) &= \frac{3\mu^2 + (1 - 3\rho)\mu + \sigma}{2(1 - 2\mu)}, \\ a_3(\mu) &= \frac{-\mu - 1 + \rho}{2}. \end{aligned} \tag{1.38}$$

As it can be shown in Lemma 1.39, different configurations appear from the signs of the functions ϕ_2 and ϕ_3 . In this new coordinates, these functions only depend on ρ and σ . Hence, in our study, we move only these two, not τ . In fact, next result shows which are the different intervals where σ moves in terms of ρ .

Lemma 1.43. *Fixed $\rho \in (0, 3)$, we have*

$$\sigma \in \begin{cases} \left(0, \frac{\rho^2}{3}\right) & \text{if } 0 < \rho \leq 1, \\ \left(\rho - 1, \frac{\rho^2}{3}\right) & \text{if } 1 < \rho \leq 2, \\ \left(2\rho - 3, \frac{\rho^2}{3}\right) & \text{if } 2 < \rho < 3. \end{cases}$$

Proof. Fixed ρ , we have that $x_0 = \rho - x_1 - x_2 \in (0, 1)$. Therefore, x_1 and x_2 must be in the region $(0, 1) \times (0, 1)$ delimited by the straight lines $\rho - x_1 - x_2 = 0$ and $\rho - x_1 - x_2 = 1$ in the plane (x_1, x_2) . These regions, in terms of ρ , are showed in Figure 1.12. Thus, the interval for σ comes from the minimum and maximum of the function $\sigma = (\rho - x_1 - x_2)(x_1 + x_2) + x_1x_2$ on the different regions for (x_1, x_2) given also in Figure 1.12. We distinguish three possible cases: $\rho \in (0, 1]$, $\rho \in (1, 2)$ and $\rho \in [2, 3)$. Solving the optimization problems with the corresponding restrictions, see [AEGP85], we obtain the intervals defined on the statement. More concretely, the maximum is always $\rho^2/3$ and it is located in the central point $(x_1, x_2) = (\rho/3, \rho/3)$, where $x_0 = \rho/3$, and the minimum is always located on the vertexes of the regions. \square

Lemma 1.44. *The point T , defined in (1.34), remains in the region $\{(a, b) : \Gamma_0 > 0, \Gamma_1 > 0, \Gamma_2 > 0, \Gamma_3 > 0\}$, where*

$$\begin{aligned} \Gamma_0 &= a^2 + b^2 - 1, \\ \Gamma_1 &= (a^2 + b^2)^2 - 2a(a^2 + b^2 + 1) - 4b^2 + 1, \\ \Gamma_2 &= 2a^3 + 2ab^2 - 2a + 1, \\ \Gamma_3 &= 2a - 1, \end{aligned}$$

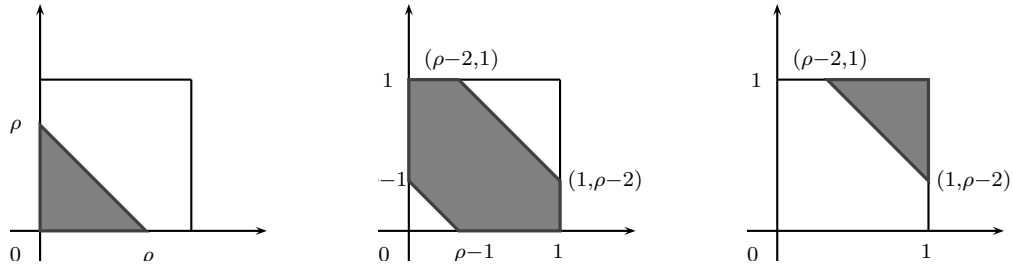


Figure 1.12 Regions for the pairs (x_1, x_2) such that the corresponding x_0 is in the interval $(0, 1)$ for the corresponding values of ρ in $(0, 1]$, $(1, 2]$ and $(2, 3)$

when (ρ, σ, τ) moves in $(0, 3)^2 \times (0, 1)$. See Figure 1.13. Moreover, the intersection points of the boundaries are

$$\begin{aligned} \{(a, b) : \Gamma_0 = 0\} \cap \{(a, b) : \Gamma_1 = 0\} &= ((1 - \sqrt{3})/2, \sqrt[4]{3}/\sqrt{2}), \\ \{(a, b) : \Gamma_1 = 0\} \cap \{(a, b) : \Gamma_2 = 0\} &= \left((1 - \sqrt{5})/4, \sqrt{18 + 10\sqrt{5}}/4 \right), \\ \{(a, b) : \Gamma_2 = 0\} \cap \{(a, b) : \Gamma_3 = 0\} &= (-1/2, \sqrt{7}/2), \\ \{(a, b) : \Gamma_3 = 0\} \cap \{(a, b) : \Gamma_0 = 0\} &= (-1/2, \sqrt{3}/2). \end{aligned}$$

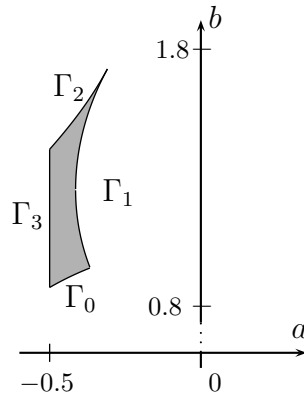


Figure 1.13 Region, depicted in gray, where the point T moves when (x_0, x_1, x_2) is in $(0, 1)^3$

Proof. First, we show that, for any ρ , T moves along a circumference arc over $\phi_3 = 0$ when we change the values x_0 , x_1 and x_2 . Second, we study the region covered by these arcs.

Fixed ρ , the point $T = (a_T, b_T)$ just depends on the value of σ . The maximum and minimum values of a_T correspond with the maximum and minimum values of σ , because a_T grows when σ grows. The corresponding value to b_T is determined by the curve $\phi_3 = 0$, which is a circumference of radius ρ . From Lemma 1.43, the maximum value of σ is $\rho^2/3$. Hence, substituting this value on the coordinates of the point T , given

in Lemma 1.39, we obtain the curve parameterized by ρ that writes, in implicit form, as $\Gamma_1 = 0$. From the different minimum values of σ given in Lemma 1.43, we obtain the curves $\Gamma_2 = 0$ when $\rho \in (2, 3)$, $\Gamma_3 = 0$ when $\rho \in (1, 2]$ and $\Gamma_4 = b^2 + b^2a + a + a^2 + a^3 = 0$ when $\rho \in (0, 1]$.

The region where T moves is depicted in gray together with the curves $\Gamma_i = 0$, $i = 1, \dots, 4$ and the compatibility condition $a^2 + b^2 > 1$, that defines the curve Γ_0 , in Figure 1.14. Notice that the curve $\Gamma_4 = 0$, that appears only when $\rho \in (0, 1]$, does not define the boundary of the region of the statement because it is totally contained in the region $a^2 + b^2 < 1$ for these values of ρ .

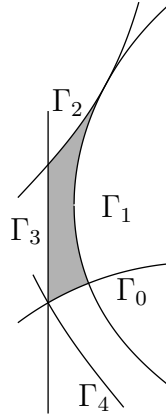


Figure 1.14 Graphs of the curves $\Gamma_i = 0$ given in the proof of Lemma 1.44 and which define the boundary of the region where the point T moves

Straightforward computations finish the proof by looking for the intersection points of the different components of the boundary curve. \square

Proposition 1.45. Let $(a, b) \in \mathbb{R}^2$ with $\mu = a^2 + b^2 > 1$. Consider the regions

$$(i) \mathcal{S}_0 = \{(a, b) \in \mathbb{R}^2 : \phi_2^M > 0, \phi_3^M > 0\},$$

$$(ii) \mathcal{S}_1 = \{(a, b) \in \mathbb{R}^2 : \phi_3^M < 0\} \setminus \mathcal{S}_2,$$

$$(iii) \mathcal{S}_2 = \{(a, b) \in \mathbb{R}^2 : \phi_2^M < 0, \Gamma_0 > 0, \Gamma_2 > 0, \Gamma_3 > 0\},$$

with

$$\phi_2^M = 3(a^2 + b^2)^2 + 4(a - 2)(a^2 + b^2) + 3 - 2a,$$

$$\phi_3^M = (a + 1)^2 + b^2 - 3,$$

$$\Gamma_0 = a^2 + b^2 - 1,$$

$$\Gamma_2 = 2a^3 + 2ab^2 - 2a + 1,$$

$$\Gamma_3 = 2a - 1.$$

For any (a, b) in \mathcal{S}_i , the number of changes of signs in the coefficients of the function ϕ , see (1.33), is at most i for any $i = 0, 1, 2$. Moreover, there exist values x_0, x_1, x_2 in $(0, 1)$ such that this number is exactly i . See the bifurcation diagram in Figure 1.15.

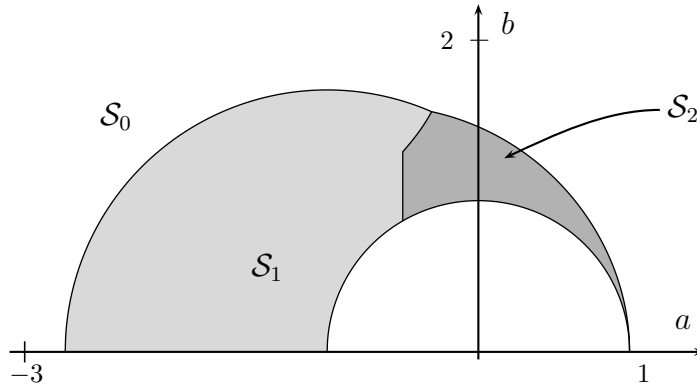


Figure 1.15 Bifurcation diagram of the number of changes of sign for the coefficient of the function ϕ

Proof. The diagram of the number of changes of sign for the coefficients of the function ϕ can be obtained considering the region covered by \mathcal{S}_i^* for $i = 0, 1, 2$, defined on Lemma 1.39, moving the values of x_0, x_1, x_2 in the interval $(0, 1)$.

First we study the areas covered by the boundaries $\phi_2 = 0$, $\phi_3 = 0$. From the expressions (1.38), we have that $a_2(\mu)$ grows when ρ is constant and σ decrease or when σ is constant and ρ grows. In both situations, the graphs do not intersect each other. The value of $a_3(\mu)$, that does not change with σ , grows when ρ grows and the graphs do not intersect each other for different values of ρ . Figure 1.16.(a) shows how these curves move in the plane (a, b) . This property of monotonous sweep shows that both, the curve that defines the region with two changes of sign, $\phi_2^M = 0$, and the one that defines the regions with one change of sign, $\phi_3^M = 0$, are obtained for the maximum values of ρ and σ . That is $\rho = 3$ and $\sigma = 3$. See Figure 1.16.(b).

Finally, the complete bifurcation diagram follows adding the region, see Lemma 1.44, where the point T moves. This diagram is plotted in Figure 1.9. □

Finally we can provide the complete bifurcation diagram of maximal configurations for our problem.

Theorem 1.46. *The maximal configuration of zeros of $\mathcal{P}(1, 2)$ depending on (a, b) is*

(i) $(3, 1, 0)$ in $\tilde{\mathcal{S}}_0 = \mathcal{S}_0 \cup \{(a, b) \in \mathcal{S}_2 : \mathcal{D} > 0\}$,

(ii) $(3, 1, 1)$ in $\tilde{\mathcal{S}}_1 = \mathcal{S}_1$,

(iii) $(3, 1, 2)$ in $\tilde{\mathcal{S}}_2 = \{(a, b) \in \mathcal{S}_2 : \mathcal{D} < 0\}$,

for a function $\mathcal{D}(a, b)$ such that the curve $\{(a, b) : \mathcal{D} = 0\} \subset \{(a, b) \in \mathbb{R}^2 : \phi_2^M < 0 \text{ and } \phi_3^M > 0\}$. Where $\mathcal{S}_0, \mathcal{S}_1, \mathcal{S}_2, \phi_2^M$ and ϕ_3^M are defined in Proposition 1.45.

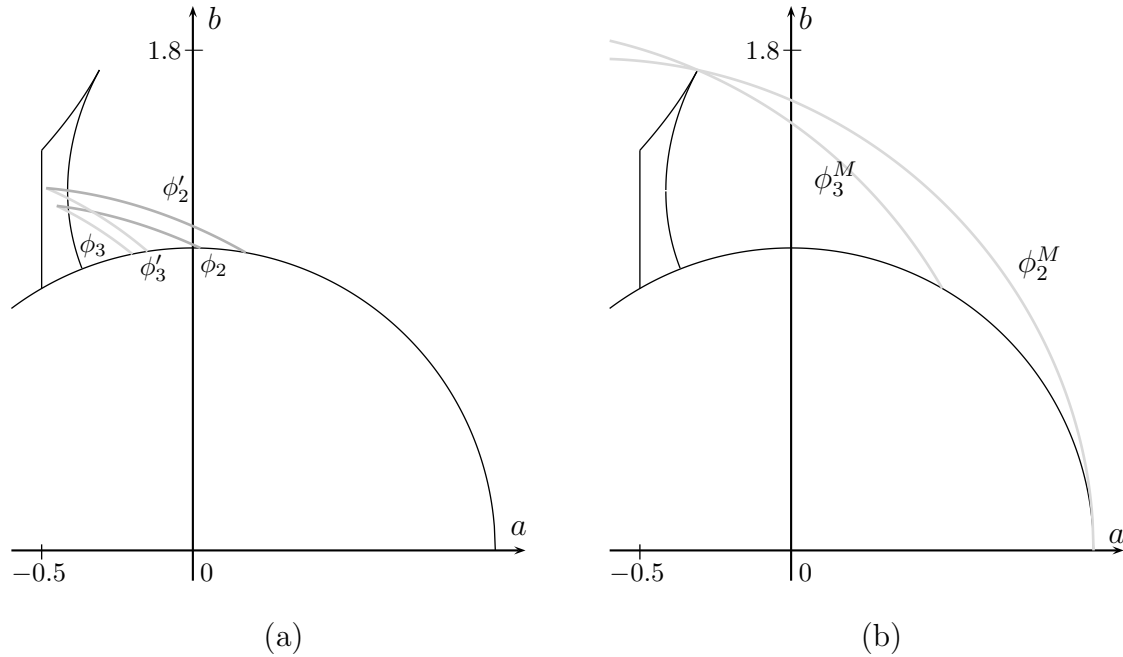


Figure 1.16 Graphs of the functions $\phi_2 = 0$ and $\phi_3 = 0$ for different values of (a, b) . A comparison for fixed σ and growing ρ is showed in (a). The boundary of the regions are represented in (b).

Proof. In the proof of Proposition 1.45, see Figure 1.15, we have studied the number of changes of sign of the coefficients of ϕ . This prove that in the regions \mathcal{S}_i for $i = 0, 1, 2$, we have that the maximal configurations are $(3, 1, 0)$, $(3, 1, 1)$ and $(3, 1, 0)$ or $(3, 1, 2)$, respectively. In fact, the sweep arguments of the proofs of Lemma 1.44 and Proposition 1.45 prove that in the region $\overline{\mathcal{S}}_2 = \mathcal{S}_2 \cap \{(a, b) \in \mathbb{R}^2 : \phi_3^M < 0\}$ we have the configuration $(3, 1, 2)$. See Figure 1.17. Also the curves $\mathcal{D}^* = 0$, given in Proposition 1.41, contained between the regions $\{(a, b) \in \mathbb{R}^2 : \phi_2 < 0 \text{ and } \phi_3 > 0\}$ for every ρ and σ force the existence of a curve $\mathcal{D} = 0$ contained in the region $\{(a, b) \in \mathbb{R}^2 : \phi_2^M < 0 \text{ and } \phi_3^M > 0\}$ such that distinguishes the configurations $(3, 1, 0)$ from $(3, 1, 2)$. \square

As it can be seen in the proof of the previous result, the complete bifurcation diagram for the exact number of zeros comes from studying how the curve $\mathcal{D}^* = 0$ moves when ρ , σ and τ change. This study is similar to the procedure for the curves $\phi_2 = 0$ and $\phi_3 = 0$ made in the proof of Proposition 1.45. From the plots of the curve $\mathcal{D}^* = 0$ for different values of ρ, σ, τ , it seems also that some monotonous properties can be observed. Taking the same values used for $\phi_2^M = 0$, $\rho = \sigma = 3$, we obtain that $\tau = 1$ and using $\mu = a^2 + b^2$, we have a possible candidate for $\mathcal{D} = 0$. That is

$$\mathcal{D} = 4a^4b^2 + 8a^2b^4 + 4b^6 + 4a^5 + 8a^3b^2 + 4ab^4 - 9a^4 - 18a^2b^2 - 9b^4 + 4a^3 + 4ab^2 + 2a^2 + 2b^2 - 1.$$

As in Proposition 1.41, this curve would be the bifurcation curve from 0 to exactly 2 zeros for $\rho = \sigma = 3$ and $\tau = 1$. Numerically we show that it is, in fact, the bifurcation

curve for the general case. The bifurcation diagram given in Theorem 1.46 is showed on Figure 1.17.

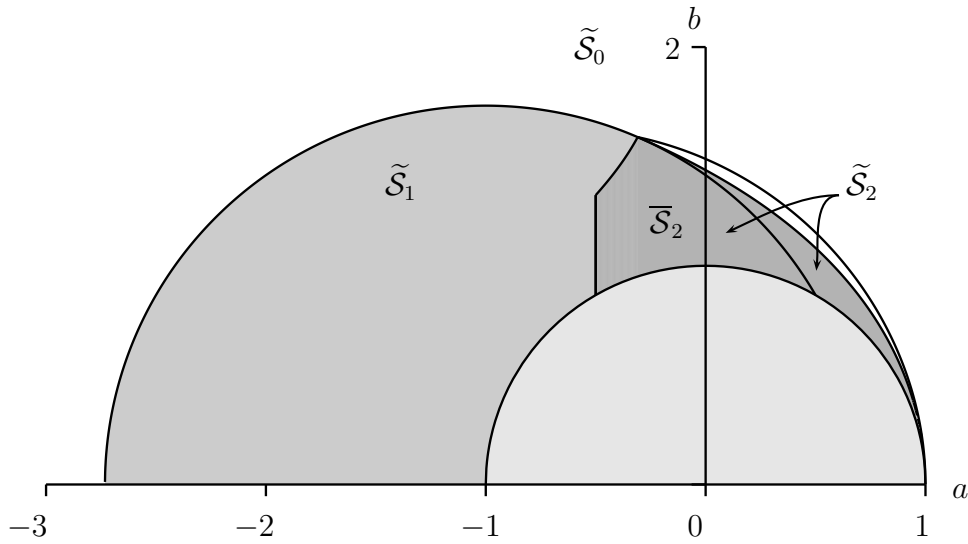


Figure 1.17 Bifurcation diagram for the configurations $(3, 1, w)$ for $w = 0, 1, 2$. \bar{S}_i are defined in Theorem 1.46 and \tilde{S}_2 in its proof

Chapter 2

Existence and Uniqueness of limit cycles for generalized φ -laplacian Liénard equations

2.1 Introduction

Liénard equation,

$$x'' + f(x)x' + g(x) = 0, \quad (2.1)$$

appears as simplified model in many domains in science and engineering. It was intensively studied during the first half of 20th century as it can be used to model oscillating circuits or simple pendulums. In the simple pendulum case, f and g represents the friction and acceleration terms. One of the first models where this equation appears was introduced by Balthasar van der Pol. See [Pol26]. Considering the equation

$$x'' + \mu(x^2 - 1)x' + x = 0,$$

for modeling the oscillations of a triode vacuum tube. See [GH02] for other references about more applications.

The first results on the existence and uniqueness of periodic solutions on the Liénard equation appear in [LS42, San49]. For some results on the existence and uniqueness of limit cycles, some papers like [Vil82] or [Vil83] and the books [YCC⁺86] and [ZDHD92] could also be referred. Additionally, more current references on related problems are [DMD11] and [LL12].

In this chapter, some criteria are presented for existence and uniqueness results on limit cycles for the generalized φ -laplacian Liénard equation

$$(\varphi(x'))' + f(x)\psi(x') + g(x) = 0 \quad (2.2)$$

Besides the obvious mathematical interest of this generalization, our main motivation for considering such equation comes from some relativistic models studied before. Special Relativity imposes a universal bound for the propagation speed of any gravitational

or electromagnetic wave. If c is the speed of light in the vacuum, in the framework of Special Relativity the momentum of a particle with unitary rest mass is given by $\varphi(x') = \frac{x'}{\sqrt{1 - \frac{x'^2}{c^2}}}$, see [Gol80]. The harmonic relativistic oscillator,

$$\left(\frac{x'}{\sqrt{1 - \frac{x'^2}{c^2}}} \right)' + x = 0,$$

is a classical topic studied in several papers, for example [Gol57, Mic98]. Other authors have included damping terms and nonlinear forces. An example is the forced pendulum with relativistic effects, which model can be expressed as

$$\left(\frac{x'}{\sqrt{1 - \frac{x'^2}{c^2}}} \right)' + kx' + a \sin x = p(t) \quad (2.3)$$

where $p(t)$ is a periodic function. It is treated in [Tor08], where conditions on the function p are given for which equation (2.3) presents periodic orbits.

In the case of Liénard equation (2.1), it is usual to apply some change of variables to express the equation as the planar system

$$\begin{cases} \dot{x} = y - F(x), \\ \dot{y} = -g(x) \end{cases}$$

or

$$\begin{cases} \dot{x} = y, \\ \dot{y} = -g(x) - f(x)y. \end{cases}$$

In this chapter a variation of this approach is considered. Our results apply to system

$$\begin{cases} \dot{x} = \varphi^{-1}(y), \\ \dot{y} = -g(x) - f(x)\psi(y\varphi^{-1}(y)), \end{cases} \quad (2.4)$$

or, after a time rescaling, to system

$$\begin{cases} \dot{x} = y\varphi'(y), \\ \dot{y} = -g(x) - f(x)\psi(y). \end{cases} \quad (2.5)$$

Before stating the results some necessary hypotheses are introduced. All the functions in (2.2) should be at least locally Lipschitz continuous, $\mathcal{C}^{0,1}$, except $\varphi(y)$ that should be in $\mathcal{C}^{1,1}$. These properties assure the existence and uniqueness of a solution for any initial value problem associated to system (2.4) or (2.5). More regularity of each function is required in some concrete results.

Let \mathcal{D} be the greater connected domain, neighborhood of the origin, for which the four functions in (2.2), $\varphi(y)$, $\psi(y)$, $f(x)$ and $g(x)$, are well defined. In this way \mathcal{D} can be consider as $\mathcal{D} = (x_1, x_2) \times (y_1, y_2)$ where $x_1, y_1 \in \mathbb{R}^- \cup \{-\infty\}$ and $x_2, y_2 \in \mathbb{R}^+ \cup \{+\infty\}$.

Along this chapter all the limits considered for x or y tending to x_i or y_i with $i = 1, 2$ are limits from the interior of the intervals of definition. It means that, for example, we denote $y \rightarrow y_2$ instead of $y \rightarrow y_2^-$.

Based on the results of the classical Liénard equation (2.1) given in [Vil82, Vil83, ZDHD92] the following conditions, denoted by (H) , are established.

(H_0) $f(x)$, $g(x)$ and $\psi(y)$ are of class $\mathcal{C}^{0,1}(\mathbb{R})$ and $\varphi(y)$ is of class $\mathcal{C}^{1,1}(\mathbb{R})$.

(H_1) $xg(x) > 0$ for all $x \in (x_1, x_2) \setminus \{0\}$ and $g(0) = 0$.

(H_2) $f(0) \neq 0$.

(H_3) $\text{Dom}(\varphi) \subseteq \text{Dom}(\psi)$.

(H_4) $\psi(0) = 0$.

(H_5) $\varphi'(y) \in \mathbb{R}^+ \setminus \{0\}$ for all $y \in (y_1, y_2)$ and $\varphi(0) = 0$.

(H_0) represents the regularity condition. (H_1) and (H_2) are inherited from the referred classic results. $(H_3 - H_5)$ are the most basic hypotheses that we impose to $\varphi(y)$ and $\psi(y)$. We have included the extra condition $\varphi(0) = 0$ for simplicity and symmetry reasons. Without loss of generality, the case $\varphi(0) \neq 0$ can also be considered after doing a translation of this function.

Briefly the aim of this chapter is to provide conditions on functions f , g , φ and ψ such that system (2.5) has at least a periodic orbit and, moreover, if it exists, when it is unique. Next two results summarize these properties.

Theorem 2.1. *[Existence Theorem] Consider system (2.5) under the hypotheses (H) . Additionally, next properties hold.*

- (i) $y\psi(y)f(x) \leq 0$ in a neighborhood of the origin, $I_x \times I_y = [x_-, x_+] \times [y_-, y_+] \subset \mathcal{D}$, except for a finite number of points where it vanishes.
- (ii) There exist δ and η in \mathbb{R} , with $x_1 < \eta < 0 < \delta < x_2$, such that $f(x) > 0$ for all $x \in (x_1, x_2) \setminus [\eta, \delta]$.
- (iii) For each $i = 1, 2$ there exists λ_i in $\mathbb{R}^+ \cup \{+\infty\}$ such that, if $|x_i| = +\infty$, then $\liminf_{x \rightarrow x_i} x(|g(x)| + f(x)) = \lambda_i$, and if $x_i \in \mathbb{R}$, then $\liminf_{x \rightarrow x_i} |x - x_i|(|g(x)| + f(x)) = \lambda_i$.
- (iv) $y\psi(y) > 0$ for all $y \neq 0$.
- (v) For $i = 1, 2$, $\lim_{y \rightarrow y_i} \psi(y)/(y\varphi'(y)) \in \mathbb{R}$.
- (vi) The integral $\int_{\eta}^{\delta} f(x)dx$ is positive or, alternatively, there exists $y_0 \in (y_1, y_2)$ such that $-\psi(y_0) \in \left[\liminf_{x \rightarrow x_i} g(x)/f(x), \limsup_{x \rightarrow x_i} g(x)/f(x) \right]$ for at least one of the x_i and there exists U , neighborhood of y_0 , such that $\text{sign}(\psi'(y))$ is constant almost for every $y \in U$.

Then system (2.5) has at least a periodic orbit contained in \mathcal{D} .

Theorem 2.2. [Unicity Theorem] Consider system (2.5) under the hypotheses (H). Additionally, next properties hold.

- (i) $f, g \in \mathcal{C}^{0,1}((x_1, x_2))$ and $\varphi, \psi \in \mathcal{C}^{1,1}((y_1, y_2))$ with $x_1, y_1 \in \mathbb{R}^- \cup \{-\infty\}$ and $x_2, y_2 \in \mathbb{R}^+ \cup \{+\infty\}$.
- (ii) There exist $a < 0 < b$ such that $f(x) < 0$ when $x \in (a, b)$ and $f(x) > 0$ when $x \in (x_1, x_2) \setminus [a, b]$,
- (iii) $\frac{d}{dx} \left(\frac{f(x)}{g(x)} \right) > 0$, for all $x \in (x_1, x_2) \setminus I_0$ where $I_0 \subset [a, b]$ such that I_0 contains the origin and $I_0 = (a, x_0)$ or $I_0 = (x_0, b)$ with x_0 satisfying that $\int_0^{x_0} g(s)ds = \min \left\{ \int_0^a g(s)ds, \int_0^b g(s)ds \right\}$.
- (iv) $\psi'(y) > 0$ and $\frac{d}{dy} \left(\frac{\psi'(y)}{y\varphi'(y)} \right) < 0$, for all y in $(y_1, y_2) \setminus \{0\}$.

Then system (2.5) has at most one limit cycle. Moreover, when it exists, it is stable.

In Section 2.2, we present the different kinds of functions that we can find in our study. The Section 2.3 is devoted to introduce a new way to compactify the domain \mathcal{D} to $\tilde{\mathcal{D}} = (-1, 1) \times (-1, 1)$. This compactification allows us to consider the *boundary of \mathcal{D}* as the inverse of the boundary of $\tilde{\mathcal{D}}$. Hence, we can study the behavior of the differential equation (2.4) close to the boundary of \mathcal{D} . Moreover, this compactification allows us to consider all the cases in a unified way. So we restrict our study to the case $\mathcal{D} = \tilde{\mathcal{D}}$. In Section 2.4, we show some first integrals of the particular cases of (2.5) when the friction term vanishes, $f(x) = 0$,

$$\begin{cases} \dot{x} = y\varphi'(y), \\ \dot{y} = -g(x), \end{cases} \quad (2.6)$$

or when the acceleration term vanishes, $g(x) = 0$,

$$\begin{cases} \dot{x} = y\varphi'(y), \\ \dot{y} = -f(x)\psi(y). \end{cases} \quad (2.7)$$

We use both first integrals as state functions of system (2.5).

These first sections include all the technical results needed to prove the main results. Hence, in Section 2.5, we prove the Existence Theorem, Theorem 2.1. The proof follows from the Poincaré-Bendixson theorem, see [CL55], because the statement ensures that the origin and the boundary of \mathcal{D} have the same stability, in fact both are repellers. Proposition 2.6 studies the stability of the origin and Propositions 2.20 and 2.21 deal with the stability of the boundary of \mathcal{D} . Finally, Section 2.6 is devoted to prove the uniqueness of limit cycle in the whole space, Theorem 2.2. The proof, as it is done in [ZDHD92], is obtained by contradiction, computing the integral of the divergence of the vector field between any two consecutive limit cycles. We remark that our proof does not need any restriction on the location of the limit cycles.

2.2 Function families

In this chapter we only consider three basic different behaviors of $\varphi(y)$ over y_i for $i = 1, 2$. We say that

- (a) $\varphi(y)$ is *singular* over y_i if $y_i \in \mathbb{R}$ and $\lim_{y \rightarrow y_i} \varphi(y) = \pm\infty$,
- (b) $\varphi(y)$ is *non-bounded regular* over y_i if $y_i = \pm\infty$ and $\lim_{y \rightarrow y_i} \varphi(y) = \pm\infty$, and,
- (c) $\varphi(y)$ is *bounded regular* over y_i if $y_i = \pm\infty$ and $\lim_{y \rightarrow y_i} \varphi(y) \in \mathbb{R}^+$.

For shortness, we denote above properties by S_i , NB_i and B_i , respectively. Some graphical representations of this basic functions are showed in Figure 2.1.

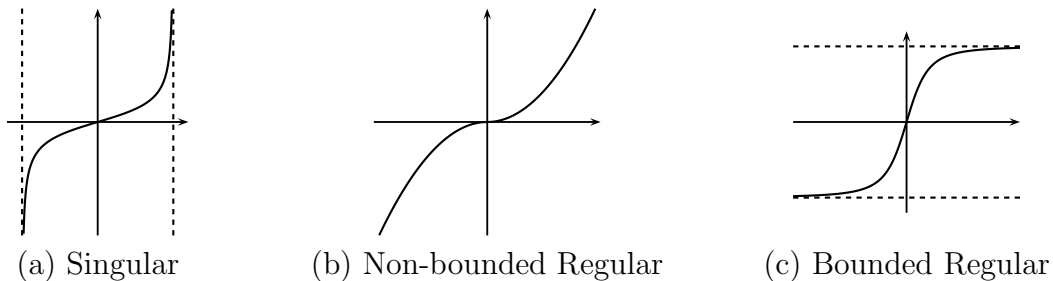


Figure 2.1 Basic φ functions

The most representative function of the singular case could be the relativistic operator, $\varphi(s) = s/\sqrt{1-s^2}$. An example of the non-bounded regular case is the p-laplacian operator, $\varphi(s) = |s|^{p-1}s$. And for the bounded regular case, we can use, for example, the mean curvature operator, $\varphi(s) = s/\sqrt{1+s^2}$. These three examples are well known in the literature about φ -laplacian problems. See for example [BJM10], [WSM⁺09] or [DCM09], respectively.

Although the previous examples are all symmetric we do not ask for any symmetry to the function $\varphi(y)$, nor a symmetric behavior at the boundary of the domain. Therefore some mixed cases can also be considered. Hence, the results of this chapter apply also for functions like $\varphi(s) = s/(1-s)$ or $\varphi(s) = e^s - 1$. See Figure 2.2.

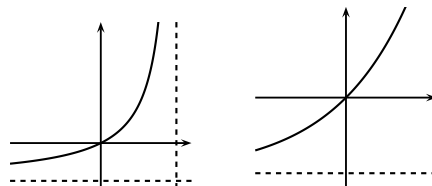


Figure 2.2 Some examples of mixed behavior at the boundary of the domain

We also consider different kinds of function $f(x)$ in terms of the type of its domain of definition. So we say that we are in a *finite (infinite) case on x_i* , denoted by $F_i (I_i)$, if $x_i \in \mathbb{R} (x_i \notin \mathbb{R})$. The results of this chapter also apply when we have not symmetry in the behavior of $f(x)$ at both $x_i, i = 1, 2$, at the same time, as in the case of the function φ . An example of this situation is the function $f(s) = \frac{s^2}{1-s} - 1$, shown in Figure 2.3.

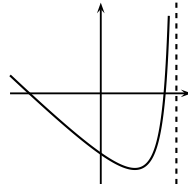


Figure 2.3 A mixed function $f(x)$

The functions g and ψ are actually determined by the hypotheses (H) and, as it can be seen in the next section, they do not play an special role in the compactification. Hence it is not necessary to study their different behaviors at the boundary of the domain.

2.3 A Polygonal Compactification

The main tool of this chapter is a transformation of the domain of definition, $\mathcal{D} = (x_1, x_2) \times (y_1, y_2)$, of the generalized Liénard differential equation (2.5). Next proposition allows us to unify all the different behaviors detailed in the previous section via a transformation to the square $(-1, 1) \times (-1, 1)$. We consider it as a polygonal compactification because the closure of the new domain is a compact set which boundary is a polygon.

Proposition 2.3. *Given system (2.5) satisfying (H) and defined in $\mathcal{D} = (x_1, x_2) \times (y_1, y_2)$ where $x_1, y_1 \in \mathbb{R}^- \cup \{-\infty\}$ and $x_2, y_2 \in \mathbb{R}^+ \cup \{+\infty\}$, there exists a change of variables of class \mathcal{C}^1 such that (2.5) writes as*

$$\begin{cases} \dot{w} &= \chi(z), \\ \dot{z} &= -\tilde{g}(w) - \tilde{f}(w)\tilde{\psi}(z), \end{cases} \quad (2.8)$$

the new domain of definition is $\tilde{\mathcal{D}} = (-1, 1) \times (-1, 1)$ and the functions $\tilde{f}, \tilde{g}, \tilde{\psi}$ and χ satisfy the following properties.

(\tilde{H}_0) $\tilde{f}(w), \tilde{g}(w)$ and $\tilde{\psi}(z), \chi(z)$ are of class $\mathcal{C}^{0,1}(\mathbb{R})$.

(\tilde{H}_1) $w\tilde{g}(w) > 0$ for all $w \in (-1, 1) \setminus \{0\}$ and $\tilde{g}(0) = 0$.

(\tilde{H}_2) $\tilde{f}(0) \neq 0$.

$$(\tilde{H}_3) \text{ Dom}(\chi) \subseteq \text{Dom}(\tilde{\psi}).$$

$$(\tilde{H}_4) \tilde{\psi}(0) = 0.$$

$$(\tilde{H}_5) z\chi(z) > 0 \text{ for all } z \in (-1, 1) \text{ and } \chi(0) = 0.$$

From now on we use either system (2.5) defined in \mathcal{D} or system (2.8) defined in $\tilde{\mathcal{D}}$. A graphical interpretation of the last result can be seen in Figure 2.4.

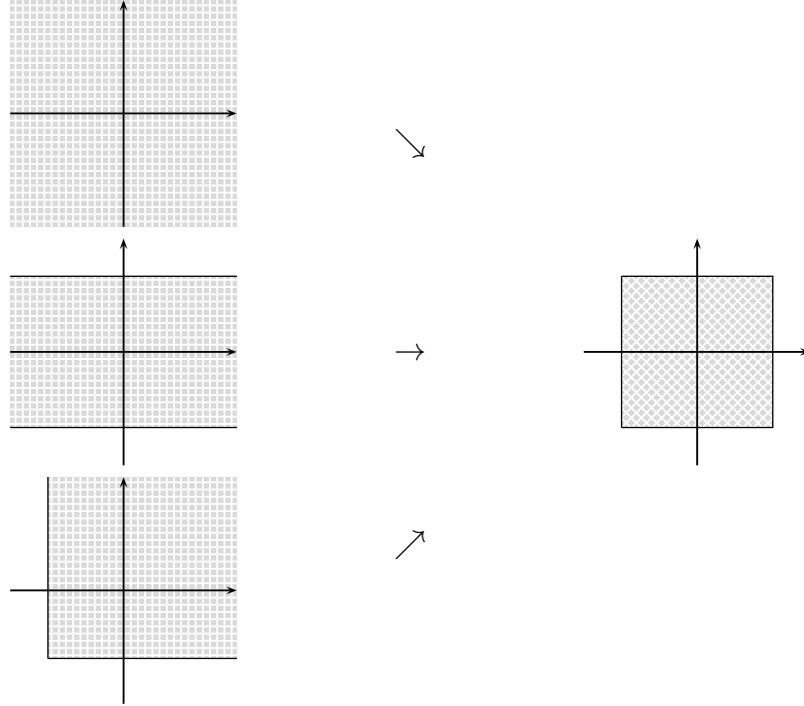


Figure 2.4 Some examples of compactified boundaries

Proof of Proposition 2.3. All the functions, f , g , φ and ϕ are functions of one variable. Taking into account the symmetry of the hypotheses (H) with respect to the origin we can consider different changes of variables for the positive and the negative axes. These changes define a global piecewise change of class \mathcal{C}^1 for the variable x and another one for the variable y . Hence system (2.5) is equivalent to system (2.8) and all the conditions of hypotheses (H) are transformed to the equivalent conditions of hypotheses (\tilde{H}). From the above considerations we only show the changes corresponding to first quadrant, that is $x > 0$ and $y > 0$. The other follow analogously.

Following the classification of Section 2.2 we consider all possible cases F_2 , I_2 , S_2 , NB_2 and B_2 because the changes of variables are different for each type.

For the type F_2 , let us consider the change of variable

$$w = \frac{x_2 x}{(x_2 - 1)x + x_2} \text{ which inverse is } x = \frac{x_2 w}{(1 - x_2)w + x_2},$$

that transforms (2.5) to

$$\begin{cases} \dot{w} &= y\varphi'(y), \\ \dot{y} &= -\tilde{g}(w) - \tilde{f}(w)\psi(y) \end{cases}$$

where

$$\tilde{g}(w) = \frac{x_2^2 g\left(\frac{x_2 w}{(1+x_2)w+x_2}\right)}{((1-x_2)w+x_2)^2} \quad \text{and} \quad \tilde{f}(w) = \frac{x_2^2 f\left(\frac{x_2 w}{(1+x_2)w+x_2}\right)}{((1-x_2)w+x_2)^2}$$

and the corresponding side of the boundary of the transformed \mathcal{D} is the line $w = 1$.

For the type I_2 , we consider the change of variable

$$w = \frac{x}{1+|x|} \quad \text{which inverse is} \quad x = \frac{w}{1-|w|}, \quad (2.9)$$

that transforms (2.5) to

$$\begin{cases} \dot{w} &= y\varphi'(y), \\ \dot{y} &= -\tilde{g}(w) - \tilde{f}(w)\psi(y) \end{cases}$$

where

$$\tilde{g}(w) = \frac{g\left(\frac{w}{1-|w|}\right)}{(1-|w|)^2} \quad \text{and} \quad \tilde{f}(w) = \frac{f\left(\frac{w}{1-|w|}\right)}{(1-|w|)^2}.$$

Moreover, the line $w = 1$ contains the corresponding side of the boundary of the transformed \mathcal{D} .

For the type S_2 , consider the change of variable

$$z = \frac{y_2^2 y}{y^2 - y_2(2 - y_2)y + y_2^2}$$

which inverse is

$$y = \frac{y_2}{2z} \left((2 - y_2)z + y_2 - \sqrt{y_2(z-1)((y_2-4)z - y_2)} \right),$$

and (2.5) writes as

$$\begin{cases} \dot{x} &= \frac{y_2}{2z} \left((2 - y_2)z + y_2 - \sqrt{y_2(z-1)((y_2-4)z - y_2)} \right) \tilde{\varphi}'(z), \\ \dot{z} &= -g(x) - f(x)\tilde{\psi}(z), \end{cases}$$

where

$$\begin{aligned} \tilde{\varphi}(z) &= \varphi \left(\frac{y_2}{2z} \left((2 - y_2)z + y_2 - \sqrt{y_2(z-1)((y_2-4)z - y_2)} \right) \right), \\ \tilde{\psi}(z) &= \psi \left(\frac{y_2}{2z} \left((2 - y_2)z + y_2 - \sqrt{y_2(z-1)((y_2-4)z - y_2)} \right) \right) \quad \text{and} \end{aligned}$$

$z = 1$ contains the boundary of the transformed \mathcal{D} .

For the type NB_2 , let us consider the change of variable

$$z = \frac{y}{1 + |y|} \text{ which inverse is } y = \frac{z}{1 - |z|}, \quad (2.10)$$

and (2.5) writes as

$$\begin{cases} \dot{x} &= z \frac{\tilde{\varphi}'(z)}{1 - |z|}, \\ \dot{z} &= -g(x) - f(x)\tilde{\psi}(z) \end{cases}$$

where

$$\tilde{\varphi}(z) = \varphi\left(\frac{z}{1 - |z|}\right), \quad \tilde{\psi}(z) = \psi\left(\frac{z}{1 - |z|}\right)$$

and $z = 1$ contains a piece of the boundary of the transformed \mathcal{D} .

Finally, for the type B_2 if $\lim_{y \rightarrow y_2} \varphi(y) = \nu_2$, the change of variable needed is

$$z = \frac{\varphi\left(\frac{\nu_2}{\varphi'(0)}y\right)}{\nu_2} \text{ which inverse is } y = \frac{\varphi'(0)}{\nu_2}\varphi^{-1}(\nu_2 z),$$

that allow us to express (2.5) as follows

$$\begin{cases} \dot{x} &= \gamma(z), \\ \dot{z} &= -g(x) - f(x)\tilde{\psi}(z), \end{cases}$$

where

$$\gamma(z) = \frac{(\varphi'(0))^2}{\nu_2}\varphi^{-1}(\nu_2 z) \frac{\varphi'\left(\frac{\varphi'(0)}{\nu_2}\varphi^{-1}(\nu_2 z)\right)}{\varphi'(\varphi^{-1}(\nu_2 z))}, \quad \tilde{\psi}(z) = \psi\left(\frac{\varphi'(0)}{\nu_2}\varphi^{-1}(\nu_2 z)\right)$$

and again $z = 1$ contains the boundary of the transformed \mathcal{D} .

The proof ends checking that the global piecewise changes are all \mathcal{C}^1 . This is done because any of the previous changes are of class \mathcal{C}^1 for $x \neq 0$ or $y \neq 0$. Moreover, the left and right derivatives at the origin coincides, in fact, $w'(0^+) = w'(0^-) = 1$ and $z'(0^+) = z'(0^-) = 1$. Therefore we combine the changes depending on the behavior at \mathbb{R}^+ and \mathbb{R}^- . \square

Under hypothesis (H_0) , system (2.5) satisfies the sufficient conditions to assure existence and unicity of any initial value problem in \mathcal{D} . Then, from the previous proposition, this is also done for the equivalent system (2.8) in the corresponding $\tilde{\mathcal{D}}$.

2.4 State functions

In a general framework, a differential equation can be thought as a dynamical system. In that case, a function of state, also called state function, E is a property of the system that depends only on the current state of it. That is, the value of the function E at some point is independent of the processes undergone by the system to arrive to this value. State functions usually appear in physical and chemical systems, for example the mass, the energy, the entropy and the temperature, among others.

The state functions, for system (2.5), described in this section are constructed as first integrals in the null friction and the null acceleration cases, (2.6) and (2.7) respectively. They are very helpful in the study of system (2.5), particularly in the proof of the Uniqueness Theorem, Theorem 2.2.

Lemma 2.4. *[Primary Energy Function] The function $E(x, y) = G(x) + \Phi(y)$, where $G(x) = \int_0^x g(u)du$ and $\Phi(y) = \int_0^y v\varphi'(v)dv$, is a first integral of system (2.6) in \mathcal{D} . Moreover $E(0, 0) = 0$ and the origin is a local center.*

Proof. Straightforward computations show that E is well defined and $\dot{E} \equiv 0$ over the solutions of system (2.6). The existence of the first integral and the monodromic structure of the origin gives the center property \square

Likewise, next result holds.

Lemma 2.5. *[Secondary Energy Function] The function $J(x, y) = F(x) + \Psi(y)$, where $F(x) = \int_0^x f(u)du$ and $\Psi(y) = \int_0^y \frac{v\varphi'(v)}{\psi(y)}dv$, is a first integral of (2.7) in \mathcal{D} . Moreover $J(0, 0) = 0$.*

2.5 Existence results

Theorem 2.1, the Existence Theorem, is a consequence of the results of this section. In order to simplify the reading of all the results we refer to system (2.5), defined in \mathcal{D} , for the functions f, g, φ, ψ and to system (2.8), defined in $\tilde{\mathcal{D}}$, for the corresponding transformed functions $\tilde{f}, \tilde{g}, \tilde{\chi}, \tilde{\psi}$, via the change of variables of Proposition 2.3. Additionally we also assume the hypothesis (H) on (2.5) and (\tilde{H}) on (2.8).

2.5.1 Local stability of the origin

Let us show some conditions so that system (2.5) has a singular point at the origin which stability can be determined.

Proposition 2.6. *Assume that f and ψ vanish only on a finite number of points on neighborhoods of the origin $I_x = [x_-, x_+] \subset (x_1, x_2)$ and $I_y = [y_-, y_+] \subset (y_1, y_2)$, respectively. If $\text{sign } f(x)$ and $\text{sign } y\psi(y)$ are constant in I_x and I_y , then the origin is a repellor (attractor) when $y\psi(y)f(x) \leq 0$ (≥ 0). Moreover the basin of repulsion (attraction) contains the biggest level curve of the Primary Energy Function E , defined in Lemma 2.4, completely contained in $I_x \times I_y$.*

Proof. By (2.5) we have

$$\dot{E} = g(x)\dot{x} + y\varphi'(y)\dot{y} = g(x)y\varphi'(y) + y\varphi'(y)(-g(x) - f(x)\psi(y)) = -y\psi(y)\varphi'(y)f(x).$$

As $\varphi'(y) > 0$ for every $y \in (y_1, y_2) \setminus \{0\}$ the sign of \dot{E} is constant in a neighborhood of the origin. Thus we can assure that the stability of the origin, applying Hartman's Theorem, is done by the sign of $y\psi(y)f(x)$. \square

2.5.2 Stability of the infinity

This section is devoted to prove that the boundary of \mathcal{D} is a repellor under the hypotheses of Theorem 2.1. First, we study how the compactification transforms the hypotheses. Second, Proposition 2.14 explains the behavior of the orbits close to the boundaries of the compactified domain $\tilde{\mathcal{D}}$ and Definition 2.15 introduces the notion of regular and singular points in the boundary. Propositions 2.17 and 2.18 establish the dynamics of the finite points and Corollary 2.19 shows that their ω -limit remains in $\tilde{\mathcal{D}}$ or is the full boundary. Finally, we prove that the boundary is a repellor considering two cases. Proposition 2.20 deals with the case with singular points on the boundary different from the vertex and Proposition 2.21 without them.

Lemma 2.7. *If $y\psi(y) > 0$ then $z\tilde{\psi}(z) > 0$.*

Lemma 2.8. *If there exist $\delta, \eta \in \mathbb{R}$, with $x_1 < \eta < 0 < \delta < x_2$, where $f(x) > 0$ for all $x \in (x_1, x_2) \setminus [\eta, \delta]$, we have that there exist $\tilde{\delta}, \tilde{\eta} \in \mathbb{R}$, with $-1 < \tilde{\eta} < 0 < \tilde{\delta} < 1$, satisfying $\tilde{f}(w) > 0$ for all $w \in (-1, 1) \setminus [\tilde{\eta}, \tilde{\delta}]$.*

Lemma 2.9. *Assume that there exists $y_0 \in (y_1, y_2)$ such that $-\psi(y_0) \in \left[\liminf_{x \rightarrow x_i} \frac{g(x)}{f(x)}, \limsup_{x \rightarrow x_i} \frac{g(x)}{f(x)} \right]$ for at least one of the x_i and a neighborhood U of y_0 where $\text{sign}(\psi'(y))$ is constant almost for every y in U . Then this properties are also satisfied in the compactified domain.*

The proofs of the above lemmas involve straightforward computations, using the appropriate change of variables from the proof of Proposition 2.3.

Lemma 2.10. *Assume that there exist $\delta, \eta \in \mathbb{R}$, with $x_1 < \eta < 0 < \delta < x_2$, such that $f(x) > 0$ for all $x \in (x_1, x_2) \setminus [\eta, \delta]$, and $\lambda_i \in \mathbb{R}^+ \cup \{+\infty\}$ such that, for $i = 1, 2$,*

$$\begin{aligned} & \text{if } |x_i| = +\infty, \quad \liminf_{x \rightarrow x_i} x(|g(x)| + f(x)) = \lambda_i, \text{ or} \\ & \text{if } x_i \in \mathbb{R}, \quad \liminf_{x \rightarrow x_i} |x - x_i|(|g(x)| + f(x)) = \lambda_i. \end{aligned}$$

Then there exist $\tilde{\lambda}_i \in \mathbb{R}^+ \cup \{+\infty\}$ such that $\liminf_{w \rightarrow w_i} |w - w_i|(|\tilde{g}(x)| + \tilde{f}(x)) = \tilde{\lambda}_i$, for $i = 1, 2$.

Proof. The statement follows immediately for $x_i \in \mathbb{R}$, so we only prove it for $|x_2| = +\infty$. The case $|x_1| = +\infty$ is analogous. From the change of variables (2.9) we have

$$\begin{aligned} \liminf_{w \rightarrow 1} |1 - w|(|\tilde{g}(w)| + \tilde{f}(w)) &= \liminf_{x \rightarrow x_2} \left(1 - \frac{x}{1+x}\right) \frac{g(x) + f(x)}{\left(1 - \frac{x}{1+x}\right)^2} = \\ &= \liminf_{x \rightarrow x_2} (1 + |x|)(|g(x)| + f(x)) = \beta + \lambda. \end{aligned}$$

And the above expression is positive because $\beta = \liminf_{x \rightarrow x_2} (|g(x)| + f(x)) \geq 0$, since $|g(x)|$ and $f(x)$ are positive functions for $|x|$ large enough. \square

Lemma 2.11. *The function χ satisfies $\lim_{|z| \rightarrow 1} |\chi(z)| = +\infty$.*

Proof. We restrict the proof to the case $z > 0$. The other cases are analogous. Following the structure of proof of Proposition 2.3 we consider the types S_2 , NB_2 and B_2 .

For S_2 we have $\chi(z) = \frac{y_2}{2z} \left((2 - y_2)z + y_2 - \sqrt{y_2(z-1)((y_2-4)z - y_2)} \right) \tilde{\varphi}'(z)$ with

$$\tilde{\varphi}'(z) = \frac{\left((2 - y_2)z + y_2 - \sqrt{y_2(z-1)((y_2-4)z - y_2)} \right) y_2^2}{2z^2 \sqrt{y_2(z-1)((y_2-4)z - y_2)}} \varphi' \left(\frac{y_2}{2z} \left((2 - y_2)z + y_2 - \sqrt{y_2(z-1)((y_2-4)z - y_2)} \right) \right).$$

As we are in the singular type, $\lim_{y \rightarrow y_2} \varphi'(y) = +\infty$. If not, φ can be regularly extended from $y = y_2$, which contradicts the maximality of the domain \mathcal{D} . Thus,

$$\lim_{z \rightarrow 1} \chi(z) = \lim_{y \rightarrow y_2} y \varphi'(y) \frac{(y^2 - y_2(2 - y_2)y + y_2^2)^2}{y_2^2(y_2 - y)(y_2 + y)} = +\infty.$$

For NB_2 we have $\chi(z) = z\tilde{\varphi}'(z)/(1-z) = z\varphi'(z/(1-z))/(1-z)^3$ with $z \in (0, 1)$ and

$$\lim_{z \rightarrow z_2} \chi(z) = \lim_{y \rightarrow y_2} y(1+y)^2 \varphi'(y) = +\infty$$

because $\lim_{y \rightarrow y_2} y^2 \varphi'(y) = +\infty$. We show this assertion by contradiction. Assume that $\lim_{y \rightarrow y_2} y^2 \varphi'(y) = \alpha$ where α is a real number. Then there exists $y_0 > 0$ such that $\varphi'(y) < (\alpha + 1)/y^2$ for all $y > y_0$. So, it follows that

$$\begin{aligned} \varphi(y) &= \int_0^y \varphi'(v) dv = \int_0^{y_0} \varphi'(v) dv + \int_{y_0}^y \varphi'(v) dv = \varphi(y_0) + \int_{y_0}^y \varphi'(v) dv < \\ &< \varphi(y_0) + \int_{y_0}^{+\infty} \frac{\alpha + 1}{v^2} dv = \varphi(y_0) + \frac{-(\alpha + 1)}{v} \Big|_{y_0}^{+\infty} = \varphi(y_0) + \frac{\alpha + 1}{y_0} \end{aligned}$$

for all $y \in (0, +\infty)$. It means that φ is a bounded function, which contradicts the condition of being in type NB_2 .

We conclude considering the type B_2 . We have

$$\lim_{z \rightarrow 1} \chi(z) = \lim_{z \rightarrow z_2} \frac{\varphi'(0)^2}{\nu_2} \varphi^{-1}(\nu_2 z) \frac{\varphi' \left(\frac{\varphi'(0)}{\nu_2} \varphi^{-1}(\nu_2 z) \right)}{\varphi'(\varphi^{-1}(\nu_2 z))} = \lim_{y \rightarrow +\infty} \varphi'(0) y \frac{\varphi'(y)}{\varphi' \left(\frac{\nu_2}{\varphi'(0)} y \right)} = +\infty,$$

because

$$\lim_{y \rightarrow +\infty} \frac{\varphi'(y)}{\varphi' \left(\frac{\nu_2}{\varphi'(0)} y \right)} = 1.$$

This equality follows from $\lim_{y \rightarrow +\infty} \varphi'(y) = 0$, hence $\varphi'(y)$ is a Cauchy function. Let $\varepsilon \in (0, 1)$ and $\delta = \frac{\varepsilon}{3}$. Thus there exists y_0 such that for all $y > y_0$, $|\varphi'(y) - \varphi'(\nu_2 y / \varphi'(0))| < \delta$ holds. Therefore,

$$\min \left\{ 1 - \delta, \frac{1}{1 + \delta} \right\} < \frac{\varphi'(y)}{\varphi' \left(\frac{\nu_2}{\varphi'(0)} y \right)} < \max \left\{ 1 + \delta, \frac{1}{1 - \delta} \right\}$$

and, consequently,

$$1 - \frac{\varepsilon}{2} < 1 - \frac{\varepsilon}{3} \leq \frac{\varphi'(y)}{\varphi' \left(\frac{\nu_2}{\varphi'(0)} y \right)} \leq \frac{3}{3 - \varepsilon} < 1 + \frac{\varepsilon}{2}.$$

□

Lemma 2.12. *If the limit $\lim_{y \rightarrow y_i} \frac{\psi(y)}{y\varphi'(y)}$ is real then $\lim_{z \rightarrow z_i} \frac{\tilde{\psi}(z)}{\chi(z)} = 0$, for $i = 1, 2$.*

Proof. Let us just consider the case $i = 2$, that is $z_2 = 1$. The case $i = 1$ follows analogously. The different types that should be considered are S_2 , NB_2 and B_2 .

We start with type S_2 ,

$$\lim_{z \rightarrow 1} \frac{\tilde{\psi}(z)}{\chi(z)} = \lim_{y \rightarrow y_2} \frac{y_2^2 (y_2 - y)(y_2 + y)}{(y^2 - y_2(2 - y_2)y + y_2^2)^2} \frac{\psi(y)}{y\varphi'(y)} = \frac{2}{y_2^3} \lim_{y \rightarrow y_2} (y_2 - y) \frac{\psi(y)}{y\varphi'(y)} = 0.$$

For type NB_2 , let us consider the change (2.10) and we obtain

$$\lim_{z \rightarrow z_2} \frac{\tilde{\psi}(z)}{\chi(z)} = \lim_{z \rightarrow z_2} (1 - z) \frac{\psi \left(\frac{z}{1 - z} \right)}{\frac{z}{1 - z} \varphi' \left(\frac{z}{1 - z} \right)} = \lim_{y \rightarrow +\infty} \frac{1}{1 + y} \frac{\psi(y)}{y\varphi'(y)} = 0.$$

Finally, let us consider type B_2 . Since $\lim_{y \rightarrow +\infty} \varphi'(y) = 0$, we have

$$\lim_{z \rightarrow z_2} \frac{\tilde{\psi}(z)}{\chi(z)} = \lim_{y \rightarrow +\infty} \frac{\psi(y) \varphi' \left(\frac{\nu_2}{\varphi'(0)} y \right)}{\varphi'(0) y \varphi'(y)} = \frac{1}{\varphi'(0)} \lim_{y \rightarrow +\infty} \frac{\psi(y)}{y\varphi'(y)} \varphi' \left(\frac{\nu_2}{\varphi'(0)} y \right) = 0.$$

□

Lemma 2.13. *Let h be a function of class $C^{0,1}([0, 1])$, if $\liminf_{s \rightarrow 1} (1 - s)h(s) > 0$ then $\int_0^1 h(s)ds = +\infty$.*

Proof. From the statement, $\liminf_{s \rightarrow 1} (1 - s)h(s) = \lambda$ for a positive real number λ . Thus, there exists $\varepsilon \in (0, 1)$ such that $h(s) \geq \lambda/(2(1 - s))$, for all $s \in (1 - \varepsilon, 1)$. Hence,

$$\int_0^1 h(s)ds = \int_0^{1-\varepsilon} h(s)ds + \int_{1-\varepsilon}^1 h(s)ds.$$

The proof ends because $h(s)$ is bounded in $[0, 1 - \varepsilon]$ and

$$\int_{1-\varepsilon}^1 h(s)ds \geq \int_{1-\varepsilon}^1 \frac{\lambda}{2} \frac{1}{1-s} ds = +\infty.$$

□

Next result extends the dynamics to the boundary of \tilde{D} . Then we study the behavior of the orbits in each quadrant.

Proposition 2.14. *Consider system (2.8) under the hypotheses (\tilde{H}) . Additionally we assume that*

(i) *there exist real numbers $\tilde{\delta}, \tilde{\eta}$, such that $-1 < \tilde{\eta} < 0 < \tilde{\delta} < 1$, and $\tilde{f}(w) > 0$ for all $w \in (-1, 1) \setminus [\tilde{\eta}, \tilde{\delta}]$,*

(ii) *there exists $\tilde{\lambda}_i \in \mathbb{R}^+ \cup \{+\infty\}$ with $\liminf_{w \rightarrow w_i} |w - w_i|(|\tilde{g}(x)| + \tilde{f}(x)) = \tilde{\lambda}_i$, for $i = 1, 2$,*

(iii) *$z\tilde{\psi}(z) > 0$ for all $z \neq 0$,*

(iv) *$\lim_{|z| \rightarrow 1} |\chi(z)| = +\infty$, and*

(v) *$\lim_{z \rightarrow z_i} \tilde{\psi}(z)/\chi(z) = 0$, for $i = 1, 2$.*

Then for $i = 1, 2$, given $w_0, z_0 \in (-1, 1)$ such that $-\tilde{\psi}(z_0) \notin \left[\liminf_{w \rightarrow w_i} \frac{\tilde{g}(x)}{f(x)}, \limsup_{w \rightarrow w_i} \frac{\tilde{g}(x)}{f(x)} \right]$, the vector field defined by (2.8) is topologically equivalent to

$$\begin{cases} \dot{w} = \text{sign}(z_i), \\ \dot{z} = 0, \end{cases} \quad \text{or} \quad \begin{cases} \dot{w} = 0, \\ \dot{z} = \lim_{w \rightarrow w_i} \text{sign}(-\tilde{g}(w) - \tilde{f}(w)\tilde{\psi}(z_0)) \end{cases}$$

in a neighborhood of (w_0, z_i) or (w_i, z_0) , respectively.

Proof. First we prove the equivalence for neighborhoods of points $(w_0, \pm 1)$. For any $z \neq 0$, we can rewrite the system (2.8) with a positive time rescaling as

$$\begin{cases} \dot{w} = \text{sign}(\chi(z)), \\ \dot{z} = \frac{-\tilde{g}(w) - \tilde{f}(w)\tilde{\psi}(z)}{|\chi(z)|}. \end{cases} \quad (2.11)$$

For any fixed $w_0 \in (-1, 1)$, applying (iv) and (v), we have $\dot{z} \rightarrow 0$ when $z \rightarrow \pm 1$. It means that the segments of the boundary of $\tilde{\mathcal{D}}$ contained in $\{z = \pm 1\}$ are invariant for (2.11). Using hypotheses (\tilde{H}) , $\chi(z)$ and z have the same sign, so the proof, for this case, ends.

Finally, we only prove the equivalence for neighborhoods of points $(1, z_0)$. For the points $(-1, z_0)$ the proof is analogous. For any z_0 satisfying $-\tilde{\psi}(z_0) \notin [\liminf_{w \rightarrow 1} \tilde{g}(w)/\tilde{f}(w), \limsup_{w \rightarrow 1} \tilde{g}(w)/\tilde{f}(w)]$ there exists a neighborhood of $(1, z_0)$ in $\tilde{\mathcal{D}}$ such that $\tilde{g}(w) + \tilde{f}(w)\tilde{\psi}(z)$ does not vanishes. In this neighborhood, system (2.8) is equivalent to

$$\begin{cases} \dot{w} = \frac{\chi(z)}{|-\tilde{g}(w) - \tilde{f}(w)\tilde{\psi}(z)|}, \\ \dot{z} = \text{sign}(-\tilde{g}(w) - \tilde{f}(w)\tilde{\psi}(z)). \end{cases}$$

Hence, the equivalence follows similarly to the previous case. □

Definition 2.15. *We say that the points $(w_0, \pm 1)$ or $(\pm 1, z_0)$, are regular points in the boundary when they satisfy the properties of the Proposition 2.14. The other points, including the vertex, are called singular.*

Remark 2.16. *Proposition 2.14 extends the dynamical behavior of system (2.8) in $\tilde{\mathcal{D}}$ to the regular points of its closure. See a possible phase portrait in Figure 2.5.*

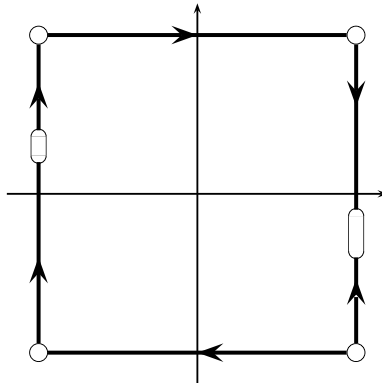


Figure 2.5 *An example of a phase portrait on the boundary. The rounded regions represent the set of singular points*

Proposition 2.17. *Under the assumptions of Proposition 2.14, the positive orbit of every point in $[0, 1) \times (0, 1)$ (resp. in $(-1, 0] \times (-1, 0)$) cuts transversally, in finite time, the segment $(0, 1) \times \{0\}$ (resp. $(-1, 0) \times \{0\}$). See Figure 2.6.*

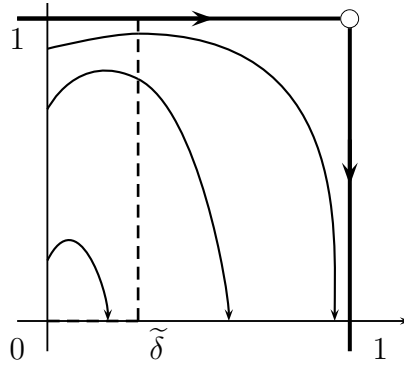


Figure 2.6 Phase portrait of system (2.8) on the first quadrant

Proof. We only prove the result on the first quadrant. The other follows by symmetry.

The first component of the vector field on the points over the positive z -axis is greater than zero. Proposition 2.14 provides a Flow Box argument for the vector field (2.8) in the neighborhood of the points $(0, 1) \times \{1\}$. As there are no critical points with $w > 0$, $z > 0$ in $\tilde{\mathcal{D}}$, the proof ends, from the Poincaré-Bendixson Theorem, showing that there are no orbits tending to $(1, z_0)$ with $z_0 > 0$. We prove it by contradiction.

In a neighborhood of the segment $\{1\} \times (0, 1)$ in $\tilde{\mathcal{D}}$, condition (ii) implies that $\lim_{w \rightarrow 1} (1-w)\tilde{g}(w)$ or $\lim_{w \rightarrow 1} (1-w)\tilde{f}(w)$ is strictly positive. Then, one of the state functions of Section 2.4. after the changes of variables of Proposition 2.3,

$$\begin{aligned}\tilde{E}(w, z) &= \tilde{G}(w) + \tilde{\Phi}(z) = \int_0^w \tilde{g}(u)du + \int_0^z \chi(v)dv \\ \tilde{J}(w, z) &= \tilde{F}(w) + \tilde{\Psi}(z) = \int_0^w \tilde{f}(u)du + \int_0^z \frac{\chi(v)}{\tilde{\psi}(v)}dv,\end{aligned}$$

goes to infinity when (w, z) tends to the boundary of $\tilde{\mathcal{D}}$ by Lemma 2.13.

Therefore, if an orbit goes to the boundary then one of the state functions goes to infinity. This contradicts with the fact that both state functions decrease over the solutions of the vector field on the region $w > \tilde{\delta}$ and $z > 0$. Because, by (i) and (\tilde{H}) ,

$$\tilde{E}(w, z) = \tilde{g}(w)\dot{w} + \chi(z)\dot{z} = -\tilde{f}(w)\tilde{\psi}(z)\chi(z) < 0$$

and

$$\tilde{J}(w, z) = \tilde{f}(w)\dot{w} + \frac{\chi(z)}{\tilde{\psi}(z)}\dot{z} = -\tilde{g}(w)\frac{\chi(z)}{\tilde{\psi}(z)} < 0.$$

□

Proposition 2.18. *Under the assumptions of Proposition 2.14, the positive orbit of every point in $(0, 1) \times (-1, 0]$ (resp. in $(-1, 0) \times [0, 1)$) cuts transversally, in finite time, the segment $\{0\} \times (-1, 0)$ (resp. $\{0\} \times (0, 1)$). See Figure 2.7.*

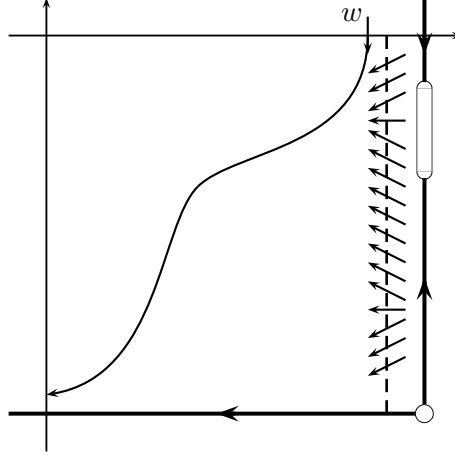


Figure 2.7 Phase portrait of system (2.8) on the fourth quadrant

Proof. We only prove the result on the fourth quadrant, the other follows by symmetry.

The second component of the vector field on the points over the positive w -axis is negative. Proposition 2.14 provides a Flow Box argument for the vector field (2.8) in the neighborhood of the points $(0, 1) \times \{-1\}$. As there are no critical points with $w > 0$, $z < 0$ in $\tilde{\mathcal{D}}$, the proof ends, from the Poincaré-Bendixson Theorem, using the condition $\dot{w} = \chi(z) < 0$ on the fourth quadrant. \square

The last two propositions imply the next corollary.

Corollary 2.19. *The ω -limit of a finite point of $\tilde{\mathcal{D}}$ can not be partially contained in the corresponding boundary.*

Finally, the proof of Theorem 2.1 follows from the next two propositions. In the first result, the boundary always presents singular points besides the vertex, while in the second does not.

Proposition 2.20. *Consider system (2.5) under the hypotheses (H) and satisfying that*

- (i) *there exist δ and η in \mathbb{R} , with $x_1 < \eta < 0 < \delta < x_2$, such that $f(x) > 0$ for all $x \in (x_1, x_2) \setminus [\eta, \delta]$,*
- (ii) *for each $i = 1, 2$ there exists λ_i in $\mathbb{R}^+ \cup \{+\infty\}$ such that, if $|x_i| = +\infty$, then $\liminf_{x \rightarrow x_i} x(|g(x)| + f(x)) = \lambda_i$, and if $x_i \in \mathbb{R}$, then $\liminf_{x \rightarrow x_i} |x - x_i|(|g(x)| + f(x)) = \lambda_i$,*
- (iii) *$y\psi(y) > 0$ for all $y \neq 0$,*

(iv) for $i = 1, 2$, $\lim_{y \rightarrow y_i} \psi(y)/(y\varphi'(y)) \in \mathbb{R}$,

(v) there exists $y_0 \in (y_1, y_2)$ such that $-\psi(y_0) \in \left[\liminf_{x \rightarrow x_i} g(x)/f(x), \limsup_{x \rightarrow x_i} g(x)/f(x) \right]$ for at least one of the x_i , $i = 1, 2$, and there exists U , neighborhood of y_0 , such that $\text{sign}(\psi'(y))$ is constant almost for every $y \in U$.

Then, the boundary of \mathcal{D} is a repellor.

Proof. Applying Lemmas 2.7 to 2.12 to system (2.8), we can compactify and we are on the hypotheses of Propositions 2.14. Then, from statement (v), see Lemma 2.9, there exists $z_0 \in (-1, 1)$ such that $-\tilde{\psi}(z_0)$ is in $I_i = \left[\liminf_{w \rightarrow w_i} \tilde{g}(w)/\tilde{f}(w), \limsup_{w \rightarrow w_i} \tilde{g}(w)/\tilde{f}(w) \right]$ for at least one of the w_i and there exists a neighborhood, \tilde{U} , of z_0 such that $\text{sign}(\tilde{\psi}'(z))$ is constant almost for every $z \in \tilde{U}$.

We only prove the case $w_2 = 1$ and $\tilde{\psi}'(z) > 0$. The other cases follow similarly.

The proof is done in two steps. In the first one, we study the behavior of the vector field close to $(1, z_0)$ and, in second place, we construct a negatively invariant region that proves that the infinity is a repellor. For the first step we distinguish two different cases, when I_2 is a proper interval or it reduces to a point.

If we are in the first case, we can assume that $\tilde{\phi}(z_0)$ is in the interior of I_2 . From the definition of \liminf and \limsup , there exists a sequence $\{w_n\}_{n=1}^{+\infty} \subset (0, 1)$ such that $\lim_{n \rightarrow +\infty} w_n = 1$ and $-\tilde{g}(w_n) - \tilde{f}(w_n)\tilde{\psi}(z_0) = 0$. Moreover, there exists $\varepsilon > 0$ such that $(z_0 - \varepsilon, z_0 + \varepsilon) \subset \tilde{U}$ and $\tilde{\psi}(z_0 - \delta) < \tilde{\psi}(z_0) < \tilde{\psi}(z_0 + \delta)$, for all δ in $(0, \varepsilon)$. Hence, it follows that for all $n \in \mathbb{N}$ and $\delta \in (0, \varepsilon)$ we have $\dot{z}(w_n, z_0 - \delta) > 0$ and $\dot{z}(w_n, z_0 + \delta) < 0$, and consequently there exists an orbit, $\Gamma(z_0)$, which α -limit set is the point $(1, z_0)$. See Figure 2.8.

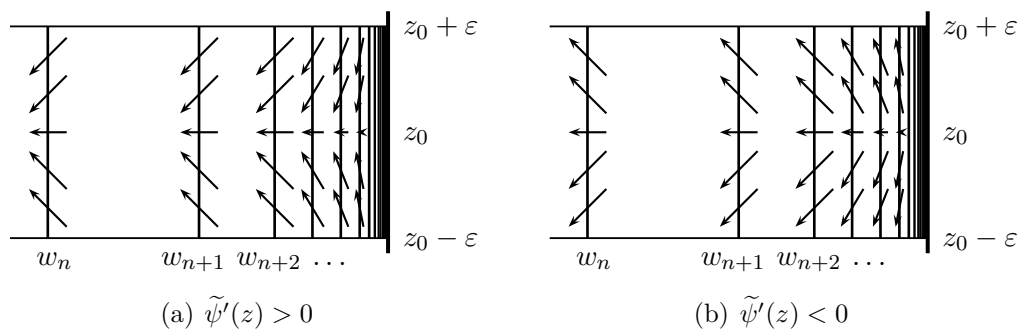


Figure 2.8 Behavior of the flux near to a continuum of singular points in the boundary

In the second case, $-\tilde{\psi}(z_0) = \lim_{w \rightarrow 1} \tilde{g}(w)/\tilde{f}(w)$ and $\tilde{\psi}'(z) > 0$ in \tilde{U} . Then the branch of $\tilde{\psi}^{-1} \left(-\tilde{g}(w)/\tilde{f}(w) \right)$ defined in \tilde{U} is a well defined function for all $w \in (1 - \gamma, 1)$ for a positive small enough γ . Similar arguments as the ones in the previous case imply that $\Gamma(z_0)$ also exists. See Figure 2.9.

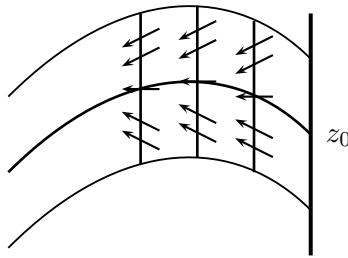


Figure 2.9 Behaviour of the flux near to an isolated singular point in the boundary

For the second step, Propositions 2.17 and 2.18 give that the orbit $\Gamma(z_0)$ touches the positive w -axis, in finite time, passing through all quadrants in counterclockwise direction. We call $(\hat{w}, 0)$ the first time that this happens and (\hat{w}, \hat{z}) the first time that the orbit $\Gamma(z_0)$ cuts the straight line $w = \hat{w}$ in the fourth quadrant. Then, by (\tilde{H}_5) , the region defined by $\Gamma(z_0)$ between (\hat{w}, \hat{z}) and $(\hat{w}, 0)$ and the segment with those endpoints, \hat{S} , is positively invariant. The proof ends because the positive orbits of all points in the complement of this region in \tilde{D} cross the segment \hat{S} . See Figure 2.10. \square

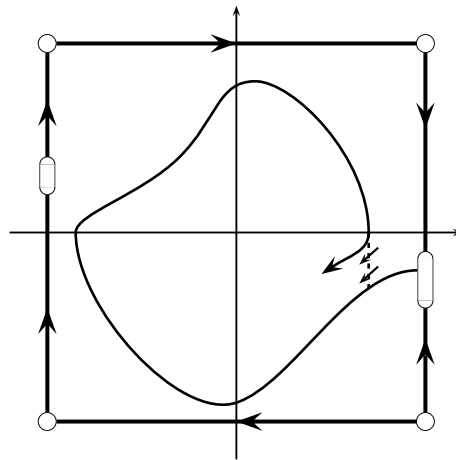


Figure 2.10 Positively invariant region when the boundary has singular points different from the vertex

Proposition 2.21. Consider system (2.5) under the hypotheses (H) and satisfying that

- (i) there exist δ and η in \mathbb{R} , with $x_1 < \eta < 0 < \delta < x_2$, such that $f(x) > 0$ for all $x \in (x_1, x_2) \setminus [\eta, \delta]$ and the integral $\int_{\eta}^{\delta} f(x) dx$ is positive,
- (ii) for each $i = 1, 2$ there exists λ_i in $\mathbb{R}^+ \cup \{+\infty\}$ such that, if $|x_i| = +\infty$, then $\liminf_{x \rightarrow x_i} x(|g(x)| + f(x)) = \lambda_i$, and if $x_i \in \mathbb{R}$, then $\liminf_{x \rightarrow x_i} |x - x_i|(|g(x)| + f(x)) = \lambda_i$,

(iii) $y\psi(y) > 0$ for all $y \neq 0$,

(iv) for $i = 1, 2$, $\lim_{y \rightarrow y_i} \psi(y)/(y\varphi'(y)) \in \mathbb{R}$.

Then the boundary of \mathcal{D} is a repellor.

Proof. System (2.5) from Proposition 2.3 and Lemmas 2.7 to 2.12, writes as the compactified equivalent system (2.8) in $\tilde{\mathcal{D}}$. In order to obtain a contradiction, we suppose that the boundary of \mathcal{D} is not a repellor. Hence, Propositions 2.14, 2.17 and 2.18 ensure the existence of a return map close to the boundary. More concretely, for $\varepsilon > 0$ small enough, there exists an orbit, Γ_ε , that starts at $(\tilde{\eta}, z_0)$ with $z_0 \in (1 - \varepsilon, 1)$, cuts after a time T the segment $\{\tilde{\eta}\} \times (0, 1)$ at $(\tilde{\eta}, z_T)$ with $z_T \in [z_0, 1)$ and remains, for positive time, in $(-1, 1) \times (-1, 1) \setminus (-1 + \varepsilon, 1 - \varepsilon) \times (-1 + \varepsilon, 1 - \varepsilon)$. See Figure 2.11. Let us denote by $(\tilde{\eta}, z_0)$, $(\tilde{\delta}, z_1)$, $(\tilde{\delta}, z_2)$, $(\tilde{\eta}, z_3)$ and $(\tilde{\eta}, z_T)$ the consecutive cutting points of Γ_ε with the segments $\{\tilde{\eta}\} \times (-1, 1)$ and $\{\tilde{\delta}\} \times (-1, 1)$. Consequently, $z_0, z_1, z_T \in (1 - \varepsilon, 1)$ and $z_2, z_3 \in (-1, -1 + \varepsilon)$.

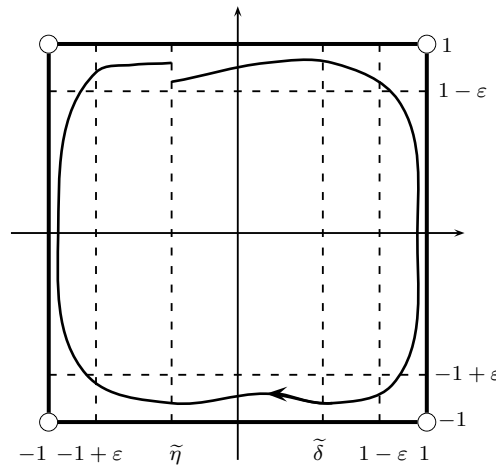


Figure 2.11 Phase portrait, close boundary, of Γ_ε when the boundary of $\tilde{\mathcal{D}}$ is not a repellor

The contradiction is obtained checking that the primary energy function \tilde{E} , see Lemma 2.4, in $(\tilde{\eta}, z_T)$ is lower than in $(\tilde{\eta}, z_0)$. Because, as $z \frac{\partial \tilde{E}}{\partial z} = z\chi(z) > 0$ for all $z \neq 0$, \tilde{E} grows when $|z|$ grows but $z_T \geq z_0$. So, we conclude proving that \tilde{E} decreases when the orbit passes through the consecutive cutting points defined before.

Straightforward computations show that, from (i), there exist $\tilde{\eta}, \tilde{\delta}$ satisfying $-1 < \tilde{\eta} < 0 < \tilde{\delta} < 1$ and $\int_{\tilde{\eta}}^{\tilde{\delta}} \tilde{f}(s) ds > 0$. Then there exists a positive real number A such that $-\int_{\tilde{\eta}}^{\tilde{\delta}} \tilde{f}(s) ds + 2M(\tilde{\delta} - \tilde{\eta})/A < 0$, where $M = \max_{w \in (\tilde{\eta}, \tilde{\delta})} |g(w)|$. By hypotheses (H), (iv) and Lemma 2.12, we obtain that $\lim_{z \rightarrow z_i} \chi(z) = +\infty$ and $\lim_{z \rightarrow z_i} \tilde{\psi}(z)/\chi(z) = 0$ or, equivalently,

$\lim_{z \rightarrow z_i} \chi(z)/\tilde{\psi}(z) = +\infty$, for $i = 1, 2$. Therefore, we fix $\varepsilon > 0$ small enough, such that $\chi(z) > A^2$ and $\frac{\chi(z)}{\tilde{\psi}(z)} > A$, for all $z \in (1 - \varepsilon, 1) \cup (-1, -1 + \varepsilon)$.

Hence, writing equation (2.8) as $dz/dw = -\tilde{g}(w)/\tilde{\psi}(z) - \tilde{f}(w)\tilde{\psi}(z)/\chi(z)$, we can estimate the differences

$$z_1 - z_0 = \int_{\tilde{\eta}}^{\tilde{\delta}} \left(-\frac{\tilde{g}(w)}{\tilde{\psi}(z)} - \frac{\tilde{f}(w)\tilde{\psi}(z)}{\chi(z)} \right) dw \leq \frac{1}{A} \left(\int_{\tilde{\eta}}^{\tilde{\delta}} -\tilde{f}(w)dw + \frac{M}{A}(\tilde{\delta} - \tilde{\eta}) \right) < 0,$$

$$\tilde{G}(\tilde{\delta}) - \tilde{G}(\tilde{\eta}) = \int_{\tilde{\eta}}^{\tilde{\delta}} \tilde{g}(w)dw \leq M(\tilde{\delta} - \tilde{\eta}) \text{ and } \tilde{\Phi}(z_1) - \tilde{\Phi}(z_0) = - \int_{z_1}^{z_0} \chi(z)dz \leq -A^2(z_0 - z_1),$$

where the \tilde{G} and $\tilde{\Phi}$ are the compactified functions defined in Lemma 2.4. Thus, the primary energy function satisfies

$$\tilde{E}(\tilde{\delta}, z_1) - \tilde{E}(\tilde{\eta}, z_0) \leq M(\tilde{\delta} - \tilde{\eta}) + A^2(z_1 - z_0) \leq 2M(\tilde{\delta} - \tilde{\eta}) - A \int_{\tilde{\eta}}^{\tilde{\delta}} \tilde{f}(w)dw < 0.$$

So, the energy decreases from $(\tilde{\eta}, z_0)$ to $(\tilde{\delta}, z_1)$ and from $(\tilde{\delta}, z_2)$ to $(\tilde{\eta}, z_3)$, applying the same argument replacing z_0 and z_1 by z_2 and z_3 , respectively.

Finally, the energy also decreases from $(\tilde{\delta}, z_1)$ to $(\tilde{\delta}, z_2)$ and from $(\tilde{\eta}, z_3)$ to $(\tilde{\eta}, z_T)$ because $\tilde{f}(w) > 0$ and $\tilde{E} = -\tilde{f}(w)\chi(z)\tilde{\psi}(z) \leq 0$, for all $w \in (-1, 1) \setminus [\tilde{\eta}, \tilde{\delta}]$ and $z \in (-1, 1)$. \square

2.6 Uniqueness of limit cycle

This section is devoted to prove the Unicity result, Theorem 2.2.

Proposition 2.6 shows that the origin is the unique singular point, which is a repeller. Additionally, there is no periodic orbits entirely contained in $(a, b) \times (y_1, y_2)$ because $\tilde{E} = -f(x)y\varphi'(y)\psi(y) > 0$, for all $(x, y) \in (a, b) \times (y_1, y_2) \setminus \{(0, 0)\}$. Moreover, all the periodic orbits contain the region $\{(x, y) \in \mathcal{D} : 0 \leq E(x, y) \leq \min(G(a), G(b))\}$, because it is negatively invariant. In the proof we assume that $G(a) \leq G(b)$, in other case we can change (x, y) by $(-x, -y)$.

The proof is done by the method of comparison. Let us suppose that we have two different limit cycles, Γ_1 and Γ_2 . Then we prove that the integral of the divergence of the vector field (2.5), between them, is different from zero, in fact, it is negative. This contradicts the existence of two limit cycles because it implies that both orbits have the same stability.

Taking into account the above considerations, there are three possible configurations of Γ_1 and Γ_2 in terms of the position of a , b and x_0 . See Figure 2.12. We only present the proof when Γ_1 contains the segment $(a, x_0) \times \{0\}$ and Γ_2 contains the segment $(a, b) \times \{0\}$. See Figure 2.12(b). The proof follows similarly for the other two cases.

The integral of the divergence of equation (2.5),

$$\operatorname{div} X = \frac{d}{dx} (y\varphi'(y)) + \frac{d}{dy} (-g(x) - f(x)\psi(y)) = -f(x)\psi'(y),$$

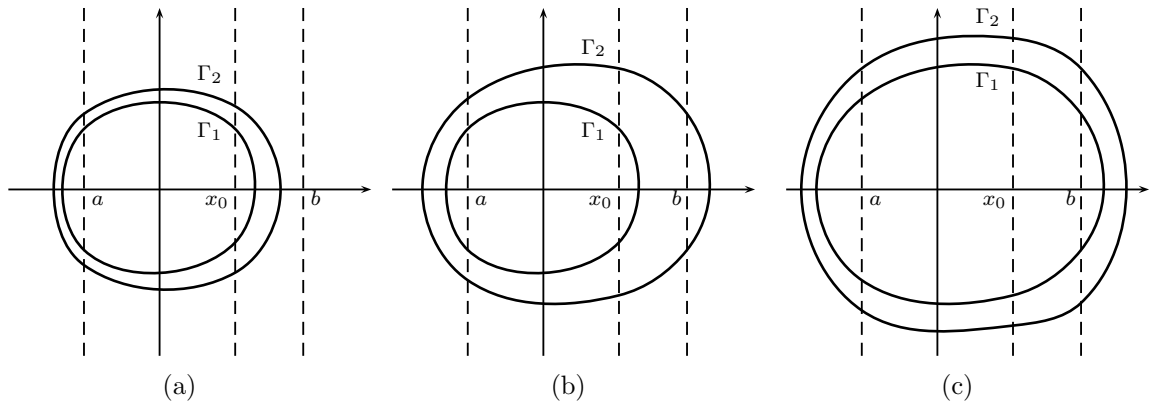


Figure 2.12 Relative positions between Γ_1 and Γ_2 with respect to the intervals (a, b) and (a, x_0)

between both periodic orbits is computed decomposing the region in five different regions G_i , $i = 1, \dots, 5$. See them in Figure 2.13.

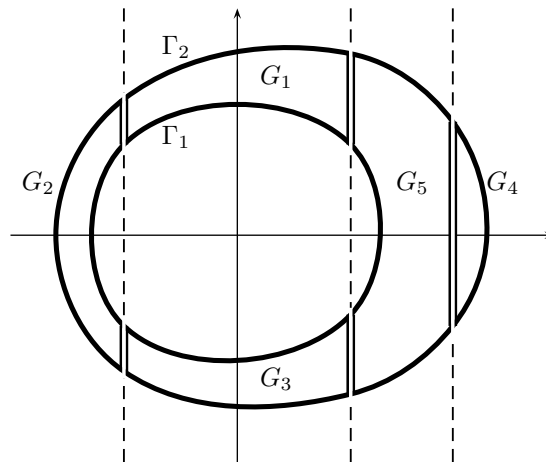


Figure 2.13 Decomposition of the enclosed region between Γ_1 and Γ_2

The different time reparametrizations that we use along the periodic orbits, in each region, are

$$dt = \begin{cases} \frac{1}{y\varphi'(y)} dx & \text{if } (x, y) \in \Gamma_{|G_1 \cup G_3}, \\ -\frac{1}{g(x) + f(x)\psi(y)} dy & \text{if } (x, y) \in \Gamma_{|G_2 \cup G_4}, \\ -\frac{\psi(y)}{g(x)y\varphi'(y)} dJ & \text{if } (x, y) \in \Gamma_{|G_5}, \end{cases}$$

where J is the secondary energy function, defined in Lemma 2.5. Then, by the Green's

Lemma, the integral of the divergence along the curve $\Gamma_1 - \Gamma_2$ can be written as

$$\begin{aligned} \int_{\Gamma_1 - \Gamma_2} \operatorname{div} X dt &= \iint_{G_1 \cup G_3} -\frac{d}{dy} \left(\frac{f(x)\psi'(y)}{y\varphi'(y)} \right) dx dy + \\ &+ \iint_{G_2 \cup G_4} \frac{d}{dx} \left(-\frac{f(x)\psi'(y)}{g(x) + f(x)\psi(y)} \right) dy dx + \\ &+ \iint_{G_5} \frac{d}{dx} \left(-\frac{f(x)\psi'(y)\psi(y)}{g(x)y\varphi'(y)} \right) dJ dx = \\ &= \iint_{G_1 \cup G_3} \Delta_1 dx dy + \iint_{G_2 \cup G_4} \Delta_2 dy dx + \iint_{G_5} \Delta_5 dJ dx, \end{aligned}$$

where

$$\begin{aligned} \Delta_1 &= -f(x) \frac{d}{dy} \left(\frac{\psi'(y)}{y\varphi'(y)} \right), & \text{for } x \in (a, b), y \in (y_1, y_2) \setminus \{0\}, \\ \Delta_2 &= -\psi'(y) \frac{g(x)^2}{(g(x) + f(x)\psi(y))^2} \frac{d}{dx} \left(\frac{f(x)}{g(x)} \right), & \text{for } x \in (x_1, x_2) \setminus [a, b], y \in (y_1, y_2) \setminus \{0\}, \\ \Delta_5 &= -\frac{\psi'(y)\psi(y)}{y\varphi'(y)} \left(-\frac{f(x)}{g(x)} \right), & \text{for } x \in (x_0, b), y \in (y_1, y_2) \setminus \{0\}. \end{aligned}$$

The proof ends because, from the statement, it can be checked that all the integrands, Δ_1 , Δ_2 and Δ_5 , are negative in each region where they are considered.

Chapter 3

On the Bogdanov-Takens bifurcation

3.1 Introduction

In general, the applications of differential systems require more than a theoretical knowledge of the qualitative behavior of the solution. Knowing the existence or the number of limit cycles that a system has is not always enough. It is usually desired to control when the limit cycles appear or disappear. The aim of our work is to provide global results about the homoclinic connection curve in the parameter space for the Bogdanov-Takens' normal form written as

$$\begin{cases} x' = y, \\ y' = -n + by + x^2 + xy, \end{cases} \quad (3.1)$$

where n and b are real numbers.

This problem is established in [Tak74, Bog75], where they introduce system (3.1) as the simplest one that provides a universal unfolding of a cusp point that just shows a bifurcation of limit cycle and a homoclinic connection curve. The cusp is a particular degenerate equilibrium point which linear part has one zero eigenvalue and the quadratic coefficient for the saddle-node bifurcation vanishes. It implies that the phase portrait, when n and b vanish, presents two tangent separatrices at the origin. The qualitative behavior of system (3.1) is utterly known. For a detailed description of the complete unfolding we refer the reader to [GH02, Kuz98]. For the analysis of other cusp unfolds, it could be referred [DRS87] where it is considered the cusp of codimension 3 (our case has codimension 2). It shows a richer behavior than (3.1) in variety and quantity of dynamical phenomena.

Roughly speaking, there are several ways in which the cusp point evolves varying n and b . Taking into account the location of (n, b) in the parameter space, near the cusp ($n = b = 0$), the number and types of singular points is none; just one, a saddle-node; or two, a saddle and a focus. Each case corresponds to the condition $n < 0$, $n = 0$ ($b \neq 0$) and $n > 0$, respectively.

Limit cycles can only appear in the case with two singular points, $n > 0$, and there

can be at most one. Furthermore, system (3.1) characterizes a rotated family of vector fields with respect to b . Hence, fixed n and varying b , a unique unstable limit cycle, born from a focus via a Hopf bifurcation ($b = \sqrt{n}$), increases, up to disappear on a homoclinic connection ($b = b^*(n)$). The evolution of the phase portrait is shown in Figure 3.1.

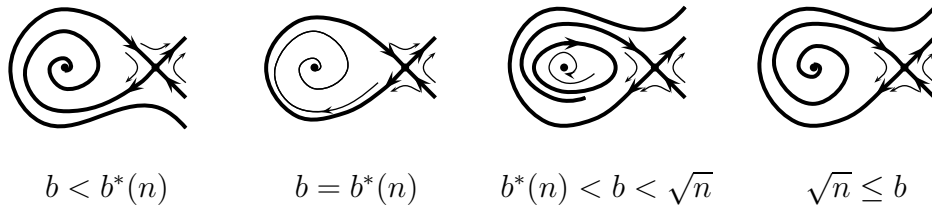


Figure 3.1 Evolution of the phase portrait of system (3.1) for $n > 0$

Lawrence Perko, in [Per92], includes the first global treatment of the bifurcations of the Bogdanov-Takens' system. For all $n > 0$, the value $b^*(n)$ is unique. See Figure 3.2(a). Perko proves that this function is analytic with respect to \sqrt{n} . Moreover, (3.1) also presents an invariant straight line in the case $b = \sqrt{n} - 1$. Hence, as Perko also shows, function $b^*(n)$ could be lower bounded. Then, for any $n > 0$, we know that $\max\{-\sqrt{n}, \sqrt{n} - 1\} < b^*(n) < \sqrt{n}$. A numerical approximation of the curve $b^*(n)$ is shown in Figure 3.2(b) as a dashed curve together with the Perko's lower and upper bounds.

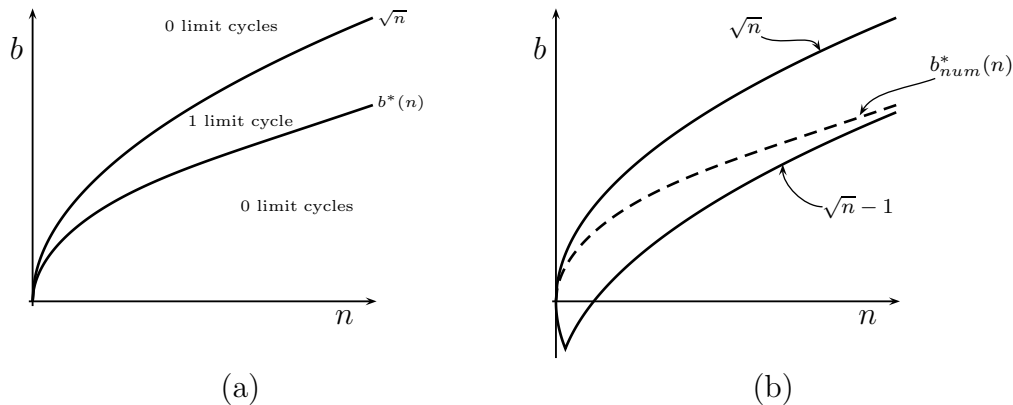


Figure 3.2 Bifurcation diagram of the existence of the limit cycle (a) and the previous bounds for the curve $b^*(n) = 0$ (b)

One of our main objectives is to provide closer explicit curves $b_d(n), b_u(n)$ such that $b_d(n) \leq b^*(n) \leq b_u(n)$ for all $n > 0$. So, we seek the values of the parameters that provide the homoclinic connection. The algebraic method that we apply is used to localize connections of singular points, heteroclines as well as homoclines. See [GGT10]. Furthermore, we also prove the Perko's Conjecture that predicts the performance of this

curve when n goes to infinity. More precisely, he conjectures that $b^*(n)$ goes to infinity as $\sqrt{n} - 1$ do. This is not the first study of the Bogdanov-Takens' system at the infinity of the parameter space. See [Bou91]. But the aim and the procedure of both works are completely different. In fact, that work does not deal with Perko's Conjecture nor with the location of the bifurcation homoclinic connection.

The main results of our work may be summarized in the following two theorems.

Theorem 3.1. *For n large enough, the homoclinic bifurcation curve of system (3.1) satisfies*

$$b^*(n) = \sqrt{n} - 1 + O(n^{-1}).$$

Theorem 3.2. *For all $n > 0$, it holds that $b_d(n) < b^*(n) < b_u(n)$ where $b_u(n)$ and $b_d(n)$ are the piecewise functions*

$$b_u(n) := \begin{cases} \Gamma_u(n) & , \text{ if } n \leq n_u, \\ \sqrt{n} - 1 + \frac{4}{\sqrt{n}} & , \text{ if } n > n_u, \end{cases} \quad \text{and} \quad b_d(n) := \begin{cases} \Gamma_d(n) & , \text{ if } n \leq n_d, \\ \sqrt{n} - 1 & , \text{ if } n > n_d, \end{cases}$$

where n_d and n_u are given squaring the unique positive real root of $72m^3 - 78m^2 - 49m - 7$, and the biggest positive real root of

$$\begin{aligned} & 96m^{16} + 88m^{15} + 462884m^{14} + 50229186m^{13} - 390289463m^{12} + 294539208m^{11} \\ & - 2224823608m^{10} + 1615614334m^9 - 2965720485m^8 + 10305829872m^7 \\ & - 34801925760m^6 + 65690924544m^5 - 98084348928m^4 + 61359980544m^3 \\ & - 14300872704m^2 - 16817061888m + 9172942848, \end{aligned}$$

respectively. Moreover Γ_u and Γ_d are the functions defined by the branches of given polynomials in \sqrt{n} and b of degrees 25 and 9 with 257 and 42 monomials, respectively. Additionally, the series expansion at $n = 0$ of Γ_u , and Γ_d are

$$b = \frac{5}{7}n^{1/2} + \frac{72}{2401}n + \frac{271944}{823543}n^{3/2} + O(n^2),$$

and

$$b = \frac{5}{7}n^{1/2} + \frac{72}{2401}n - \frac{30024}{45294865}n^{3/2} + O(n^2).$$

The explicit expressions for the polynomials Γ_u and Γ_d are presented in the Appendix of this chapter.

The bounds provided by Theorem 3.2 are graphically represented in Figure 3.3. The large dashed curve is a numerical approximation of $b^*(n)$ and the short dashed curves are the previous known bounds given in [Per92].

In order to obtain our results, we follow the method introduced in [GGT10]. In fact, we adapt the method in two different ways depending in the region that we are interested in each case, small or large values of n . The basic idea of the proof is the following: If we have positive fixed values of b and n such that $b < \sqrt{n}$, we want to

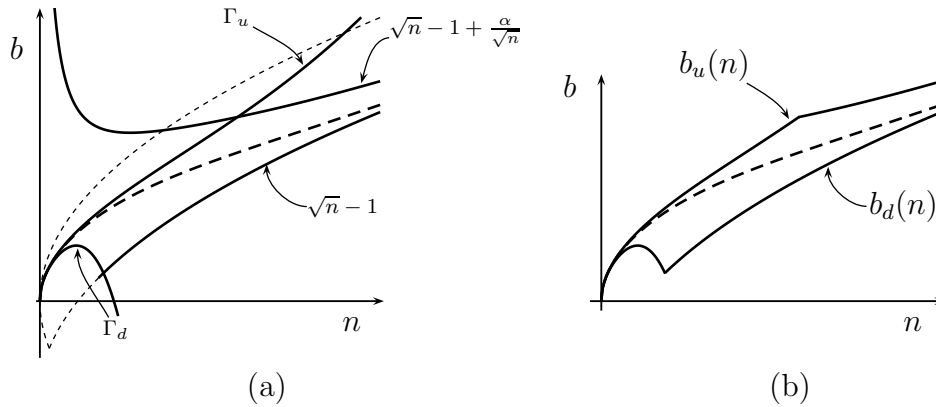


Figure 3.3 Previous (short dashed) and new (solid) upper and lower bounds together with the numerical approximation (long dashed curve) of the graph of the function $b^*(x)$

distinguish if $b > b^*(n)$ or $b < b^*(n)$, which means the existence or not of the limit cycle. So, first of all, we consider a closed curve passing through the saddle point and surrounding the focus, that in this case is an attractor. Therefore, we could apply the Poincaré-Bendixson theorem and distinguish both cases depending if the delimited region is negative or positively invariant. Hence, the limit cycle exists and it is unstable or does not exist. Both cases are represented in Figure 3.4.

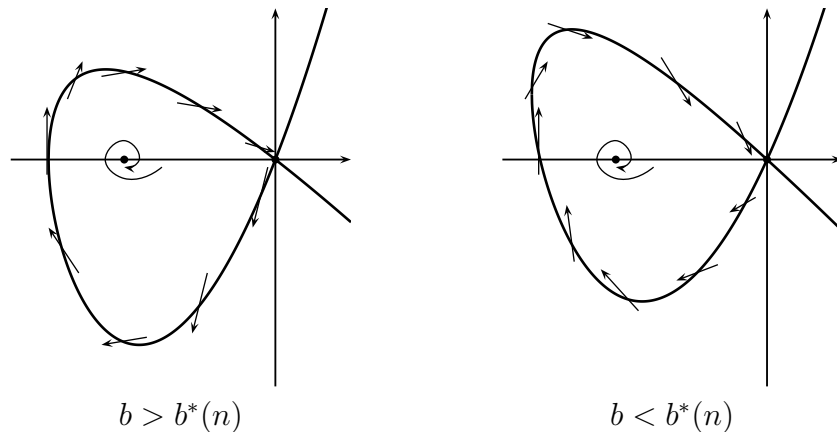


Figure 3.4 Negative and positive invariant loops around the focus

In [GGT10], the closed curve around the attracting point is proposed to be the loop of an algebraic self-intersecting curve which vertex is on the saddle point and the branches of the curve on this point approximate its separatrices. In this chapter we use the same construction for the closed curve when n is small. But we adapt the proof when n is large designing a piecewise algebraic closed curve which also approximates the separatrices of the saddle point. Moreover, we also provide the biggest possible interval where this argument holds.

The chapter is organized as follows. In Section 3.2, changes of variables, in phase and parameter spaces, are presented to shorten expressions for the bifurcation curves described in Theorem 3.2. Moreover, the previous results and curves are also transformed. The new results of the bifurcation curve are proved in Section 3.3, close to the origin in the parameter space, and in Section 3.4 for bigger values of n . Section 3.5 is devoted to proof Theorem 3.2 and to deal with some small rational expressions that provide a good approximation to this curve. Additionally, a short study of the differences with the numerical bifurcation curve are also presented. And we summarize the ranges of validity of the upper bounds constructed. At the end of this chapter, due to their size, we include the expressions of the functions in the statement of Theorem 3.2.

The required computations to obtain all the results have been done using the algebraic manipulator MAPLE.

3.2 Changes of variables

First, we move the saddle point of system (3.1) to the origin. Second, we change the parameter space in such a way that the eigenvalues of the saddle point do not have square roots. This last change allows us to obtain smaller expressions for the bifurcation curves than in the original coordinates.

System (3.1) is transformed, by the change of variables $(x, y) \rightarrow (x + \sqrt{n}, y)$, into

$$\begin{cases} x' = y, \\ y' = 2\sqrt{n}x + (b + \sqrt{n})y + x^2 + xy. \end{cases} \quad (3.2)$$

In order to simplify the expression of the eigenvalues of the linearization of the saddle point, we also propose a change in the parameters (n, b) . The new parameters, M and B , satisfy

$$M^2 = \frac{(b + \sqrt{n})^2 + 8\sqrt{n}}{4}, \quad B = \frac{b + \sqrt{n}}{2}, \quad (3.3)$$

and system (3.2) writes as

$$\begin{cases} x' = y, \\ y' = (M^2 - B^2)x + 2By + x^2 + xy. \end{cases} \quad (3.4)$$

In what follows, in order to facilitate the reading, we refer, when necessary, to (n, b) and (M, B) as the small and the capital parameter space respectively.

With the first change, the origin of the previous system is a saddle point and the focus of (3.1), $(-\sqrt{n}, 0)$, changes to $(B^2 - M^2, 0)$.

In the parameter space, the Hopf bifurcation curve, $b = \sqrt{n}$, becomes $B^2 + 2B - M^2 = 0$. The curve of the existence of an invariant straight line, $b = \sqrt{n} - 1$, is moved to $M^2 = (B + 1)^2$. And the curve where the divergence of the saddle point vanishes, $b = -\sqrt{n}$, is contained in the horizontal axis, $B = 0$. Moreover, the origin goes to the origin and the large values of n also correspond with large values of M .

The homoclinic bifurcation curve, $b = b^*(n)$, has also a new expression for system (3.4). We denote it by $B = B^*(M)$. And, as far as it is located between the curves listed in the previous paragraph, we have that $B = B^*(M)$ is contained in the set

$$\mathcal{R} = \{(M, B) \in \mathbb{R}^2 \text{ such that } M > 0, B > 0, B^2 + 2B - M^2 < 0, B > M - 1\}. \quad (3.5)$$

Without loss of generality, we consider only system (3.4) in region \mathcal{R} . Thus Theorems 3.1 and 3.2 are the translation of the analogous results for system (3.4). In order to ease the reading of the rest of the chapter, the curves described in Figure 3.3 in the small parameter space are plotted in Figure 3.5 in the capital parameter space. In Figure 3.5 set \mathcal{R} and a numerical representation of the curve $B = B^*(M)$ are also printed.

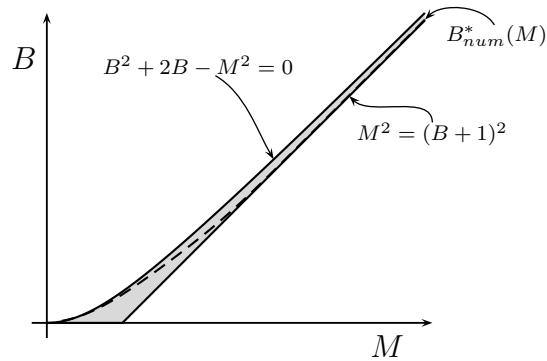


Figure 3.5 Region \mathcal{R} and the curves which define its boundary. The numerical approximation of $B = B^*(M)$ is represented by the dashed line

Since the curves in Figure 3.5 are not distinguishable at all, the plots in this parameter space is not very useful. So we use a different scale for some of the diagrams included in this chapter. Figure 3.6 is equivalent to Figure 3.5 using \tilde{B} instead of B , where $\tilde{B} = (B - M + 1)M$. This rescaling is due to the fact that the bifurcation B^* curve goes asymptotically to the straight line $B - M + 1 = 0$.

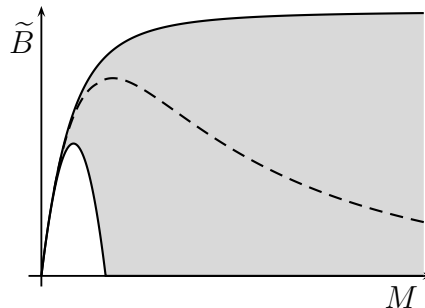


Figure 3.6 Region \mathcal{R} and the bifurcation curve $B = B^*(M)$ in the (M, \tilde{B}) plane

3.3 Bounds from the origin

This section is devoted to the study of upper and lower bounds for $b^*(n)$ for small values of n . The results on this section are presented in terms of the capital parameters introduced in the previous section, M and B . In these new coordinates, small values of n corresponds also with small values of M .

Proposition 3.3. *There exists a positive real value M_u , such that for all $0 < M < M_u$ there exists $B^*(M) < \tilde{\Gamma}_u(M)$ where $\tilde{\Gamma}_u(M)$ is the function defined by the branch of the algebraic curve*

$$\begin{aligned} & -327M^7B - 714M^6B^2 - 253M^5B^3 + 458M^4B^4 + 519M^3B^5 + 250M^2B^6 + 61MB^7 \\ & + 6B^8 - 198M^7 - 579M^6B + 253M^5B^2 + 1590M^4B^3 + 1488M^3B^4 + 707M^2B^5 \\ & + 177MB^6 + 18B^7 - 144M^6 + 300M^5B + 1402M^4B^2 + 1339M^3B^3 + 658M^2B^4 \\ & + 171MB^5 + 18B^6 + 336M^4B + 378M^3B^2 + 201M^2B^3 + 55MB^4 + 6B^5 = 0 \end{aligned}$$

which series expansion at the origin is

$$B = \frac{3}{7}M^2 - \frac{180}{2401}M^4 + \frac{3321}{33614}M^5 - \frac{225153}{3294172}M^6 + O(M^7).$$

And M_u is the M -component of the first common point of this function and the Hopf bifurcation curve, $B = -1 + \sqrt{1 + M^2}$ which is the smallest positive zero of the polynomial $8640M^7 - 28800M^6 + 29876M^5 - 19392M^4 + 14939M^3 - 13200M^2 + 8400M - 2304$. That is, approximately, 2.036795457.

Moreover, there exists a positive real M_d , such that for all $0 < M < M_d$ there exists $\tilde{\Gamma}_d(M) < B^*(M)$ where $\tilde{\Gamma}_d(M)$ is the function defined by the branch of the algebraic curve

$$\begin{aligned} & 18M^5 + 51M^4B - 6M^3B^2 - 78M^2B^3 - 48MB^4 - 9B^5 + 24M^4 \\ & - 24M^3B - 138M^2B^2 - 90MB^3 - 18B^4 - 56M^2B - 42MB^2 - 9B^3 = 0 \end{aligned}$$

which series expansion at the origin is

$$B = \frac{3}{7}M^2 - \frac{180}{2401}M^4 - \frac{1107}{16807}M^5 + \frac{77085}{1647086}M^6 + O(M^7).$$

And M_d is the M -component of the first common point of this function and the invariant straight line curve, $B = M - 1$, which is the smallest positive zero of the polynomial $72M^3 - 186M^2 + 83M - 11$. That is, approximately, 2.059652018.

Proof. We recall that system (3.4) has a saddle point at the origin and the linear approximation to the separatrices of the origin is given by the equation

$$C_2(x, y) := -(M^2 - B^2)x^2 - 2Bxy + y^2 = 0. \quad (3.6)$$

It defines two straight lines which explicit equations are $y = (B \pm M)x$. The one which slope is $B + M$ is tangent at the origin to the unstable separatrix. And, the other one, which slope is $B - M$, is tangent to the stable separatrix.

Let us consider the algebraic curve characterized by equation

$$C(x, y) := C_2(x, y) + c_{30}x^3 + c_{21}x^2y + c_{12}xy^2 + c_{03}y^3 = 0. \quad (3.7)$$

Following the method described in [GGT10], we impose that this equation defines a curve as close to the separatrices as possible. It means that this curve should coincide at the origin with the separatrices in the highest possible derivative orders. For this purpose, first we set the Taylor series expansions of both separatrices close to the origin. We express the separatrices as functions of y ,

$$x = \Phi^\pm(y) := \sum_{k=1}^{\infty} a_k^\pm y^k, \quad (3.8)$$

where the superscript sign determines the separatrix that we approach in each case. Then a_k^\pm are real numbers obtained from the identity

$$\frac{\partial(x - \Phi^\pm(y))}{\partial x}y + \frac{\partial(x - \Phi^\pm(y))}{\partial y}((M^2 - B^2)x + 2By + x^2 + xy)|_{x=\Phi^\pm(y)} \equiv 0.$$

Straightforward computations show that $a_1^\pm = 1/(B \pm M)$,

$$a_2^\pm = \frac{a_1^\pm(1 + a_1^\pm)}{-4B + 3a_1^\pm(B^2 - M^2)}, \quad a_3^\pm = -\frac{1}{2} \frac{a_2^\pm(-4(a_1^\pm)^2 + 2a_2^\pm B^2 - 3a_1^\pm - 2a_2^\pm M^2)}{-3B + 2a_1^\pm(B^2 - M^2)},$$

and the following coefficients of Φ^\pm have analytical expressions depending on a_1^\pm . Note that their denominators do not vanish in region \mathcal{R} defined in (3.5).

Substituting (3.8) in (3.7) we get the functions, that defines both branches of the algebraic curve near the origin,

$$G^\pm(y) := C(\Phi^\pm(y), y) = \sum_{k=3}^{\infty} g_k^\pm y^k. \quad (3.9)$$

From definition (3.6) g_k^\pm vanishes for $k = 1, 2$. When the curve defined by $C(x, y) = 0$ becomes closer to the separatrices, it provides extra conditions $g_k^\pm = 0$ for higher values of k . In (3.7), we choose c_{ij} with $i, j = 0, 1, 2, 3$ such that $i + j = 3$, in order to vanish g_k^\pm for the first values of k . As we have four coefficients c_{ij} , we can cancel four coefficients g_k^\pm and we are free to distribute them between both separatrices. For example, we can choose the value of three of these parameters in aim to be closer to the unstable separatrix and the other parameter to be closer to the stable one. It means, in this case, that we fix c_{ij} solving the equations $g_3^+ = 0$, $g_4^+ = 0$, $g_5^+ = 0$ and $g_3^- = 0$, and consequently

$$G^+(y) = \sum_{k=6}^{\infty} g_k^+(M, B)y^k,$$

and

$$G^-(y) = \sum_{k=4}^{\infty} g_k^-(M, B)y^k,$$

where g_6^+ and g_4^- are not identically zero polynomials in M and B .

After these considerations, we can vanish an extra term in G^+ or in G^- . This extra assumption relates the parameters M and B via, for our case, a polynomial relation given vanishing one more g_k^{\pm} . In our previous example, we may consider $g_6^+ = 0$ or $g_4^- = 0$ and we can establish two different relations between M and B . Straightforward computations show that if we set $g_6^+ = 0$, we obtain the equivalent condition

$$\begin{aligned} E_{41}(M, B) := & -327M^7B - 714M^6B^2 - 253M^5B^3 + 458M^4B^4 + 519M^3B^5 \\ & + 250M^2B^6 + 61MB^7 + 6B^8 - 198M^7 - 579M^6B + 253M^5B^2 \\ & + 1590M^4B^3 + 1488M^3B^4 + 707M^2B^5 + 177MB^6 + 18B^7 - 144M^6 \\ & + 300M^5B + 1402M^4B^2 + 1339M^3B^3 + 658M^2B^4 + 171MB^5 \\ & + 18B^6 + 336M^4B + 378M^3B^2 + 201M^2B^3 + 55MB^4 + 6B^5 = 0. \end{aligned}$$

And for $g_4^- = 0$, we obtain the equivalent condition

$$\begin{aligned} E_{32}(M, B) := & 18M^5 + 51M^4B - 6M^3B^2 - 78M^2B^3 - 48MB^4 - 9B^5 + 24M^4 \\ & - 24M^3B - 138M^2B^2 - 90MB^3 - 18B^4 - 56M^2B - 42MB^2 - 9B^3 = 0. \end{aligned}$$

The non vanishing factors in \mathcal{R} have been removed. The subindex notation shows the orders of approximation of the curve $C(x, y) = 0$ to the separatrices. The first digit corresponds to the unstable separatrix and the second digit to the stable one.

With the same procedure we obtain all the conditions E_{ij} for $i + j = 5$. Studying the plots of all these curves in region \mathcal{R} , we can see that between the graphs of the curves $E_{41} = 0$ and $E_{32} = 0$ there are no other curves $E_{ij} = 0$ for all values of $i + j = 5$. Additionally the graph of $E_{41} = 0$ appears above the graph of $E_{32} = 0$ in the space (M, B) and these are the curves that appear in the statement.

The proof continues showing that curves $E_{41} = 0$ and $E_{32} = 0$ define negative and positive invariant closed regions that contain the focus point. See Figure 3.4. This assertion is proved in two steps for each value (M, B) on the curve $E_{ij} = 0$ and for some values of M bigger than the ones that appear in the statement. First, we prove that the respective curves $C(x, y) = 0$ are without contact for the vector field when $x < 0$. Second, we prove that $C(x, y) = 0$ has a loop that emerges for $x < 0$ from the origin when (M, B) is close to $(0, 0)$.

These last properties ensure that $E_{41} = 0$ is an upper bound for $B = B^*(M)$. Moreover, both curves never touch each other in \mathcal{R} . The proof finishes, for this case, checking that $E_{41}(M, B) = 0$ intersect the Hopf bifurcation curve, $B = -1 + \sqrt{1 + M^2}$, in a point that is approximately $(M, B) = (2.036795457, 1.269038504)$. This is the value of M_u that appear in the statement. Hence, the upper bound is defined as a piecewise function because, for fixed values of M , the Hopf curve takes lower values of B than the curve $E_{41}(M, B) = 0$.

Curve $E_{32} = 0$ gives the lower bound of the statement. For that case the proof follows similarly but this curve intersect the curve of the existence of an invariant straight line, $B = -1 + M$. Hence, the lower bound is also a piecewise function because, for fixed values of M , this straight line takes bigger values of B than the curve $E_{32} = 0$. This intersection point defines the value of M_d that appears in the statement.

We only prove these properties for the curve $E_{41}(M, B) = 0$. Then, we describe the differences that appear when we take $E_{32}(M, B) = 0$.

We start proving that the curve $C(x, y) = 0$ is without contact. This means that the vector field (3.4) does not change the side that it points out along $C(x, y) = 0$. Equivalently, the region delimited by $C(x, y) = 0$ is negatively invariant. To prove it, we study the roots of the resultant, respect to y , of $C(x, y)$ and its derivative respect the vector field,

$$D(x, y) := \frac{\partial C(x, y)}{\partial x}y + \frac{\partial C(x, y)}{\partial y}((M^2 - B^2)x + 2By + x^2 + xy).$$

Some computations with an algebraic manipulator show that

$$P(x; M, B) := \text{Res}(C, D, y) = \alpha(M, B)x^{10} (r_0(M, B) + r_1(M, B)x + r_2(M, B)x^2),$$

where $\alpha(M, B)$ does not vanish in \mathcal{R} . Hence, with the exception of the multiple root in $x = 0$, we can restrict our study to the quadratic polynomial.

Straightforward computations show that the polynomial $E_{41}(M, B)$ is one of the factors of $r_0(M, B)$. So, under the assumption that $E_{41}(M, B) = 0$, $P(x; M, B)$ can have at most one root different from $x = 0$. Let us check where this zero is located applying the Descartes' rule of signs, [Kos82]. The resultant of $r_1(M, B)$ and $E_{41}(M, B)$ respect to M , except for some non-vanishing factors in \mathcal{R} , is

$$1402B^4 + 3361B^3 + 2503B^2 + 483B - 72.$$

Therefore, there is just one possible value for B where both polynomials can vanish at the same time, which is the positive root of the previous polynomial. It approximately takes the value $B = 0.095501437$. But we observe that $r_1(M, B)$ does not change its sign in small segments on $E_{41}(M, B) = 0$ for this concrete value of B . So $r_1(M, B)$ has a fixed sign for any (M, B) in \mathcal{R} satisfying $E_{41}(M, B) = 0$. Additionally, all the factors of the resultant of $r_2(M, B)$ and $E_{41}(M, B)$ respect to M do not have positive roots. So $r_2(M, B)$ has also a fixed sign for (M, B) in \mathcal{R} satisfying $E_{41}(M, B) = 0$. Finally, if we consider any (M, B) in \mathcal{R} such that $E_{41}(M, B) = 0$, it is easy to check that the sign of r_1 and r_2 are positive and negative, respectively. Hence, there are not negative values of x where $P(x; M, B)$ vanishes if M and B satisfy $E_{41}(M, B) = 0$. Consequently, the curve $C(x, y) = 0$ is without contact for negative values of x if $E_{41}(M, B) = 0$.

Our next goal is to show that $C(x, y) = 0$ under the condition $E_{41}(M, B) = 0$ actually contains a loop around the focus, $(x, y) = (B^2 - M^2, 0)$, having a vertex on the saddle, $(x, y) = (0, 0)$. That is, the loop remains in the region of the phase space with $x < 0$, where the curve $C(x, y) = 0$ is without contact. From the construction of $C(x, y)$

follows easily that the curve has a vertex at the origin. And, following [GGT10], we have proved the existence of this loop taking M small enough, since the curve obtained here and the bounds there have the same first coefficients in the power series expansion for M close to 0. The procedure is to find a box on the phase plane such that its boundary has no contact points with $C(x, y) = 0$ except for the saddle point. Figure 3.7 represents the graphical idea of the proof.

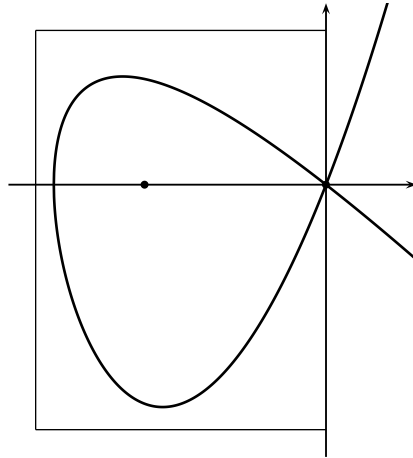


Figure 3.7 *Proving the existence of the loop surrounding the focus*

In order to have an approximate idea about the size of that box, we study some points of $C(x, y) = 0$ and their evolution when we move the value of M in the range of the statement. Therefore we observe that, if $E_{41}(M, B) = 0$, the contact point between $C(x, y) = 0$ and the negative x -axis has a power series expansion in M that starts like

$$-\frac{3}{2}M^2 + \frac{99}{392}M^4 + O(M^5).$$

Similarly we obtain that, when $x = B^2 - M^2$, two points on $C(x, y) = 0$ has a power series expansion in M that starts like

$$\pm \frac{1}{\sqrt{3}}M^3 + O(M^4).$$

So, in order to be far enough from these known points on $C(x, y) = 0$ we take the vertical segment in the boundary of the box in $x = -2M^2$ and both horizontal segments set $y = \pm M^3$.

Now, in order to see that these segments have no contact points with $C(x, y) = 0$ we proceed as follows. Let us first see the case of the vertical segment. Thus, we fix the value of $x = -2M^2$ in the expression $C(x, y)$ and we obtain a polynomial in y with degree 3. Then, we compute the discriminant of this polynomial, $DC(M, B)$, respect to y and it is a polynomial in M and B with degree 19, with the exception of some factors

that do not vanish in \mathcal{R} . That is

$$\begin{aligned}
& -75087M^{19} - 771039M^{18}B - 2955075M^{17}B^2 - 5791935M^{16}B^3 - 5146031M^{15}B^4 \\
& + 1781489M^{14}B^5 + 9452533M^{13}B^6 + 9484153M^{12}B^7 + 2834507M^{11}B^8 \\
& - 2648069M^{10}B^9 - 3457697M^9B^{10} - 1922677M^8B^{11} - 637517M^7B^{12} - 131085M^6B^{13} \\
& - 15633M^5B^{14} - 837M^4B^{15} - 358668M^{18} - 2124324M^{17}B - 3745326M^{16}B^2 \\
& + 2970806M^{15}B^3 + 22821408M^{14}B^4 + 38575340M^{13}B^5 + 26504182M^{12}B^6 \\
& - 4720570M^{11}B^7 - 24364172M^{10}B^8 - 22111932M^9B^9 - 11194994M^8B^{10} \\
& - 3555102M^7B^{11} - 701832M^6B^{12} - 76428M^5B^{13} - 2646M^4B^{14} + 162M^3B^{15} \\
& + 13716M^{17} + 2664756M^{16}B + 16908150M^{15}B^2 + 45638620M^{14}B^3 + 59703551M^{13}B^4 \\
& + 21302235M^{12}B^5 - 47237365M^{11}B^6 - 81798503M^{10}B^7 - 64623550M^9B^8 \\
& - 30599870M^8B^9 - 8876028M^7B^{10} - 1369538M^6B^{11} - 15877M^5B^{12} \\
& + 32319M^4B^{13} + 4779M^3B^{14} + 189M^2B^{15} + 787536M^{16} + 5975352M^{15}B \\
& + 14852124M^{14}B^2 + 4533506M^{13}B^3 - 51863670M^{12}B^4 - 122994760M^{11}B^5 \\
& - 139930230M^{10}B^6 - 94582910M^9B^7 - 39218024M^8B^8 - 9157952M^7B^9 \\
& - 689260M^6B^{10} + 160638M^5B^{11} + 16446M^4B^{12} - 10512M^3B^{13} - 2538M^2B^{14} \\
& - 162MB^{15} + 280800M^{15} - 989712M^{14}B - 14989824M^{13}B^2 - 53870868M^{12}B^3 \\
& - 96112515M^{11}B^4 - 97704531M^{10}B^5 - 58816770M^9B^6 - 19809750M^8B^7 \\
& - 2620939M^7B^8 + 248377M^6B^9 - 79113M^5B^{10} - 136865M^4B^{11} - 42130M^3B^{12} \\
& - 4662M^2B^{13} + 27MB^{14} + 27B^{15} - 432000M^{14} - 4017600M^{13}B - 14057712M^{12}B^2 \\
& - 24420888M^{11}B^3 - 21471336M^{10}B^4 - 7832826M^9B^5 + 1463546M^8B^6 \\
& + 2159994M^7B^7 + 293270M^6B^8 - 366660M^5B^9 - 202136M^4B^{10} - 41114M^3B^{11} \\
& - 1926M^2B^{12} + 486MB^{13} + 54B^{14} - 216000M^{13} - 1036800M^{12}B - 1626480M^{11}B^2 \\
& + 21600M^{10}B^3 + 2548296M^9B^4 + 2883624M^8B^5 + 1344389M^7B^6 + 114879M^6B^7 \\
& - 167964M^5B^8 - 80154M^4B^9 - 13654M^3B^{10} + 36M^2B^{11} + 297MB^{12} + 27B^{13}.
\end{aligned}$$

And the resultant of $E_{41}(M, B)$ and $DC(M, B)$ respect to M is

$$\begin{aligned}
& 2899622803184994484224B^{39} - 16412078457787621834752B^{38} \\
& - 1535278927440587362664448B^{37} - 23688411426884067396681728B^{36} \\
& - 202065146355663413954215936B^{35} - 1165768158549406117303156736B^{34} \\
& - 4984332287223795443419840512B^{33} - 16713724114703483938180956160B^{32} \\
& - 45701239445532739824210935808B^{31} - 103918499777337919858974654464B^{30} \\
& - 193238176255440188900157685760B^{29} - 263438033121700724968201912320B^{28} \\
& - 123607365356201133380114644992B^{27} + 666058154571668577346557771776B^{26} \\
& + 2822400982402589808333290930176B^{25} + 7196246763889539671297738784768B^{24} \\
& + 14510713801720917602146669703168B^{23} + 25109505424899238589611461595136B^{22}
\end{aligned}$$

$$\begin{aligned}
& + 38643695639740926329904520141824B^{21} + 53484117194462348676172039630848B^{20} \\
& + 66159294872247029375902242141184B^{19} + 71908684250951283143638955503872B^{18} \\
& + 67049279646371641117126261502720B^{17} + 51878581071831116191429598677504B^{16} \\
& + 31411694759635147646807567239360B^{15} + 12695083681184078702766440589216B^{14} \\
& + 684244727385813834968011768720B^{13} - 3953362876299772878463898370636B^{12} \\
& - 3798165932246799827469207218864B^{11} - 2038472318847501714435355222559B^{10} \\
& - 608908340006243591242901125072B^9 + 24242766622506635502196884126B^8 \\
& + 139900991864465566982394566550B^7 + 85749198474821573268513637569B^6 \\
& + 31118739181290495159018284520B^5 + 7339447375107889386068008965B^4 \\
& + 1037653460604717219779746482B^3 + 54572204525720465976293322B^2 \\
& - 6064006883266578137934096B - 834443269200948104180559.
\end{aligned}$$

The smallest valid root takes a value approximately $B = 2.062295032$ and it corresponds approximately to $M = 2.871454426$. So, we can assure that the vertical boundary for $x = -2M^2$ does not contain points in $C(x, y) = 0$ at least for M between 0 and 2.871454426. Notice that this value is bigger than the value given in the statement.

Doing similar computations for the horizontal segments in the boundary of the box, we obtain that the segment at the top is valid until $M = 3.263890289$, approximately, and the segment at the bottom has no contact points with $C(x, y) = 0$ for any positive value of M . Summarizing, the box represented in Figure 3.7 has no contact with $C(x, y) = 0$ while M is lower than 2.871454426. Then, the loop remains in the interior of the box.

Finally, we check that the branch of $E_{41}(M, B) = 0$ containing the origin and satisfying the existence of the loop is the expression given in the statement.

The proof for the curve $E_{32} = 0$ follows similarly as the above case. The main difference is that almost all the segments without contact with the loop, that prove its existence, are fixed. That is $x = -12$, $y = 13$ and $y = -M^3$. \square

The next result gives new upper and lower bounds considering a particular case of non contact quartic curves in the phase space for localize the bifurcation curves in the parameter space. The key point of next result is that the proof of the existence of a loop in the non contact curve is easier.

Proposition 3.4. *There exists a positive real number M_u and a function $\tilde{\Gamma}_u(M)$ such that for all $0 < M < M_u$, $B^*(M) < \tilde{\Gamma}_u(M)$. Moreover, $\tilde{\Gamma}_u(M)$ is the function defined by the branch of a given polynomial, see the Appendix, on M and B (of degree 14 with 72 monomials) which series expansion at $M = 0$ is*

$$B = \frac{3}{7}M^2 - \frac{180}{2401}M^4 + \frac{2366307}{90589730}M^6 + \frac{71523}{32353475}M^7 + O(M^8)$$

Additionally, M_u is the biggest positive zero of the polynomial

$$\begin{aligned} &15925248M^{13} - 529072128M^{12} + 1472221440M^{11} - 2220910656M^{10} + 7743711296M^9 \\ &- 23908694736M^8 + 42538637040M^7 - 50911036332M^6 + 46590774012M^5 \\ &- 31063624839M^4 + 12150489456M^3 - 1556369640M^2 - 366210720M + 69984000, \end{aligned}$$

which is, approximately, 30.30805089.

Proof. The proof follows using the same ideas and techniques developed in the proof of Proposition 3.3. Hence, due to the size of the expressions that appear during the proof, we only show the differences between both results.

The main difference is that we consider a special quartic algebraic curve

$$F(x, y) := C_2(x, y) + a_{30}x^3 + a_{21}x^2y + a_{12}xy^2 + a_{40}x^4 + a_{31}x^3y + a_{22}x^2y^2 = 0.$$

As the above curve is quadratic in y , the proof of the existence of the loop is easier. Then, following the notation of the proof of Proposition 3.3 the expression of $\tilde{\Gamma}_u$ comes from the condition $E_{52} = 0$. \square

Similar results but with a complete quartic algebraic curve do not give better results. Even though better approximation curves are obtained, we are not been able to prove that they are upper and lower bounds, because the expressions that appear in the proof are extremely huge. Notice that the above result does not provides a better lower bound.

3.4 Bounds up to infinity

In this section we study the function $B = B^*(M)$ on intervals that arrive to infinity, $(M_\alpha, +\infty)$. The procedure is similar than the one described in the last section. In this case only upper bounds are provided because only negatively invariant regions can be obtained. The main difference between next result and the given in previous section is that this region is constructed via a piecewise rational curve. More concretely, the proof follows the same procedure that Proposition 3.3. In this case the method considered in [GGT10] does not give good expressions of $C(x, y)$, since the property of been without contact usually breaks down. Therefore, we design it as a composition of sections of three different algebraic curves. The negatively invariant region in \mathbb{R}^2 , which boundary is defined by the curve $C(x, y) = 0$ is plotted in Figure 3.8. Finally, we also proof the main result of the chapter, Theorem 3.1.

Proposition 3.5. *For any real $\alpha > 0$, there exists $M_\alpha > \sqrt{\alpha} > 0$ such that for any $M > M_\alpha$,*

$$M - 1 < B^*(M) < M - 1 + \frac{\alpha}{M^2}.$$

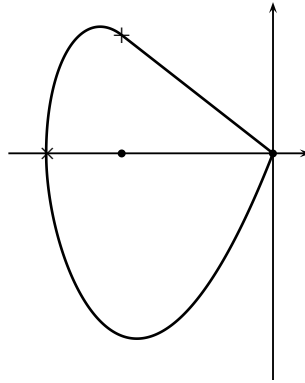


Figure 3.8 Piecewise loop for the bounds at infinity

Proof. From the existence of an invariant straight line for $B = M - 1$ we only prove that, for any α , there exists a curve $B = M - 1 + \alpha/M^2$ in the region of existence of limit cycle for M large enough. Without loss of generality we can assume that $B = M - 1 + \alpha/M^2$ and we can restrict our study to the values of M where this curve remains in \mathcal{R} .

Following the procedure of Proposition 3.3 we propose a curve $C(x, y) = 0$ formed by three different polynomials $F_i(x, y)$ of degree i , for $i = 1, 2, 3$. Figure 3.9 shows the geometry of the curve $C(x, y) = 0$ and the sections that we propose. By abuse of notation, we use the same F_i to denote the algebraic curves that contain each one of them.

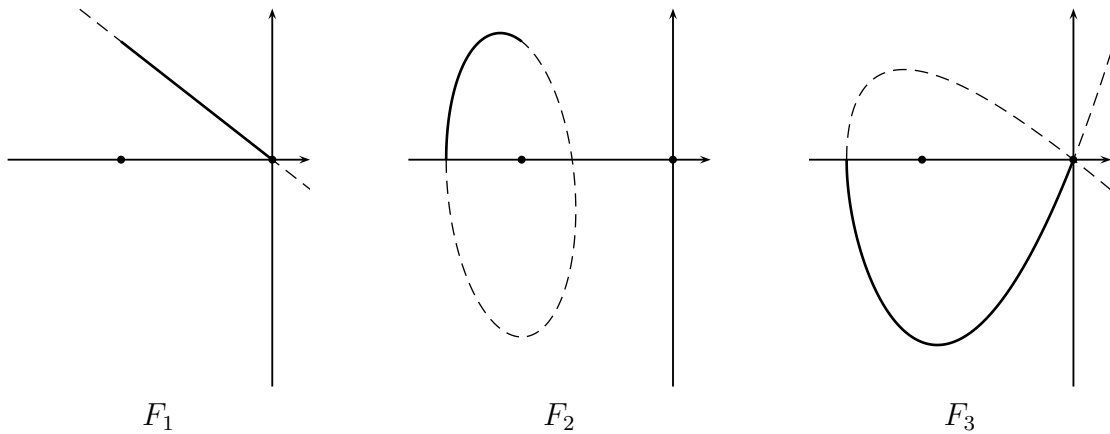


Figure 3.9 Graphical representation of the different F_i considered

First of all, let us consider the straight line containing the origin, the saddle point, such that is tangent to the stable separatrix. It satisfies the equation $y = (B - M)x$. We say F_1 to the segment of this straight line defined between the origin and the point (x_1, y_1) with $x_1 = B^2 - M^2$, which is the x -coordinate of the focus.

Second, we take F_2 to be a section of a quadratic curve that does not contain the origin. In general, it is expressed as $1 + a_{10}x + a_{01}y + a_{20}x^2 + a_{11}xy + a_{02}y^2 = 0$. And

we fixed the values of the a_{ij} to have that F_2 passes through (x_1, y_1) and is tangent to F_1 at this point. It gives us two of the five necessary conditions to get a unique quadratic expression. The other three are obtained imposing that F_2 contains and approximates until the second order the vector field at $(x_2, 0)$, where $x_2 = -3M$. The choice of this value for x_2 is justified in Remark 3.6(a). F_2 is defined as the section of the quadratic curve between the points (x_1, y_1) and $(x_2, 0)$.

Finally, F_3 is contained in a cubic curve whose quadratic part is $(B^2 - M^2)x^2 - 2Bxy + y^2$ as the one defined in (3.7), in the proof of Proposition 3.3. This fact assures that this curve is tangent to both separatrices at the origin. The four coefficients of the homogeneous part of degree three will be fixed to get that F_3 approaches two times more the unstable separatrix at the origin and contains and is tangent to the vector field at $(x_2, 0)$. F_3 is restricted to the section between the origin and $(x_2, 0)$ and which is contained in the third quadrant.

Let us check now the behavior of the vector field on each F_i for $i = 1, 2, 3$.

The gradient of F_1 at (x_1, y_1) is $(M - B, 1)$ for any α , which is an orthogonal exterior vector to F_1 . The gradient of F_2 at $(x_2, 0)$ is $\left(-\frac{2(3M+B^2-M^2)^3}{3(B+M)^2(M-B)^4M}, 0\right)$ which always points to the exterior of F_2 if $M > 0$ and $\alpha > 0$. And the gradient of F_3 at $(x_2, 0)$ is $(-3(B+M)(M-B)M, 0)$ which always points to the exterior of F_3 if $M > \sqrt{\alpha}$. Thus we can conclude that the vector field points to the exterior of F for M large enough, if we see that the curves defined by $F_i = 0$ and $\dot{F}_i = 0$, the derivation of F_i respect to the vector field, has no common points. Note that F_i and \dot{F}_i are both polynomials in x and y . Hence we can consider the resultant of both respect to any of the variables.

The resultant of F_1 and \dot{F}_1 respect to y is

$$R_1 := \text{Res}(F_1, \dot{F}_1, y) = \frac{\alpha x^2}{M^2}.$$

It just vanishes at $x = 0$, which means that the behavior of the vector field along F_1 does not change for any point on F_1 . As the vector field at (x_1, y_1) , $(x', y')|_{(x,y)=(x_1,y_1)} = ((M-B)^2(M+B), (M-B)^2(M+B)(B^2+2B-M^2))$, points to the exterior of F , this property holds at any point in F_1 and any value of $M > 0$.

The resultant with respect to y of F_2 and \dot{F}_2 , R_2 , has a zero with multiplicity two at $x = x_2$ and a factor of degree four on x , $p(x)$. Let us consider the Sturm sequence associated to $p(x)$, that we denote by $[p_0(x), p_1(x), p_2(x), p_3(x), p_4(x)]$. Once we evaluate the sequence at x_2 and x_1 , we obtain ten rational functions of M and α . If we consider the series expansion of them at $M = +\infty$, we can obtain the sign of these rational functions for M large enough. The sign configuration of the Sturm sequence, for $\alpha > 0$, at x_2 is $[+, -, -, +, +]$ and at x_1 is $[+, +, \pm, -, +]$. Thus, independently to the value of $\alpha > 0$, the number of changes of sign is in both cases two. Therefore, R_2 does not vanish in the interval (x_2, x_1) . From the previous case, the vector field at (x_1, y_1) points to the exterior of $C(x, y) = 0$. So, by the construction of F_2 , the vector field points to the exterior of $C(x, y) = 0$ along F_2 , for M large enough and any $\alpha > 0$. The value of M , \widetilde{M}_2 , where F_2 satisfies the desired property can be taken as the largest positive root of any of $p_0(x_1), p_1(x_1), p_2(x_1), p_3(x_1), p_4(x_1), p_0(x_2), p_1(x_2), p_2(x_2), p_3(x_2), p_4(x_2)$, which, for fixed α , are all polynomials in M .

The resultant of F_3 and \dot{F}_3 respect to x , R_3 , is of the form $y^9q(y)$, with q a polynomial of degree three. The series expansion of the coefficients of $q(y)$ for $y = +\infty$ show that the sign configuration of this coefficients for M large enough is $[+, -, +, -]$. Thus by the Descartes' rule of signs, all the zeros of $q(y)$ are positive. Then R_3 , for M large enough, has no vanishing points in the lower half plane, where F_3 is defined. And, similarly to the previous cases, we check that the vector field points to the exterior of $C(x, y) = 0$ along F_3 . This behavior of F_3 can be assure while the coefficients of $q(y)$ do not vanish. Thus, for a fixed value of α , we can take \widetilde{M}_3 , a real value from which we can assure this behavior, as the maximal root of the coefficients of $q(y)$, which are polynomials in M .

This finishes the proof, since M_α can be taken as the maximum of \widetilde{M}_2 and \widetilde{M}_3 and for $M > M_\alpha$ we have the situation given in Figure 3.10. \square

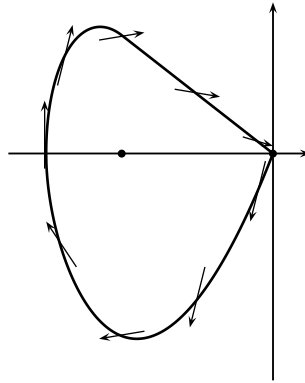


Figure 3.10 *The negatively invariant region corresponding to the piecewise loop*

Next remark clarifies some details about the previous proof. First, we explain why we fix the point $(x_2, 0)$ to be $(-3M, 0)$ in the previous proof. Second, we show the expression of M_α for a particular α .

Remark 3.6. (a) *In order to guarantee the choice of point x_2 in the proof of Proposition 3.5, we have computed numerically the first contact point of the separatrices of the saddle point with the negative x-axis, $(P_s, 0)$ for the stable and $(P_u, 0)$ for the unstable. See Figure 3.11(a).*

For some fixed values of α , we use a Fehlberg fourth-fifth order Runge-Kutta method with degree four interpolation to obtain numerical approximations of the coordinates P_s and P_u for any M . With the obtained values we compute approximations of the first coefficient of the power series expansion of these points. Figure 3.11(b) shows the plot of $-P_s/M$ and $-P_u/M$ together with the corresponding value of the abscissa of the focus point. We should remark that for any α that we have checked the limit behavior has been always the same. Thus, fixing $x_2 = -3M$, we desire that our loop will contact the x-axis between the points $(P_s, 0)$ and $(P_u, 0)$ for M large enough.

(b) *From the proof of last proposition, fixed α , M_α can be obtained as the largest positive root of a list of fourteen polynomials in M . For example, if we take $\alpha = 51/40$, we*

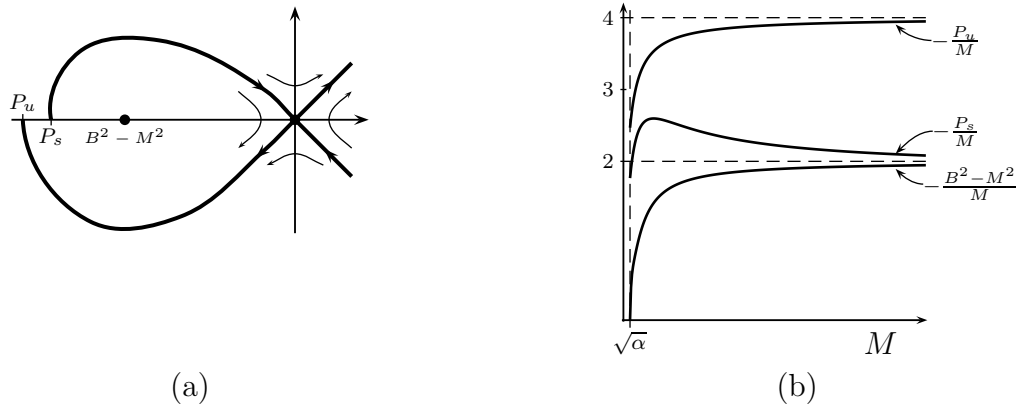


Figure 3.11 Separatrices of the saddle point

have that M_α is the largest positive zero of the polynomial of degree 17 given by

$$\begin{aligned}
& 196608000000M^{17} - 1441792000000M^{16} - 535756800000M^{15} \\
& + 1480294400000M^{14} - 1310515200000M^{13} - 1151979520000M^{12} \\
& + 1314478080000M^{11} - 727741440000M^{10} - 273666816000M^9 \\
& + 443460096000M^8 - 458441856000M^7 + 61550064000M^6 \\
& + 227310753600M^5 - 162364824000M^4 - 41403030120M^3 \\
& + 82806060240M^2 - 17596287801,
\end{aligned}$$

that is, approximately, 7.578650186. Numerical computations show that this concrete value of α is close to the one that minimize M_α . And it is taken in order to have a kind expression. A more accurate choice gives a value of M_α with a difference lower than a few thousandths.

We conclude this section with the proof of Theorem 3.1. It states the behavior, for the small parameters, of the curve $b = b^*(n)$ when n goes to infinity. Straightforward computations give the transformation of the upper bound of the previous result in capital parameters to small ones. Next lemma provides the transformed curve.

Lemma 3.7. Denoting $m = \sqrt{n}$, the change of variables (3.3) converts the curve $B = M - 1 + \alpha M^{-2}$ to the branch of the curve

$$\begin{aligned}
& -4m^5 - 12m^4b - 8m^3b^2 + 8m^2b^3 + 12mb^4 + 4b^5 - 60m^4 - 48m^3b + 88m^2b^2 \\
& + 80mb^3 + 4b^4 + (-192 - 16\alpha)m^3 + (384 - 48\alpha)m^2b + (64 - 48\alpha)mb^2 \\
& - 16\alpha b^3 + (256 - 160\alpha)m^2 - 192\alpha mb - 32\alpha b^2 - 256\alpha m + 64\alpha^2 = 0
\end{aligned} \tag{3.10}$$

such that, when m goes to $+\infty$, it is written as

$$b = m - 1 + 2\alpha \frac{1}{m} - \alpha \frac{1}{m^2} + \left(\frac{\alpha}{2} - 2\alpha^2\right) \frac{1}{m^3} + O\left(\frac{1}{m^4}\right).$$

Moreover, it remains below the curve $b = m - 1 + 2\alpha m^{-1}$ for any positive m and α .

Proof. Straightforward computations show that equation (3.10) follows immediately from the transformation under the change of variables (3.3).

In order to prove the comparison property in the statement of the lemma, we only need to show that both curves do not have common points. Then, the power series expansion at infinity, given in the statement, implies the desired order.

The common points of both curves are characterized by the roots of the polynomial obtained substituting $b = m - 1 + 2\alpha m^{-1}$ in (3.10),

$$q(m) := 8m^7 + (16\alpha + 12)m^6 + (24\alpha + 6)m^5 + (-12\alpha + 1 + 48\alpha^2)m^4 - 8\alpha(3\alpha + 1)m^3 + 24\alpha^2(2\alpha + 1)m^2 - 32m\alpha^3 + 16\alpha^4.$$

The computation of its Sturm sequence evaluated at 0 and at $+\infty$ gives us the configurations of signs $[+, -, -, -, +, +, -, -]$ and $[+, +, +, -, -, +, -, -]$, respectively, for any positive α . Hence, $q(m)$ does not have any positive root, and the curves of the statement have no common points for any positives m and α . \square

Proof of Theorem 3.1. From Lemma 3.7 the upper bound $B = M - 1 + \alpha M^{-2}$ is transformed to $b = \sqrt{n} - 1 + 2\alpha(\sqrt{n})^{-1} + O((\sqrt{n})^{-2})$. Therefore, by Proposition 3.5, we have that for every $\gamma = 2\alpha > 0$ there exists $n_\gamma \in \mathbb{R}^+$ such that for every $n > n_\gamma$,

$$\sqrt{n} - 1 < b^*(n) < \sqrt{n} - 1 + \frac{\gamma}{\sqrt{n}}.$$

Then, as we have that function $b^*(n)$ is analytic respect to \sqrt{n} , see [GGT10], we can assure, for n large enough, that

$$b^*(n) = \sqrt{n} - 1 + O(n^{-1}).$$

That is the expression given in the statement. \square

3.5 Global bounds for n in \mathbb{R}^+

This section is devoted to prove and analyze the bounds given in the statement of Theorem 3.2. First of all, we include the proof of Theorem 3.2. Then, as a corollary of it, we provide a rational expression for an upper bound of $b^*(n)$. We conclude with an analysis of the maximum error committed in the location of $b^*(n)$.

Proof of Theorem 3.2. Let $\Gamma_d(n)$ and $\Gamma_u(n)$ be the translation to small parameters of functions $\tilde{\Gamma}_d(M)$ and $\tilde{\Gamma}_u(M)$ given in Propositions 3.3 and 3.4, respectively. It follows that Γ_d connects with the curve $b = \sqrt{n} - 1$ at $n = n_d$, which can be obtained by squaring the positive root of the polynomial of the statement. That is the translated characterization of M_d in Proposition 3.3.

By Lemma 3.7 and Remark 3.6(b), the curve $b = \sqrt{n} - 1 + 51/(20\sqrt{n})$ is an upper bound of $b = b^*(n)$ for $n > n'_u$. Where n'_u is obtained by squaring the positive root of

the polynomial

$$\begin{aligned}
& 50331648000000000m^{17} - 243269632000000000m^{16} \\
& - 2129238425600000000m^{15} - 7211878973440000000m^{14} \\
& + 11166817320960000000m^{13} + 264470739812352000000m^{12} \\
& - 130466347912396800000m^{11} - 9197101546824499200000m^{10} \\
& - 6302900112535388160000m^9 + 6325778059290335232000m^8 \\
& + 2289016716587559936000m^7 - 46572462911915224012800m^6 \\
& + 8515659923453703340800m^5 - 4901243812728523876800m^4 \\
& - 45716337137659722706080m^3 + 6052551315638078774880m^2 \\
& - 8203038242422388605200m - 7953608649353382254007,
\end{aligned}$$

obtained translating the polynomial in Remark 3.6(b) to the small parameters and introducing the auxiliary parameter $m = \sqrt{n}$. That is $n \approx (6.9323668)^2 \approx 48.05770774$. However, this curve does not satisfy the condition of generating a global continuous upper bound. Because this curve cuts $b = \Gamma_u(n)$ for a value of n lower than n'_u , the starting point where we can assure that the curve is an upper bound. This situation is shown in Figure 3.12.

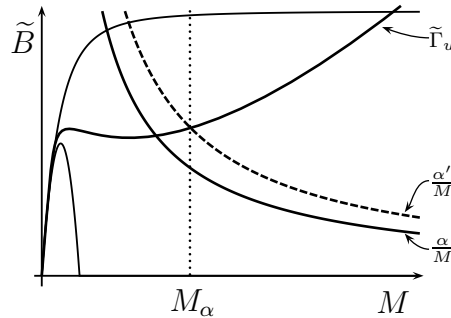


Figure 3.12 Connection of the piecewise upper bound, $b_u(n)$

In fact, for any $\alpha > 51/40$, $b = \sqrt{n} - 1 + 2\alpha/\sqrt{n}$ is also an upper bound of $b = b^*(n)$ when $n > n'_u$. The value of α such that the curve $b = \sqrt{n} - 1 + 2\alpha/\sqrt{n}$ cuts $b = \Gamma_u(n)$ for $n = n'_u$ is 1.913537947, approximately. For simplicity, we can finish the proof fixing $\alpha = 2$, for example. Thus we obtain the upper bound and the corresponding value of n_u given in the statement. \square

The global bounds included in Theorem 3.2 have been provided joining several local upper bounds. And they have motivate the seek of rational candidates, as simple as possible, to be also global upper bounds of the bifurcation curve $b = b^*(n)$.

Corollary 3.8. *There exist n_0, n_∞ positive real numbers such that for any $0 < n < n_0$ or $n_\infty < n < +\infty$,*

$$b^*(n) < b_r(n) := \frac{\sqrt{n}(5 + 2\sqrt{n})}{7 + 2\sqrt{n}}.$$

Proof. It is easy to check that

$$b_r(n) = \sqrt{n} - 1 + \frac{7}{2\sqrt{n}} + O(n^{-1}),$$

when n goes to $+\infty$. Therefore, there exist $\gamma > 0$ and $n_\gamma > 0$ such that for $n > n_\gamma$,

$$\sqrt{n} - 1 + \frac{\gamma}{\sqrt{n}} < b_r(n).$$

Then, by Theorem 3.1, we have proved the statement up to infinity

When n is close to 0 the statement follows using a similar argument since, for n small enough,

$$b_r(n) = \frac{5}{7}n^{1/2} + \frac{4}{49}n + O(n^{3/2}),$$

the definition of $\Gamma_u(n)$ in Theorem 3.2 says that for n small enough

$$\Gamma_u(n) = \frac{5}{7}n^{1/2} + \frac{72}{2401}n + O(n^{3/2}),$$

and $4/49 > 72/2401$. □

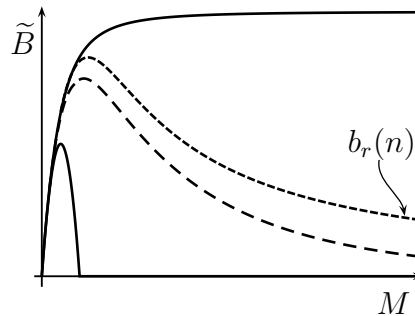


Figure 3.13 Graphical representation of the rational upper bound given in Corollary 3.8

Remark 3.9. The function provided in Corollary 3.8 is motivated by the knowledge of the Bogdanov-Takens curve at its limits of definition, gathering [GGT10] and the results contained in this chapter. It has just been designed fixing a first order approach to the origin and infinity as Bogdanov-Takens' curve does. This idea can also be considered for higher order approximations in order to obtain a family of rational candidates to be upper bounds. But we cannot assure that all these functions are global upper bounds of $b^*(n)$.

The main problem for the rational curve $b_r(n)$ of Corollary 3.8, for example, is that our proof does not work for the full real line. But it is an upper bound as it can graphically be seen in Figures 3.13 or 3.14.

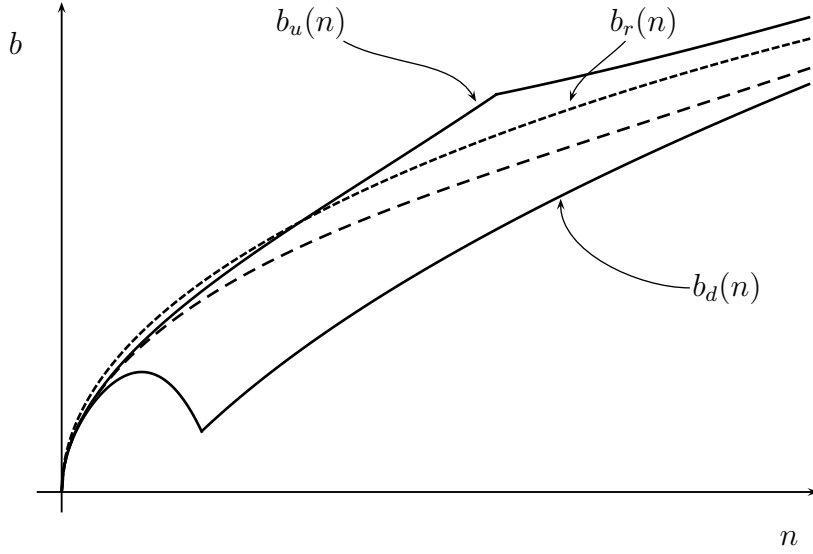


Figure 3.14 The bounds given in Theorem 3.2 and Corollary 3.8

The lower and upper bounds given in Theorem 3.2 and Corollary 3.8 are represented in Figure 3.14. The knowledge of the maximum difference between these curves motivates the following proposition.

Proposition 3.10. For any $n > 0$ we have

$$\left| \frac{b_u(n) + b_d(n)}{2} - b^*(n) \right| < \frac{1}{6}.$$

Proof. As far as $b_d(n) < b^*(n) < b_u(n)$, for every $n > 0$, we have

$$\max_{0 < n} \left| \frac{b_u(n) + b_d(n)}{2} - b^*(n) \right| < \max_{0 < n} \left| \frac{b_u(n) - b_d(n)}{2} \right|.$$

Let us consider the capital parameters (M, B) and (M, \tilde{B}) , introduced in Section 3.2. Let us denote by $B_u(M)$, $B_d(M)$, $\tilde{B}_u(M)$ and $\tilde{B}_d(M)$ the bounds of $B = B^*(M)$ and $\tilde{B} = \tilde{B}^*(M)$ obtained translating to capital parameters the ones given in Theorem 3.2, $b_u(n)$ and $b_d(n)$ respectively. It follows that

$$\max_{0 < n} \left| \frac{b_u(n) - b_d(n)}{2} \right| = \max_{0 < M} |B_u(M) - B_d(M)| = \max_{0 < M} \left| \frac{\tilde{B}_u(M) - \tilde{B}_d(M)}{M} \right|.$$

In the rescaled capital parameter space, (M, \tilde{B}) , the graph of the above differences is plotted in Figure 3.15.

□

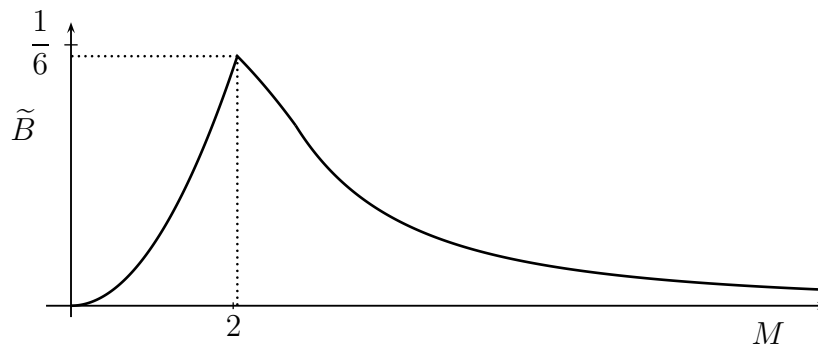


Figure 3.15 Numerical representation of $\left(\tilde{B}_u(M) - \tilde{B}_d(M)\right) / M$

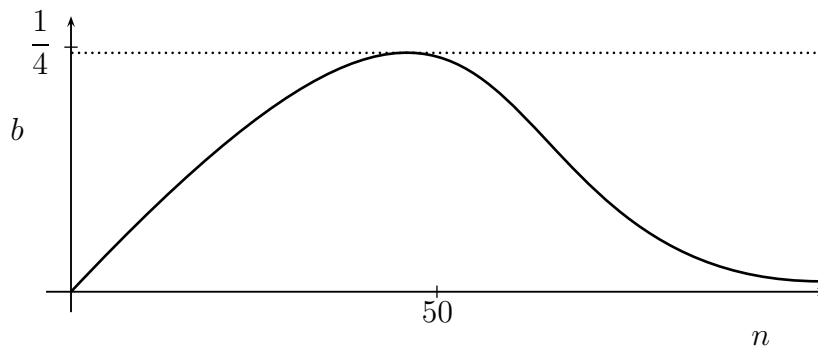


Figure 3.16 Differences between the rational curve given in Corollary 3.8 and the numerical approximation of $b^*(n)$

Figure 3.16 shows a numerical representation of the distance between $b_r(n)$, the rational upper bound, and $b^*(n)$. There are some labels included in the axes of the graphic in order to give some ideas on the size of the maximum distance.

Finally, we summarize the results of this chapter. We have constructed several upper and lower bounds of $b^*(n)$, each one with its own interval validity range. As the functions in Theorem 3.2 are global upper bounds, their validity range is \mathbb{R}^+ . We have included in Table 3.1 the approximative values of their connection points in both capital and small parameters.

	M	n
$b_d(n), n_d$	2.05965201805	2.43251441741
$b_u(n), n_u$	8.47598802427	60.0356036188

Table 3.1: Connection points

Table 3.2 contains the extrema of the range, different from 0 or ∞ , of the main functions obtained along the chapter. The values are expressed, at the same time, in the capital parameter space, M , and in the small parameter case, n , in order to help

the comprehension of the text. To simplify notation, the functions $\sqrt{n} - 1 + \alpha(\sqrt{n})^{-1}$ have been denoted by $\Gamma_\infty(n)$.

	M	n
$\Gamma_u(M)$ for the cubic, M_u	2.03679545744	1.61045872621
$\Gamma_u(M)$ for the quartic, M_u	30.3080508889	859.928861348
$\Gamma_\infty(M)$ for $\alpha = 51/40$	7.57865018594	48.0577077492
$b_r(n)$ near the origin, n_0	3.57286231485	8.26191928192
$b_r(n)$ near the infinity, n_∞	7.70499194495	49.8543430782

Table 3.2: Validity range of the bounds

Appendix. Explicit expressions of the functions that appear in Theorem 3.2

This appendix is devoted to present the functions that appear in Theorem 3.2 and Proposition 3.4, due to their extension.

The upper bound $b = \Gamma_u(n)$ satisfies a polynomial in the coordinates (n, b) of degree 50 with 488 monomials. But we do not show its expression due to its extension, more than six pages. But using $m = \sqrt{n}$, $b = \Gamma_u(n)$ in the coordinates (m, b) , satisfies the polynomial of degree 25 with 257 monomials given by

$$\begin{aligned}
& 6220800m^{25} + 118350720m^{24}b + 1048204800m^{23}b^2 + 5702607360m^{22}b^3 \\
& + 21110284800m^{21}b^4 + 55300734720m^{20}b^5 + 101692039680m^{19}b^6 \\
& + 118963468800m^{18}b^7 + 42514813440m^{17}b^8 - 146429078400m^{16}b^9 \\
& - 349219537920m^{15}b^{10} - 390209633280m^{14}b^{11} - 182847974400m^{13}b^{12} \\
& + 150497948160m^{12}b^{13} + 371723904000m^{11}b^{14} + 349219537920m^{10}b^{15} \\
& + 159138017280m^9b^{16} - 26815536000m^8b^{17} - 107002114560m^7b^{18} \\
& - 95081817600m^6b^{19} - 52546475520m^5b^{20} - 20244660480m^4b^{21} \\
& - 5502297600m^3b^{22} - 1015856640m^2b^{23} - 115084800mb^{24} - 6065280b^{25} \\
& + 1479409920m^{24} + 25447898304m^{23}b + 202329253728m^{22}b^2 + 979317796608m^{21}b^3 \\
& + 3186916616736m^{20}b^4 + 7208345545920m^{19}b^5 + 11072259099936m^{18}b^6 \\
& + 9820774357632m^{17}b^7 - 414106289568m^{16}b^8 - 15666786170496m^{15}b^9 \\
& - 24027019191360m^{14}b^{10} - 16663536470016m^{13}b^{11} + 1347045380928m^{12}b^{12} \\
& + 15195214770048m^{11}b^{13} + 15632837061696m^{10}b^{14} + 6653243923200m^9b^{15} \\
& - 1880901186624m^8b^{16} - 4811908120128m^7b^{17} - 3610247316768m^6b^{18} \\
& - 1620648850176m^5b^{19} - 463010329440m^4b^{20} - 76596134976m^3b^{21} \\
& - 4020877152m^2b^{22} + 808507008mb^{23} + 115420896b^{24} + 84621220992m^{23}
\end{aligned}$$

$$\begin{aligned}
& + 1288340194176m^{22}b + 8943457635072m^{21}b^2 + 37069000720416m^{20}b^3 \\
& + 100161191495808m^{19}b^4 + 177344384238144m^{18}b^5 + 181594323823104m^{17}b^6 \\
& + 19275968341152m^{16}b^7 - 262450460047104m^{15}b^8 - 435356383758336m^{14}b^9 \\
& - 305743750018560m^{13}b^{10} + 35124339871296m^{12}b^{11} + 285911704675584m^{11}b^{12} \\
& + 269090901263232m^{10}b^{13} + 86875012859904m^9b^{14} - 59520056347584m^8b^{15} \\
& - 90139294406016m^7b^{16} - 54946790640000m^6b^{17} - 19293792226560m^5b^{18} \\
& - 3592251065952m^4b^{19} - 69102271872m^3b^{20} + 117226391616m^2b^{21} \\
& + 21951530496mb^{22} + 1185062688b^{23} + 2414194507008m^{22} + 31884131336256m^{21}b \\
& + 188101079408928m^{20}b^2 + 641511875796384m^{19}b^3 + 1342298764700832m^{18}b^4 \\
& + 1568475643682592m^{17}b^5 + 264611549651904m^{16}b^6 - 2378121008711040m^{15}b^7 \\
& - 4093915225074048m^{14}b^8 - 2723647705357824m^{13}b^9 + 774728156299968m^{12}b^{10} \\
& + 3089356510209216m^{11}b^{11} + 2490135914265792m^{10}b^{12} + 430735862300352m^9b^{13} \\
& - 886533985695744m^8b^{14} - 921728907278208m^7b^{15} - 446086120265856m^6b^{16} \\
& - 112848983025984m^5b^{17} - 7058442069216m^4b^{18} + 4180301322912m^3b^{19} \\
& + 1226178837408m^2b^{20} + 129224460576mb^{21} + 4880168256b^{22} + 42190814634240m^{21} \\
& + 470451286136448m^{20}b + 2267586703804992m^{19}b^2 + 5947184281170944m^{18}b^3 \\
& + 8196404089444864m^{17}b^4 + 1961477154569152m^{16}b^5 - 13489230549722880m^{15}b^6 \\
& - 24086083022740480m^{14}b^7 - 14563176105958912m^{13}b^8 + 8399916239310336m^{12}b^9 \\
& + 21304373361561472m^{11}b^{10} + 13965013282195456m^{10}b^{11} - 634889482612736m^9b^{12} \\
& - 7494193465936256m^8b^{13} - 5732203990987520m^7b^{14} - 2103486848228352m^6b^{15} \\
& - 301815126950656m^5b^{16} + 54945819748736m^4b^{17} + 30793636929600m^3b^{18} \\
& + 5201438891008m^2b^{19} + 404622489088mb^{20} + 11807514560b^{21} + 495876937655040m^{20} \\
& + 4487513887926976m^{19}b + 16545974125913120m^{18}b^2 + 28705605197816768m^{17}b^3 \\
& + 10361321113019104m^{16}b^4 - 51428818413182080m^{15}b^5 - 97250974110823168m^{14}b^6 \\
& - 51062683016071808m^{13}b^7 + 53909569367995904m^{12}b^8 + 99763713113532672m^{11}b^9 \\
& + 48658371413630528m^{10}b^{10} - 20265216018078464m^9b^{11} - 3970143335521856m^8b^{12} \\
& - 22523461498507136m^7b^{13} - 5608349848081408m^6b^{14} + 33707576360576m^5b^{15} \\
& + 391024139706880m^4b^{16} + 103292053239872m^3b^{17} + 13074188960928m^2b^{18} \\
& + 818367701824mb^{19} + 17278284128b^{20} + 4104092821667840m^{19} \\
& + 28312843969412224m^{18}b + 69819279415142400m^{17}b^2 + 41105786416460832m^{16}b^3 \\
& - 135727881844667520m^{15}b^4 - 285155185291330176m^{14}b^5 - 122657032814469248m^{13}b^6 \\
& + 229441151090534400m^{12}b^7 + 328573475038163328m^{11}b^8 + 94513852166579840m^{10}b^9 \\
& - 126102088861397632m^9b^{10} - 136959392539723968m^8b^{11} - 54632796990975360m^7b^{12} \\
& - 6349251404392320m^6b^{13} + 2446689031102080m^5b^{14} + 1104877347606784m^4b^{15}
\end{aligned}$$

$$\begin{aligned}
& + 212390401970304m^3b^{16} + 22515377821440m^2b^{17} + 1083685497984mb^{18} \\
& + 12749065120b^{19} + 24248170909005568m^{18} + 113731913419226304m^{17}b \\
& + 119958794637441760m^{16}b^2 - 243701994794514656m^{15}b^3 - 631262639455112736m^{14}b^4 \\
& - 208889256536238688m^{13}b^5 + 689780650186495712m^{12}b^6 + 771640395849770144m^{11}b^7 \\
& + 20677092181085792m^{10}b^8 - 441095940107501920m^9b^9 - 302939716318727136m^8b^{10} \\
& - 70796915314736288m^7b^{11} + 5373818838661024m^6b^{12} + 6504196546318560m^5b^{13} \\
& + 1838275684562336m^4b^{14} + 308765642213600m^3b^{15} + 27475035662624m^2b^{16} \\
& + 760457061920mb^{17} + 3462524032b^{18} + 100457345029900032m^{17} \\
& + 240725155697962496m^{16}b - 258867884174916288m^{15}b^2 - 1080119137649827136m^{14}b^3 \\
& - 274544472903095552m^{13}b^4 + 1521072514023740544m^{12}b^5 \\
& + 1276250735468781760m^{11}b^6 - 451649186474963392m^{10}b^7 \\
& - 965591142884274816m^9b^8 - 385192534878103296m^8b^9 - 16903608672155968m^7b^{10} \\
& + 22642961413505856m^6b^{11} + 8440201658162176m^5b^{12} + 2095708173335680m^4b^{13} \\
& + 352768753056576m^3b^{14} + 18661462897600m^2b^{15} + 199493090432mb^{16} \\
& + 275361200182773760m^{16} - 24274497847361664m^{15}b - 1426810749661406080m^{14}b^2 \\
& - 355729778198722944m^{13}b^3 + 2527873309894242432m^{12}b^4 \\
& + 1373958026708376320m^{11}b^5 - 1425291112416852480m^{10}b^6 \\
& - 1253415774351883008m^9b^7 - 172100052464404224m^8b^8 \\
& + 61296882134398336m^7b^9 + 25865269037062272m^6b^{10} \\
& + 5095684448861312m^5b^{11} + 2266577973638784m^4b^{12} + 238671809538048m^3b^{13} \\
& + 4772158151936m^2b^{14} + 429715428082300800m^{15} - 1367619432428810240m^{14}b \\
& - 616381816261551232m^{13}b^2 + 3315854533454275840m^{12}b^3 + 515888813505861376m^{11}b^4 \\
& - 2188921705654174720m^{10}b^5 - 654543783718337792m^9b^6 + 43418085599272448m^8b^7 \\
& + 118533112492607872m^7b^8 - 6216783207470080m^6b^9 + 4875395092361600m^5b^{10} \\
& + 1632837097817344m^4b^{11} + 60385667667968m^3b^{12} + 154827387518464000m^{14} \\
& - 2129589491551820800m^{13}b + 4643874344694302720m^{12}b^2 \\
& - 2336798290309246976m^{11}b^3 - 328070062174093312m^{10}b^4 - 609415804072036352m^9b^5 \\
& + 349813351851782144m^8b^6 + 17053843181522944m^7b^7 - 15357613659959296m^6b^8 \\
& + 5110418770789376m^5b^9 + 421514883500032m^4b^{10} - 523689297294080000m^{13} \\
& + 1495937764656128000m^{12}b - 1096022762364108800m^{11}b^2 + 131072400717946880m^{10}b^3 \\
& - 311704372471083008m^9b^4 + 298824261287272448m^8b^5 - 60486934990241792m^7b^6 \\
& + 1064348487114752m^6b^7 + 1483249690617856m^5b^8 - 33072590592000000m^{12} \\
& + 134603494502400000m^{11}b - 170202048768000000m^{10}b^2 + 38839430062080000m^9b^3 \\
& + 50705558378496000m^8b^4 - 20443669596241920m^7b^5 + 1602400672825344m^6b^6 \\
& - 597196800000000m^{11} + 3344302080000000m^{10}b - 7023034368000000m^9b^2 \\
& + 6554832076800000m^8b^3 - 2294191226880000m^7b^4.
\end{aligned}$$

In the coordinates (M, B) , the function $B = \tilde{\Gamma}_u(M)$ satisfies the polynomial of degree 14 and 72 monomials with expression

$$\begin{aligned}
& -383292M^{14} - 1910439M^{13}B - 3223665M^{12}B^2 - 314748M^{11}B^3 + 5603940M^{10}B^4 \\
& + 5541141M^9B^5 - 2323401M^8B^6 - 7154664M^7B^7 - 3397092M^6B^8 + 2020587M^5B^9 \\
& + 3218997M^4B^{10} + 1742052M^3B^{11} + 499644M^2B^{12} + 76071MB^{13} + 4869B^{14} \\
& - 500742M^{13} - 787023M^{12}B + 4493070M^{11}B^2 + 14795091M^{10}B^3 + 11566572M^9B^4 \\
& - 11585754M^8B^5 - 24443044M^7B^6 - 8307134M^6B^7 + 12772706M^5B^8 \\
& + 16289545M^4B^9 + 8662166M^3B^{10} + 2509195M^2B^{11} + 388536MB^{12} + 25344B^{13} \\
& - 174798M^{12} + 1420524M^{11}B + 7005177M^{10}B^2 + 4483350M^9B^3 - 16943919M^8B^4 \\
& - 28501282M^7B^5 - 3691132M^6B^6 + 27741570M^5B^7 + 31479694M^4B^8 + 16742014M^3B^9 \\
& + 4938651M^2B^{10} + 781536MB^{11} + 52119B^{12} - 48600M^{11} + 855846M^{10}B + 404136M^9B^2 \\
& - 8473533M^8B^3 - 14178838M^7B^4 + 2903273M^6B^5 + 26313718M^5B^6 + 28894211M^4B^7 \\
& + 15714446M^3B^8 + 4769205M^2B^9 + 775554MB^{10} + 53046B^{11} + 226800M^9B \\
& - 1138914M^8B^2 - 2990748M^7B^3 + 2116351M^6B^4 + 10975549M^5B^5 \\
& + 12542602M^4B^6 + 7156446M^3B^7 + 2261723M^2B^8 + 380289MB^9 + 26766B^{10} \\
& - 264600M^7B^2 + 218442M^6B^3 + 1575182M^5B^4 + 2042992M^4B^5 + 1262428M^3B^6 \\
& + 421554M^2B^7 + 73806MB^8 + 5364B^9.
\end{aligned}$$

For the lower bound in the coordinates (n, b) , the function $b = \Gamma_d(n)$ satisfies the polynomial of degree 18 with 74 monomials given by

$$\begin{aligned}
& 26244b^{18} - 282852nb^{16} + 492804b^{17} + 1318032n^2b^{14} - 5279904nb^{15} + 3542049b^{16} \\
& - 3510864n^3b^{12} + 24093936n^2b^{13} - 59646456nb^{14} + 12332628b^{15} + 5919480n^4b^{10} \\
& - 61282656n^3b^{11} + 284874732n^2b^{12} - 396688860nb^{13} + 21865626b^{14} - 6572664n^5b^8 \\
& + 95304600n^4b^9 - 569429352n^3b^{10} + 2244693060n^2b^{11} - 1556797266nb^{12} + 18664224b^{13} \\
& + 4817232n^6b^6 - 93070944n^5b^7 + 511250454n^4b^8 - 4198843116n^3b^9 + 12862236618n^2b^{10} \\
& - 3613760064nb^{11} + 6056521b^{12} - 2251152n^7b^4 + 55882224n^6b^5 - 158931720n^5b^6 \\
& + 962744508n^4b^7 - 22001723442n^3b^8 + 51550980192n^2b^9 - 4831263702nb^{10} + 609444n^8b^2 \\
& - 18903456n^7b^3 - 16136820n^6b^4 + 3431184300n^5b^5 - 7185849282n^4b^6 - 76306790784n^3b^7 \\
& + 139214319207n^2b^8 - 3390790528nb^9 - 72900n^9 + 2763396n^8b - 8845848n^7b^2 \\
& - 1884890196n^6b^3 + 7787631546n^5b^4 - 39218570784n^4b^5 - 180864465140n^3b^6 \\
& + 244658871808n^2b^7 - 959415296nb^8 + 13322961n^8 - 170532324n^7b - 7508602530n^6b^2 \\
& - 27656677440n^5b^3 - 65653161849n^4b^4 - 288902018304n^3b^5 + 265576943616n^2b^6 \\
& - 764646966n^7 - 5166608736n^6b - 73099403862n^5b^2 - 30984045056n^4b^3 \\
& - 294849320960n^3b^4 + 159664046080n^2b^5 + 11621481961n^6 - 2593704832n^5b \\
& + 46422134784n^4b^2 - 167754334208n^3b^3 + 40282095616n^2b^4 + 17934515200n^5 \\
& + 44027084800n^4b - 41104179200n^3b^2 + 10485760000n^4.
\end{aligned}$$

Using the auxiliary variable $m = \sqrt{n}$, in the coordinates (m, b) , the polynomial has degree 9 with 42 monomials and is given by

$$\begin{aligned}
& -270m^9 - 1998m^8b - 6264m^7b^2 - 10584m^6b^3 - 9828m^5b^4 - 3780m^4b^5 + 1512m^3b^6 \\
& + 2376m^2b^7 + 1026mb^8 + 162b^9 - 3591m^8 - 21456m^7b - 51804m^6b^2 - 61344m^5b^3 \\
& - 29250m^4b^4 + 10224m^3b^5 + 19764m^2b^6 + 9216mb^7 + 1521b^8 + 792m^7 - 33504m^6b \\
& - 119160m^5b^2 - 121968m^4b^3 + 5928m^3b^4 + 77184m^2b^5 + 37944mb^6 + 3792b^7 \\
& + 111661m^6 + 1950m^5b - 290733m^4b^2 - 71260m^3b^3 + 181635m^2b^4 + 74334mb^5 \\
& + 2461b^6 + 70240m^5 + 18304m^4b - 424896m^3b^2 + 334720m^2b^3 + 44128mb^4 \\
& + 102400m^4 - 286720m^3b + 200704m^2b^2.
\end{aligned}$$

The size increases in (n, b) instead of (m, b) because the square root disappears squaring.

Finally, in the coordinates (M, B) , the lower bound $B = \tilde{\Gamma}_d(M)$ satisfies the quintic polynomial

$$\begin{aligned}
& -18M^5 - 51M^4B + 6M^3B^2 + 78M^2B^3 + 48MB^4 + 9B^5 - 24M^4 + 24M^3B \\
& + 138M^2B^2 + 90MB^3 + 18B^4 + 56M^2B + 42MB^2 + 9B^3.
\end{aligned}$$

Clearly, the most useful coordinates are (M, B) . Because the expressions involved in all the results of this chapter are shorter.

Bibliography

- [AEGP85] O. Armitano, J. Edelman, and U. García Palomares. *Programación no lineal*. Editorial Limusa, México, Bogotá, 1985.
- [Arn77] V. I. Arnol'd. Loss of stability of self-induced oscillations near resonance, and versal deformations of equivariant vector fields. *Funkcional. Anal. i Priložen.*, 11(2):1–10, 95, 1977.
- [Arn83] V. I. Arnol'd. *Geometrical methods in the theory of ordinary differential equations*, volume 250 of *Grundlehren der Mathematischen Wissenschaften [Fundamental Principles of Mathematical Science]*. Springer-Verlag, New York, 1983. Translated from the Russian by Joseph Szücs, Translation edited by Mark Levi.
- [Ben01] I. Bendixson. Sur les courbes définies par des équations différentielles. *Acta Math.*, 24(1):1–88, 1901.
- [Bir66] G. D. Birkhoff. *Dynamical systems*. With an addendum by Jurgen Moser. American Mathematical Society Colloquium Publications, Vol. IX. American Mathematical Society, Providence, R.I., 1966.
- [BJM10] C. Bereanu, P. Jebelean, and J. Mawhin. Periodic solutions of pendulum-like perturbations of singular and bounded ϕ -Laplacians. *J. Dynam. Differential Equations*, 22(3):463–471, 2010.
- [BL07] A. Buică and J. Llibre. Limit cycles of a perturbed cubic polynomial differential center. *Chaos Solitons Fractals*, 32(3):1059–1069, 2007.
- [Bog75] R. I. Bogdanov. Versal deformation of a singular point of a vector field on the plane in the case of zero eigenvalues. *Funkcional Anal. i Priložen.*, 9(2):63, 1975.
- [Bou91] M. Boutat. *Familles de champs de vecteurs du plan de type Takens-Bogdanov*. PhD thesis, Université de Bourgogne, Bourgogne (France), 1991.
- [Chi06] C. Chicone. *Ordinary differential equations with applications*, volume 34 of *Texts in Applied Mathematics*. Springer, New York, second edition, 2006.

-
- [Cie02] K. Ciesielski. On the poincaré-bendixson theorem (rehacer). *Lecture Notes in Nonlinear Analysis*, 3:49–69, 2002.
- [CL55] E. A. Coddington and N. Levinson. *Theory of ordinary differential equations*. McGraw-Hill Book Company, Inc., New York-Toronto-London, 1955.
- [CL95] C. Christopher and N. G. Lloyd. Polynomial systems: a lower bound for the Hilbert numbers. *Proc. Roy. Soc. London Ser. A*, 450(1938):219–224, 1995.
- [CL07] C. Christopher and Chengzhi Li. *Limit cycles of differential equations*. Advanced Courses in Mathematics. CRM Barcelona. Birkhäuser Verlag, Basel, 2007.
- [CLP09] B. Coll, Chengzhi Li, and R. Prohens. Quadratic perturbations of a class of quadratic reversible systems with two centers. *Discrete Contin. Dyn. Syst.*, 24(3):699–729, 2009.
- [Con65] S. D. Conte. *Elementary numerical analysis: An algorithmic approach*. McGraw-Hill Book Co., New York, 1965.
- [DCM09] Z. Došlá, M. Cecchi, and M. Marini. Asymptotic problems for differential equations with bounded Φ -Laplacian. *Electron. J. Qual. Theory Differ. Equ.*, (Special Edition I):No. 9, 18, 2009.
- [DL03] F. Dumortier and Chengzhi Li. Perturbation from an elliptic Hamiltonian of degree four. IV. Figure eight-loop. *J. Differential Equations*, 188(2):512–554, 2003.
- [DMD11] P. De Maesschalck and F. Dumortier. Bifurcations of multiple relaxation oscillations in polynomial Liénard equations. *Proc. Amer. Math. Soc.*, 139(6):2073–2085, 2011.
- [DRS87] F. Dumortier, R. Roussarie, and J. Sotomayor. Generic 3-parameter families of vector fields on the plane, unfolding a singularity with nilpotent linear part. The cusp case of codimension 3. *Ergodic Theory Dynam. Systems*, 7(3):375–413, 1987.
- [GGJ08] A. Garijo, A. Gasull, and X. Jarque. Simultaneous bifurcation of limit cycles from two nests of periodic orbits. *J. Math. Anal. Appl.*, 341(2):813–824, 2008.
- [GGT10] A. Gasull, H. Giacomini, and J. Torregrosa. Some results on homoclinic and heteroclinic connections in planar systems. *Nonlinearity*, 23(12):2977–3001, 2010.
- [GH02] J. Guckenheimer and P. Holmes. *Nonlinear oscillations, dynamical systems, and bifurcations of vector fields*, volume 42 of *Applied Mathematical Sciences*.

- Springer-Verlag, New York, 2002. Revised and corrected reprint of the 1983 original.
- [GL07] J. Giné and J. Llibre. Limit cycles of cubic polynomial vector fields via the averaging theory. *Nonlinear Anal.*, 66(8):1707–1721, 2007.
- [GLT12] A. Gasull, T. Lazaro, and J. Torregrosa. Upper bounds for the number of zeroes for some abelian integrals. *Nonlinear Anal.*, 75:5169–5179, 2012.
- [Gol57] L. Gold. Note on the relativistic harmonic oscillator. *J. Franklin Inst.*, 264:25–27, 1957.
- [Gol80] H. Goldstein. *Classical mechanics*. Addison-Wesley Publishing Co., Reading, Mass., second edition, 1980. Addison-Wesley Series in Physics.
- [GPT08] A. Gasull, R. Prohens, and J. Torregrosa. Bifurcation of limit cycles from a polynomial non-global center. *J. Dynam. Differential Equations*, 20(4):945–960, 2008.
- [Har64] P. Hartman. *Ordinary differential equations*. John Wiley & Sons Inc., New York, 1964.
- [HS74] M. W. Hirsch and S. Smale. *Differential equations, dynamical systems, and linear algebra*. Academic Press [A subsidiary of Harcourt Brace Jovanovich, Publishers], New York-London, 1974. Pure and Applied Mathematics, Vol. 60.
- [Ily02] Y. Ilyashenko. Centennial history of Hilbert’s 16th problem. *Bull. Amer. Math. Soc. (N.S.)*, 39(3):301–354 (electronic), 2002.
- [Kos82] A. I. Kostrikin. *Introduction to algebra*. Springer-Verlag, New York, 1982. Translated from the Russian by Neal Koblitz, Universitext.
- [Kuz98] Y. A. Kuznetsov. *Elements of applied bifurcation theory*, volume 112 of *Applied Mathematical Sciences*. Springer-Verlag, New York, second edition, 1998.
- [Li03] Jibin Li. Hilbert’s 16th problem and bifurcations of planar polynomial vector fields. *Internat. J. Bifur. Chaos Appl. Sci. Engrg.*, 13(1):47–106, 2003.
- [LL12] Chengzhi Li and J. Llibre. Uniqueness of limit cycles for Liénard differential equations of degree four. *J. Differential Equations*, 252(4):3142–3162, 2012.
- [LLLZ00] Chengzhi Li, Weigu Li, J. Llibre, and Zhifen Zhang. Linear estimate for the number of zeros of abelian integrals for quadratic isochronous centres. *Nonlinearity*, 13(5):1775–1800, 2000.

- [LLLZ02] Chengzhi Li, Weigu Li, J. Llibre, and Zhifen Zhang. Linear estimation of the number of zeros of abelian integrals for some cubic isochronous centers. *J. Differential Equations*, 180(2):307–333, 2002.
- [LS42] N. Levinson and O. K. Smith. A general equation for relaxation oscillations. *Duke Math. J.*, 9:382–403, 1942.
- [Mic98] R. E. Mickens. Periodic solutions of the relativistic harmonic oscillator. *J. Sound Vibration*, 212(5):905–908, 1998.
- [Per92] L. M. Perko. A global analysis of the Bogdanov-Takens system. *SIAM J. Appl. Math.*, 52(4):1172–1192, 1992.
- [PGT12] S. Pérez-González and J. Torregrosa. Limit cycles on a linear center with extra singular points. Prepublicacions del Departament de Matemàtiques, Núm. 25/2012, 2012.
- [PGTT12] S. Pérez-González, J. Torregrosa, and P. J. Torres. Existence and uniqueness of limit cycles for generalized φ -laplacian liénard equations. Prepublicacions del Departament de Matemàtiques, Núm. 24/2012, 2012.
- [Phi03] G. M. Phillips. *Interpolation and approximation by polynomials*. CMS Books in Mathematics/Ouvrages de Mathématiques de la SMC, 14. Springer-Verlag, New York, 2003.
- [Poi81] H. Poincaré. Mémoire sur les courbes définies par une équation différentielle. *Journal de mathématiques pures et appliquées*, 1881. (1) 7:375–422, 1881, (2) 3:251–296, 1882, (3) 4:167–244, 1885, (4) 2:151–217, 1886.
- [Poi90] H. Poincaré. Sur le problème des trois corps et les équations de la dynamique. *Acta Mathematica*, 13:1–270, 1890.
- [Pol26] B. van der Pol. On relaxation-oscillations. *Philosophical Magazine*, 2(11):978–992, 1926.
- [Pon34] L. S. Pontrjagin. Über autoschwingungssysteme, die den hamiltonschen nahe liegen. *Physikalische Zeitschrift der Sowjetunion*, 6(1-2):25–28, 1934.
- [San49] G. Sansone. Sopra l'equazione di A. Liénard delle oscillazioni di rilassamento. *Ann. Mat. Pura Appl. (4)*, 28:153–181, 1949.
- [Sma98] S. Smale. Mathematical problems for the next century. *Math. Intelligencer*, 20(2):7–15, 1998.
- [Sot79] J. Sotomayor. *Lições de equações diferenciais ordinárias*, volume 11 of *Projeto Euclides [Euclid Project]*. Instituto de Matemática Pura e Aplicada, Rio de Janeiro, 1979.

- [Tak74] Floris Takens. Singularities of vector fields. *Inst. Hautes Études Sci. Publ. Math.*, (43):47–100, 1974.
- [Tor08] P. J. Torres. Periodic oscillations of the relativistic pendulum with friction. *Physics Letters A*, 372(42):6386–6387, 2008.
- [Vil82] G. Villari. Periodic solutions of Liénard’s equation. *J. Math. Anal. Appl.*, 86(2):379–386, 1982.
- [Vil83] G. Villari. On the existence of periodic solutions for Liénard’s equation. *Nonlinear Anal.*, 7(1):71–78, 1983.
- [WSM⁺09] Lijuan Wang, Jianying Shao, Hua Meng, Bing Xiao, and Fei Long. Periodic solutions for Liénard type p -Laplacian equation with two deviating arguments. *J. Comput. Appl. Math.*, 224(2):751–758, 2009.
- [XH04a] Guanghui Xiang and Maoan Han. Global bifurcation of limit cycles in a family of multiparameter system. *Internat. J. Bifur. Chaos Appl. Sci. Engrg.*, 14(9):3325–3335, 2004.
- [XH04b] Guanghui Xiang and Maoan Han. Global bifurcation of limit cycles in a family of polynomial systems. *J. Math. Anal. Appl.*, 295(2):633–644, 2004.
- [YCC⁺86] Yan Qian Ye, Sui Lin Cai, Lan Sun Chen, Ke Cheng Huang, Ding Jun Luo, Zhi En Ma, Er Nian Wang, Ming Shu Wang, and Xin An Yang. *Theory of limit cycles*, volume 66 of *Translations of Mathematical Monographs*. American Mathematical Society, Providence, RI, second edition, 1986. Translated from the Chinese by Chi Y. Lo.
- [ZDHD92] Zhi Fen Zhang, Tong Ren Ding, Wen Zao Huang, and Zhen Xi Dong. *Qualitative theory of differential equations*, volume 101 of *Translations of Mathematical Monographs*. American Mathematical Society, Providence, RI, 1992. Translated from the Chinese by Anthony Wing Kwok Leung.

Index

- B , 73
- B^* close to infinity, 83
- $B^*(M)$, 74
- $C(x, y)$, 76
- E_{ij} , 77
- F_i , 83
- $I(h)$, 3
- I_j , 5
- $K(x, y)$, 3
- M , 73
- M_d , 75
- M_u , 75
- M_α , 83
- R_l , 13
- S_l , 13
- Γ_d , 71
- Γ_u , 71
- Φ^\pm , 76
- α_{lm} , 13
- β_{lm} , 13
- $\mathbf{H}(n)$, v, 1
- $\mathcal{H}(n, k)$, 3, 4
- $\mathcal{P}(n, k)$, 3
- \mathcal{R} , 74
- \mathcal{R}_j , 4
- \mathcal{Z} , 5
- \mathcal{Z}^M , 6
- φ functions, 49
- φ -laplacian Liénard equation, 45
- \tilde{B} , 74
- $\tilde{\Gamma}_d(M)$, 74
- $\tilde{\Gamma}_u(M)$, 74
- $b^*(n)$, 70, 71
- $b_d(n)$, 71
- $b_u(n)$, 71
- $d_0(r)$, 2
- $\mathcal{P}_a(n)$, 4
- (M,B), 73
- Abelian integral, vi, 3
- autonomous differential system, iii
- Basic φ functions, 49
- bifurcate, 1
- Bogdanov-Takens system, vii, 69
- bounded regular, 49
- box without contact, 79
- capital parameter, 73
- Chebyshev's polynomials, 12
- compactified boundaries, 51
- compactified boundary with singular points, 63
- compactified boundary without singular points, 64
- configuration of signs, 28
- configuration of simultaneous zeros, 5
- cusp, 69
- dynamical system, iii
- energy function, 54
- Existence of limit cycle, 47
- first return map, 1
- harmonic relativistic oscillator, vi, 46
- heteroclinic orbit, iv
- Hilbert 16th Problem, 2
- Hilbert 16th problem, iv, 1
- homoclinic connection, iv, 69, 70

-
- Hopf bifurcation, v, 70, 75
 - Hypotheses (\tilde{H}), 50
 - Hypotheses (H), 47

 - Liénard system, v, 45
 - limit cycle, iv, 1
 - loop without contact, 78
 - lower bound, 71

 - maximal configuration, 6
 - maximum of configurations, 6
 - mean curvature operator, 49
 - minimal configuration, 24, 27
 - mixed behavior, 49

 - negative invariant loop, 72
 - non-bounded regular behavior, 49

 - orbit, iii

 - p-laplacian operator, 49
 - Perko's bounds, 70
 - Perko's Conjecture, 70
 - piecewise loop, 83
 - Poincaré map, 1
 - Poincaré-Bendixson theorem, iv
 - polygonal compactification, 50
 - Pontrjagin Criterion, 2
 - positively invariant loop, 72

 - rational decomposition, 9
 - regular point in the boundary, 59
 - relativistic operator, 49
 - rotated family of vector fields, vii, 70

 - separatrices, 76
 - singular behavior, 49
 - singular point, iv
 - singular point in the boundary, 59
 - Smale 13th problem, v
 - small parameter, 73
 - state function, 54
 - Sturm sequence, 85

 - trajectory, iii
 - transversal section, 3

 - Unicity of limit cycle, 48
 - upper bound, 71

 - van der Pol system, 45

 - Weak Hilbert 16th Problem, 2